HYDROLOGIC PROPERTIES
OF ONE MAJOR AND TWO MINOR SOIL SERIES
OF THE COAST RANGES OF NORTHERN CALIFORNIA

by

Edward Pearson Wosika

A Thesis

Presented to

The Faculty of Humboldt State University

In Partial Fulfillment

of the requirements for the Degree

Master of Science

HYDROLOGIC PROPERTIES

OF ONE MAJOR AND TWO MINOR SOIL SERIES

OF THE COAST RANGES OF NORTHERN CALIFORNIA

by

Edward Pearson Wosika

Approved by the Master's Thesis Committee

Carlton S. Yee, Chairman

Robert R. Ziemer

Dean F. Freeland

Natural Resources Graduate Program

Approved by the Dean of Graduate Studies

Alba M. Gillespie

ABSTRACT

The following properties of the Hugo, Mendocino, and Caspar soil series were analyzed at the 10 cm, 20 cm, 30 cm, 50 cm, 100 cm, and 150 cm depths: bulk density; porosity; particle density; saturated and unsaturated hydraulic conductivity; particle-size distribution; pore-size distribution; and water retention characteristics.

The Hugo soil series exhibits great variation in its hydrologic properties from location to location. This series differs from the Mendocino and. Caspar series by having a higher gravel content, a greater proportion of large diameter pores, and a lower degree of development of the B_t horizon. The Caspar and Mendocino series vary only slightly in their hydrologic properties. The main factor producing differences between these three series and within the Hugo series is the degree of colluvial mixing, which is closely related to slope position. The lower the slope position, the greater they degree of colluvial mixing and burial. The unsaturated hydraulic conductivities of the three series are sufficiently high at all soil depths to preclude the large-scale development of saturated subsurface flow.

ACKNOWLEDGEMENT

Invaluable guidance and moral support throughout the selection and course of this project were provided by my major advisor, Dr. Carlton S. Yee. Dr. Yee's thorough knowledge of soil physics, watershed management and grantsmanship, coupled with his ready availability not only expedited the project's completion but made it possible in the first place. Appreciation is extended to my other committee members, Dr. Robert R. Ziemer and Dr. F. Dean Freeland for their promptness in reviewing the drafts. Dr. Ziemer’s thorough, constructive criticism greatly reduced the number of drafts necessary, and gave me a valuable education in balancing project size with the limitations of statistical inference. Dr. Freeland provided both a student assistantship and valuable moral support. Mr. Robert B. Thomas, of the Pacific Southwest Forest and Range Experiment Station's (P.S.W.) Redwood Sciences Laboratory, provided astute advise on statistical approaches and limitations.

The project was funded principally by a McIntire-Stennis grant, with matching funds and laboratory space provided by Humboldt State University. I wish to thank the P.S.W.'s Redwood Sciences Laboratory for providing laboratory space and equipment, generous computer time, arid a summer position as hydrologist wherein my principal assignment was the furtherance of my initial field work. The Redwood Sciences Laboratory's geologist, Mr. Philip B. Durgin, helped provide the original idea for the project.

My wife, Hannelore, did the final typing and helped me through the long months of field and laboratory work.

TABLE OF CONTENTS

TABLE OF CONTENTS (continued) Page

APPENDICES

TABLE OF CONTENTS (continued) Page

APPENDICES (continued)

LIST OF TABLES

LIST OF FIGURES

LIST OF SYMBOLS

The following symbols are used in this thesis:

Symbol	Description	Units
AS	Degree of aggregate stability (% by weight of total aggregates)	%
B_t	B soil horizon rich in illuvial clay and silt	
D	Particle diameter	mm
g'	The acceleration due to gravity	cm sec^{-2}
G_s	Specific gravity of the soil, solids (dimensionless)	
h	Distance below the free water surface	cm
H	Total hydraulic head (cm of water)	cm
H_g	Gravitational head (cm of water	cm
H_p	Pressure head (cm of water)	cm
H	Head loss (cm of water)	cm
i	Potential energy gradient or hydraulic gradient (dimensionless)	
K	Hydraulic conductivity	cm hr^{-1}
$K(P_c)$	Hydraulic conductivity at a capillary pressure of P_c	cm hr^{-1}
K_r	Relative hydraulic conductivity (decimal fraction of K_s)	
K_S	Saturated hydraulic conductivity	cm hr^{-1}
L	Length of flow, measured parallel to the mean vector component of the flow	cm
n	Total porosity of the soil	%
N'	Corrected percent-finer, based upon the total dry soil weights	%
N_f	Percent-finer than a specified size within the fine fraction, based upon the fine fraction only	%
P_b	Bubbling pressure; approximately the minimum capillary pressure on the drainage cycle at which the non-wetting fluid is continuous (cm of water)	cm

Symbol	Description	Units
P_C	Capillary pressure; the difference in pressure across the interface between the wetting and non-wetting fluid (cm of H_2O)	cm
Pc'	Capillary pressure (bars used for high pressures)	bar
P_g	Gravitational potential (cm of water)	cm
P_k	Kinetic potential (cm of water)	cm
P_o	Osmotic potential (cm of water)	cm
P_p	Pressure potential (cm of water)	cm
P_t	Total potential (cm of water)	cm
r	Hydrometer reading in the suspension	g/1
r_w	Hydrometer reading in water at the same temperature as the suspension	g/l
R	Radius of curvature of meniscus	mm
R_e	Reynolds Number (dimensionless)	
S	Degree of saturation (decimal fraction)	
S_a	Degree of total saturation (decimal fraction)	
S_e	Effective saturation (decimal fraction)	
S_r	Residual saturation (decimal fraction)	
t	Total elapsed time since beginning of the hydrometer run	sec
T_s	Surface tension of liquid	g sec^{-2}
V'	Volume of the suspension in the Bouyoucos cylinder	cm^3
w	Water content (% by weight)	%
W_c	Total oven dried mass of the coarse fraction of a bulk sample	g
W_s	Equivalent dry mass of the total bulk soil sample	g
W_1	Equivalent dry mass of the total soil sample passing the 2 mm sieve	g

Symbol	Description	Units
W_2	Equivalent dry mass of the soil used in the hydrometer analysis	g
w%	Equilibrium moisture content (% by weight)	%
Z	Elevation above the reference datum	cm
Z_r	Distance from the surface of the suspension to the center of volume of the hydrometer	mm
Y_c	Density of water at the calibration temperature	g cm^{-3}
Y_s	Particle density	g cm^{-3}
Y_w	Unit mass of water at the temperature of the test	g cm^{-3}
η	Pore-size distribution index (dimensionless)	
θ	Volumetric water content (decimal fraction of the total soil volume)	
λ	Pore-size distribution index (dimensionless)	
ζ_w	Density of water	g cm^{-3}
μ	Viscosity of water	newton sec. m^{-2}
ϕ	Contact angle of the meniscus	rad

INTRODUCTION

Purpose

The purpose of this thesis was to quantify certain hydrologic properties of three soil series of the redwood region. A statistical approach was not possible, due to the large number of interactions between the various parameters examined, yet much useful information has resulted from the study.

Geology

Geology and Geomorphology of the Study Area

The Caspar Creek Watershed contains two types of bedrock: graywacke of the Franciscan Formation, and wave-cut terrace deposits. No significant faults transect the watershed (U.S. Geologic Survey, 1960).

The Franciscan Formation is a eugeosynclinal sequence that was deposited in the later part of the Mesozoic Era (late Jurassic to latest Cretaceous). It has a complex structural history and a diverse lithology. The most common rock is graywacke, with lesser shale, conglomerate, basalt, greenstone, chert and limestone. Subsequent burial, faulting and folding of these rocks, coupled with varying degrees of low temperature metamorphism and scattered ultramafic intrustions has produced the chaotic assemblage which dominates the California Coast Ranges today. Faulting is so common that no conformable contact has been found between the Franciscan and geographically adjacent formations. In addition, the Franciscan is so thick that despite all the regional faulting, neither the base nor the original top of the formation have ever been recognized (Page, 1966). Erosion has tended to follow the zones of lithologic weakness associated with the fault traces, producing a northwest to southeast trending drainage pattern development regionally. The Franciscan within the Caspar Creek drainage is a massive, well indurated, brecciated graywacke of latest Cretaceous age (U.S. Geologic Survey, 1960). The geomorphology of the area, exclusive of the narrow band of wave-cut terraces along the coast, is in the "mature" stage of the mountainous erosion cycle: Most of the land is steeply sloped, the valleys are narrow and V-shaped; streams and rivers tend to be narrowly confined, without significant floodplains; ridges tend to be sharp.

The large fluctuations in sea level which occurred world-wide during the Pleistocene epoch ("glacial age") produced a series of five wave-cut terraces in the Fort Bragg-Mendocino area (Jenny, 1973). Wavecut terraces are formed when the sea level rises so slowly that the waves are able to erode the sea cliffs down to sea level continually as the shore line marches inland. Any geologically abrupt rise in sea level drops the wave-cut terrace below the level of erosive scour, thereby preserving it and beginning a new terrace at a higher level. Sediments derived from the erosion of the terrace are deposited on the next lower terraces, which are in less turbulent water. This "stairstep" effect is preserved during the recessional sequence because the receding water tends to merely rearrange the loose terrace deposits, leveling them but not altering the basic bedrock geomorphology. Often wind blown sand from the receding shoreline will be saltated up to the next higher terrace. This sand is deposited by onshore winds at the edge of the terrace drop-off, due to the vortex induced by the wind's passage over the terrace edge. The resultant terrace deposits have a mineralogy similar to that of the parent formation, but are higher in abrasion resistant quartz and lack induration. In some areas, the lithology of the parent formation precludes the formation of terraces by being either too soft or too hard to match the rates of erosion and transgression. For this reason, Pleistocene terraces were developed along some coastlines and not along others. The terraces of the Mendocino area are particularly well-developed.

Soil Morphology

The soils that develop on wave-cut terraces in a cool-humid climate are unusual in character. The loose terrace deposits are normally very permeable, while the underlying bedrock is relatively impermeable. These conditions promote eluviation of clays from the surface horizons, eventually producing an albic A_2 and a tonal B horizon (B_t). The large lateral extent of the terrace deposits, relative to their thickness, combined with the impermeability of the bedrock and illuvial clay pan, causes a perched water-table to form. The resulting poor drainage causes gleying to occur. The geomorphology thus produces a toposequence in which the soils of the flattest, poorest drained sites exhibit all the above-mentioned characteristics (e.g. Blacklock soil series). The better drained edges of the terraces retain only the albic A_2 and B_t horizons, exhibiting no gleying. The Caspar soil series is an example of this type of soil profile development. Halfway between these extremes lies the Noyo soil series, which develops on the gently sloping parts of the terraces and on the dunes.

Except for the Pleistocene wave-cut terraces, the entire Caspar Creek watershed is in the "mature" stage of geomorphic evolution, with most of the area being in. steeply sloping terrain. Typical slopes within the watershed range from 35% to 75%. Steep, V-shaped canyons and sharp crested ridges characterize the area.

The colluvial movement, unaltered Franciscan parent material, and improved drainage characteristics on the slopes produce different soils than those that occur on the nearby wave-cut terraces. The Hugo soil series is typical of the soils which develop under these conditions and is the most common soil in both the Caspar Creek drainage arid the redwood region as a whole. The colluvial movement precludes the establishment of a distinct pedon. The good drainage tends to reduce the amount of clays left in the pedon, though B_t horizons do develop from place to place due to variations in colluvial mixing. The thickness and degree of development of this soil varies considerably within the study area.

Isolated remnants of wavecut terraces are to be found on many of the broader ridgetops of the Caspar watershed. Here, the Mendocino series occurs. It is similar to the Caspar series in many respects, but lacks the albic A_2 horizon, and is not part of the Blacklock-Noyo-Caspar toposequence. Its parent material is slightly different from that of the Caspar series in that it consists mostly of reworked gravels. The Caspar series, by comparison, represents a modification of the older Blacklock and Noyo series, in response to improved drainage conditions. The Mendocino series has a well developed B_t horizon, but its surface horizons are very well aggregated, like those of the Hugo series.

The Energy State of Soil Water

The tendency for water to move through the soil is controlled by the energy state of the soil water and its variation throughout the soil profile. Movement of water within the soil is always from points of higher potential energy to points of lower potential energy. The rate of this movement is controlled by both the potential energy gradient (i) (the ratio of the change in total potential over distance), that exists and by the hydraulic conductivity (K) of the soil. The hydraulic conductivity at any point is a function of the soil's pore and particle-size distributions, the arrangement of the pores, the total porosity (n) and the degree of saturation (S). The direction of water movement is determined by the resultant vector of the potential energy gradient.

Total Energy Concept

Total potential (P_t) is the vector summation of several different energy potential components. Gravitational potential (P_g), pressure potential (P_p), osmotic potential (P_o), and kinetic potential (P_k) are the most common potentials governing water movement. However, the velocity of soil water movement is so slow that the kinetic potential is essentially zero and is therefore usually disregarded. For the osmotic potential to become relevant, a semipermeable membrane must be present between areas where the soil water salinity differs. Since this situation does not usually occur, except at soil-root interfaces, it also can be ignored in this discussion. Therefore, the gravitational and pressure potentials are the primary contributors to the total energy potential in a soil mass. Mathematically speaking, the total potential of soil water is the sum of all relevant components, such that

$$P_t = P_g + P_p + \ldots \quad (1)$$

The dots to the right of the formula signify that other terms may be included when their contribution is significant.

The gravitational potential of the soil water at any point is a function of that point's elevation above some arbitrary reference datum. This datum is normally chosen such that all values of P_g will be either positive or zero for a given situation. The gravitational potential acts only in the vertical direction. The magnitude of P_g at any point is strictly a function of that point's elevation (Z) above the referenced datum, the density of water (ζ_w), the volume of water involved (V), and the acceleration due to gravity (g'). The gravitational potential for a unit volume is given by

$$P_g = \zeta_w \, g' \, Z. \qquad (2)$$

The pressure potential is normally referenced to atmospheric pressure. Where a free water surface exists, the pressure potential is equal to atmospheric pressure, at the water's surface. Atmospheric pressure is, by convention, often set equal to zero, the so-called gage pressure, when pressure potential differences are of primary concern. The pressure potential of water at any point in a soil may be positive, negative, or zero. If the potential is positive, it is commonly termed "pressure". The pressure potential is always positive at any point below a free water surface. Under the water table, for instance,

$$P_p = \zeta_w \, g' \, h, \qquad (3)$$

where h is the vertical distance below the free water surface. If P_p has a negative value, it is termed "tension", "suction", "capillary pressure", or "matric potential".

Above the water table, the soil contains both water and air in its pores. A meniscus forms wherever an interface exists between the water and air. The presence of the menisci introduces capillary forces into the system. The nature of the capillary phenomenon is such that the pressure of the water beneath the meniscus is less than zero. The magnitude of this negative pressure potential is

$$P_p = -2T_s \, \mathrm{Cos}\phi \, R^{-1}, \qquad (4)$$

where T_S is the surface tension of water, ϕ is the contact angle of the meniscus with the soil particles (0 rad. is normally assumed), and R is the radius of curvature of the meniscus (Hillel, 1971).

Flow may be induced in any direction by the pressure potential. If, for example, the upward pressure potential gradient is greater than the opposing gravitational potential gradient (downward), then the net potential gradient will be upward, and flow will occur against gravity.

The potential equations presented above yield units of force per unit area (g cm^{-1} sec^{-2}). It is often more convenient to express the pressure potential and gravitational potential in terms of an equivalent hydraulic head (H), the height of a column of water that would produce the same potential. When this convention is adopted, both gravitational and pressure heads are expressed in centimeters of water and hydraulic gradients are unitless. The energy state of the soil water is then expressed in terms of its "total potential head", "pressure potential head", and "gravitational potential head" (Hillel, 1971). Equation 1 may then be rewritten as

$$H = H_g + H_p + \ldots., \qquad (5)$$

where H, H_g, and H_p are, respectively, the total, gravitational and pressure potential heads, in centimeters of water. Another simplifying unit convention is to express the potential in terms of the equivalent of 9800 g cm^{-1} sec^{-2} is equivalent to 10 cm of head or 9.79 x 10^{-3} bars.

Darcy's Equation

The potential energy gradient between points within the soil, as mentioned above, causes the soil water to move. The heterogeneity of pore-size and shape within soils is such that theoretically derived mathematical expressions describing saturated flow of water through individual pores are beyond our capabilities. Henry Darcy, in 1856, circumvented this problem by approaching saturated flow from an empirical and holistic standpoint (Hubert, 1956). His work involved the study of the seepage rate of water passing through saturated sand filters. He found that a simple, linear relationship existed between the flux (q), or flow rate per unit cross-sectional area of soil, and the hydraulic gradient (Δ H/L),

$$q = -K_s (\Delta H/L), \qquad (6)$$

where K_s is a constant of proportionality for the, medium involved and is termed the "saturated hydraulic conductivity". The hydraulic gradient(i) is the amount of head-loss per unit distance of travel, or H/L.

The flux is a linear function of i only so long as laminar flow prevails. In a porous medium such as soil, this means that the Reynolds number (R_e) must be less than one (Hille1, 1971). This limit is usually not exceeded if the hydraulic gradient is less than five (Sowers and Sowers, 1951). This range of hydraulic gradients encompasses the majority of water flow situations within the soil. Should these limits be exceeded, increasingly greater applied hydraulic gradients produce increasingly smaller increments of additional flow, since more of the additional energy is consumed in turbulence.

Hydraulic Conductivity

The hydraulic conductivity (K) is essentially a parameter describing the ease with which water will pass through the soil matrix. The saturated hydraulic conductivity (K_s) may be thought of as the apparent velocity of water passage in response to a unit hydraulic gradient.

The concept of saturated flow through porous media is thoroughly discussed in many texts and professional papers on soil physics (Hillel, 1971; Sowers and Sowers, 1951; Wu, 1970; Lambe, 1951).

Hydraulic conductivity decreases exponentially when the degree of saturation decreases from 100%. This phenomenon occurs because only those pores continuing to contain water contribute to flow. Because, by the law of capillarity, large pores will be the first to drain (Harr and Yee, 1975), the large, interconnected pore spaces are responsible for a large majority of a soil's hydraulic conductivity. In soils with a pore-size distribution that is skewed towards the larger pore diameters (e.g. sandy soils), the hydraulic conductivity drops very quickly when subjected to a small capillary tension. A soil with the same porosity, but dominated by micropores (e.g. clay soils), will have a higher relative conductivity at that capillary tension, since the majority of its pores will resist desorption until a much higher tension is experienced. Soils midway between these two extremes often exhibit high values of both saturated and unsaturated hydraulic conductivity.

The laboratory method for the determination of unsaturated hydraulic conductivity at various tensions ($K(P_c)$) is a tedious procedure. Various methods have been developed which permit the estimation of $K(P_c)$, using other soil parameters. The method of Laliberte _et al_. (1968) is by far the simplest of these methods (Harr and Yee, 1975). It is applicable only to the drainage cycle, and at moisture contents greater than field capacity. Hysteresis effects prohibit its use on the sorbing cycle. The only inconvenience this causes is that most analyses of subsurface storm flow are done on soils that are in the process of taking on water (sorbing). Still, the technique yields valuable estimates. Presumably, values of $K(P_c)$ for the sorbing cycle would be less than those for the drainage cycle, for any given value of tension (P_c).

Laliberte _et_ _al_. found that the relationship of unsaturated hydraulic conductivity to tension could be described by the parameters λ, η, and P_b (Laliberte _et_ _a1_.,1968). Brooks and Corey (1964) had previously defined, λ and η as pore-size distribution, indices and P_b as the bubbling pressure. They defined P_b as the tension level at which gas begins to enter the soil and hypothesized that this air-entry value was related to the hydraulic radius of the larger pores in the soil. These larger pores could be expected to be the first to desaturate, since their larger diameter would render them less resistant to water loss than the smaller pores.

The parameter λ is a constant which is dependent on the nature of the porous medium in question. It is equal to the absolute value of the slope of a log-log plot of effective saturation (S_e) versus capillary pressure (P_c), as shown in Figure 1. A description of the parameter S_e is included in the results section. The larger the value of λ for the soil, the faster the soil desaturates, as tension is increased. A larger value of λ indicates that the soil lacks a wide range of pore sizes. Extremely large values of λ can be obtained from artificial soils made from uniformly packed glass spheres of identical size.[1)]

The other pore-size distribution index, λ, is also an absolute slope value of a log-log plot, that of relative hydraulic conductivity (K_r) versus capillary pressure. Figure 2 illustrates this relationship. Brooks and Corey (1964) showed that an empirical relationship existed between λ and η, whereby

$$\eta = 2 + 3\lambda. \tag{8}$$

1) Yee, C.S., 1977. Personal communication, Arcata, California.

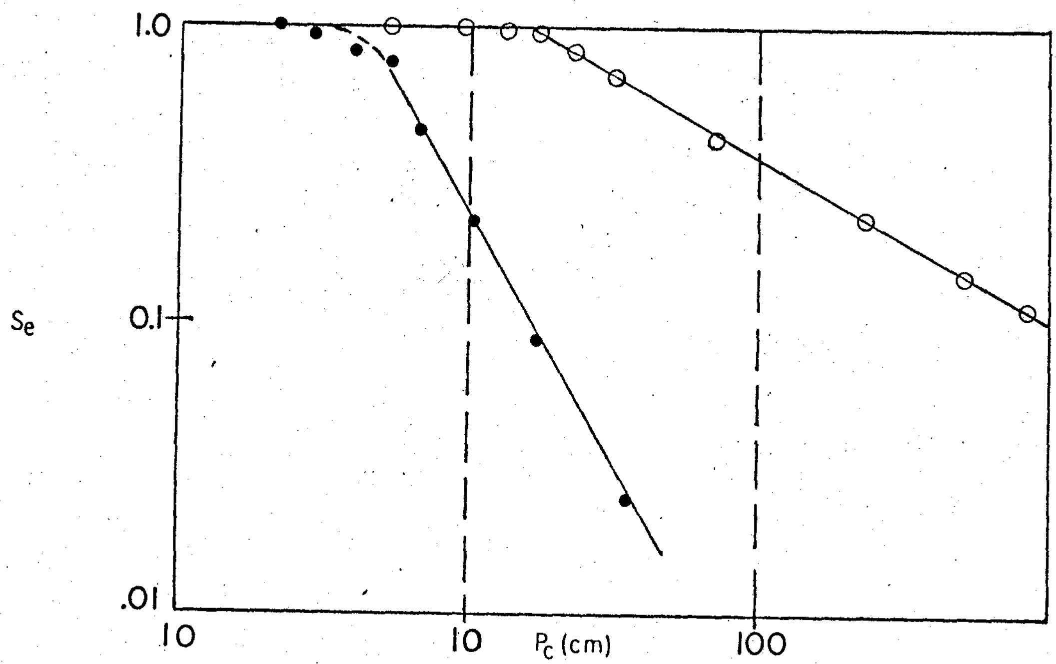

Figure 1. Effective saturation as a function of capillary pressure (after Corey, 1969).

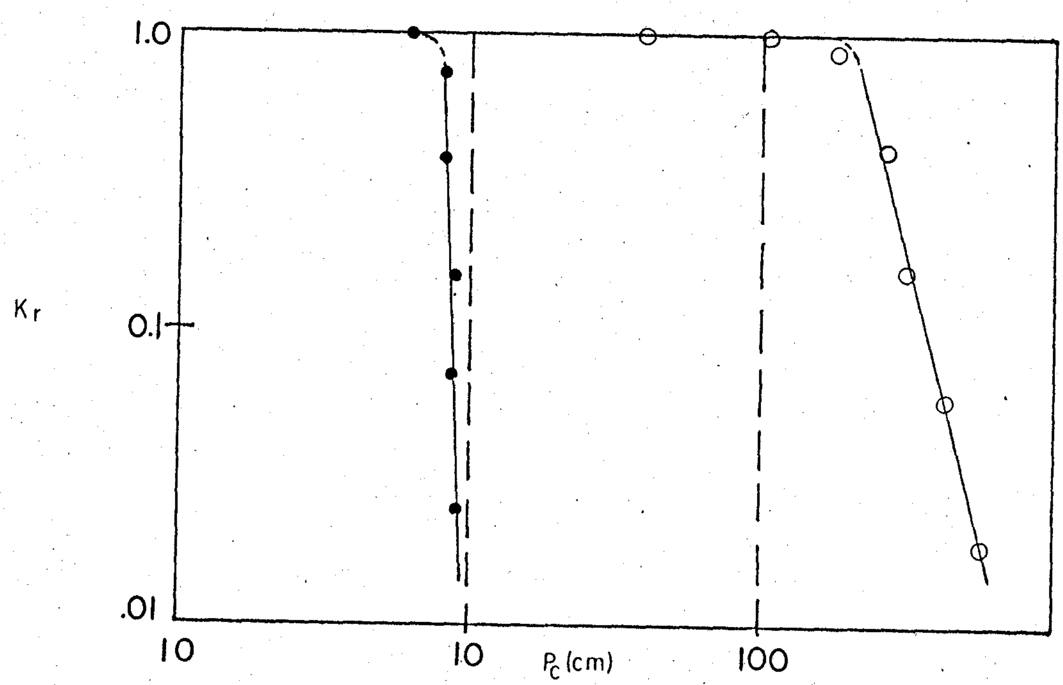

Figure 2. Relative hydraulic conductivity as a function of capillary pressure (after Corey, 1969).

In addition, they found that K_r is related to P_b, P_c and η by

$$K_r = \left(\frac{P_b}{P_c}\right)^{\eta}, \text{ for } P_c \geqq P_b \,. \tag{9}$$

K_r is the decimal fraction of K_s which the soil exhibits at a tension of P_c, so that

$$K(P_c) = (K_r)\,(K_s) \tag{10}$$

Subsequent work by Laliberte *et al*. (1968) has verified the validity of these relationships.

DESCRIPTION OF THE STUDY AREA

Location

The Caspar Creek Watershed was selected as the most suitable for this study in terms of its geomorphology, climate, soils, vegetation, and previous related work. It is located along the coastal edge of the California Coast Ranges (Figure 3), in the northeast portion of T17N, R7W, Mount Diablo Meridian, Mendocino County, approximately 6 km E.S.E. of the village of Caspar, and midway between the towns of Mendocino and Fort Bragg. The study watershed is on land administered by the Jackson State Forest, California Department of Forestry. The areas chosen for study comprise those portions of the Caspar Creek watershed that lie upstream of the wiers on the north and south forks (Figure 3). The areas of the north and south fork watersheds are 508 ha and 424 ha, respectively.

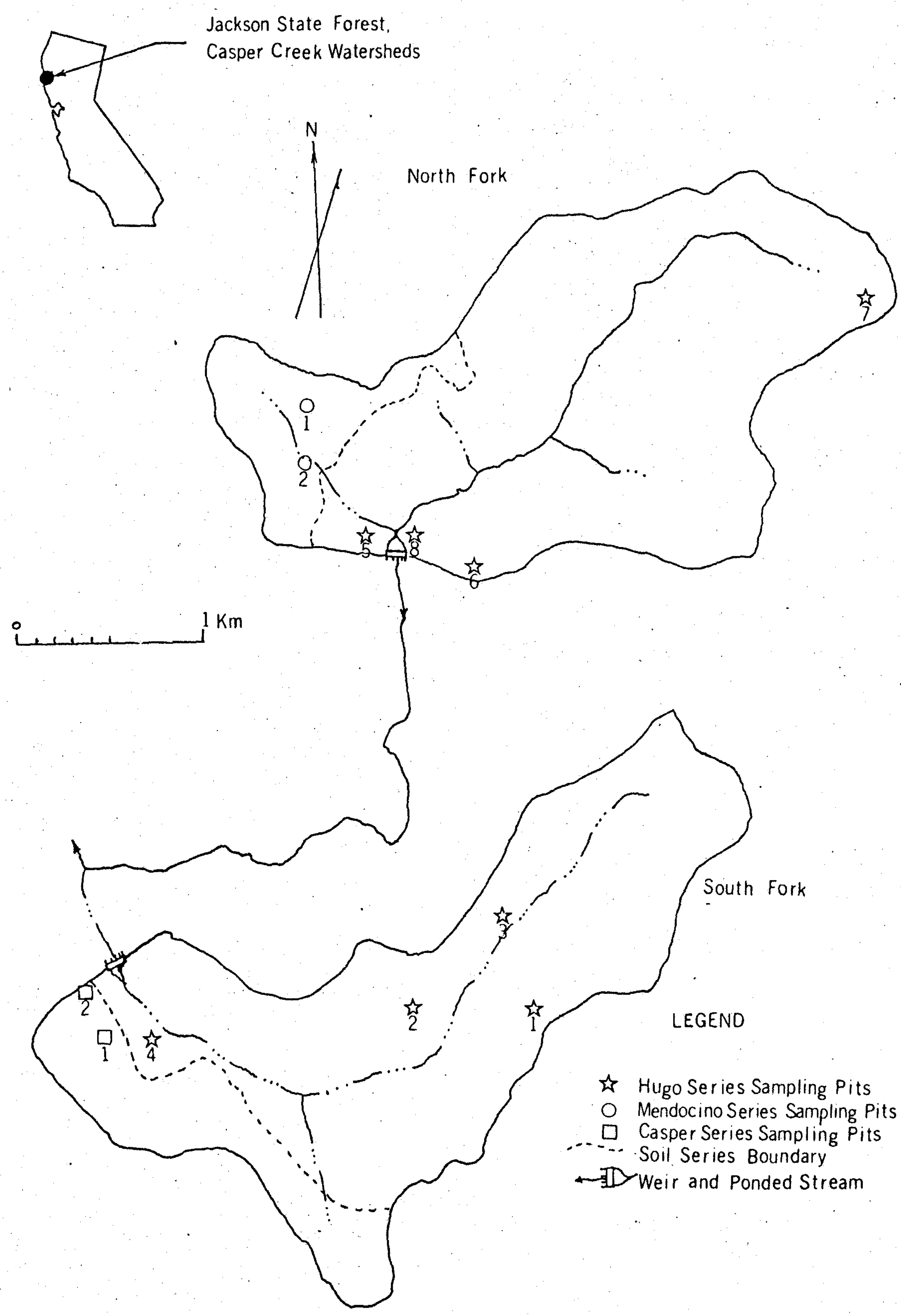

Figure 3. Location map of the Caspar Creek Watersheds.

The Jackson State Forest

The Caspar Creek drainage and study area lies within the Jackson State Forest. The first lands for the forest were purchased in 1947 by the State of California. The primary focus of this forest has been the application of state-of-the-art forestry practices on old-growth and second-growth redwood forest types. In addition, the State Forest is an outdoor laboratory in which new concepts may be tried and developed. Work in the following areas is an ongoing endeavor within the forest: timber growing and harvesting research; forest tree improvement; improved seedling establishment; manipulation of growing stock; prediction of growth and yield; methods of timber harvesting; watershed management research in the California commercial timber zone; inland fisheries research; wildland recreation research; forest insect research and forest disease research. These lands are available to the faculty and students of the California College and University System, as well as to other scientific groups and to individuals, for basic and applied research related to the above areas of interest. Many of the concepts and techniques developed within the Jackson State Forest have become adopted as standard practices by the logging industry of northern coastal California. Since so much research effort is concentrated in this one geographic area, data and results from a particular study are often helpful to later researchers (Krammes and Burns,1973, and Rice *et al*., 1979).

Geology of the Area

The study watershed is underlain by the Franciscan Formation, a late Mesozoic eugeosynclinal sequence of diverse lithology. The principal rock in the study area is a well indurated, brecciated graywacke, with the minor exception of a pocket of scoriaceous basalt at the site of soil pit Hugo No. l. Surficial deposits of sand exist on the scattered remnants of Pleistocene wave-cut terraces. This mildly indurated material comprises the parent rock for the Caspar soil series, which covers 9.2% of the study area (Figure 3). The Mendocino soil series is derived from coarser wave-cut terrace deposits and occurs on broad ridges which are the remnants of terraces. This soil series covers 6.4% of the study area (Figure 3).

Physiography

The topography of the study area is characterized by fairly steep slopes, averaging 28 degrees (53%), which is typical of the mountainous areas of the redwood region. The drainage pattern is dendritic, resulting in a complete range of slope aspects (O° to 360°) The elevational range is from 36.6 m at the south fork wier, to over 317 m at the northeastern end of the south fork watershed.

There are two exceptions to the steep, mountainous terrain mentioned previously. One is a broad ridge-top along the western edge of the north fork watershed. This is the location of the Mendocino soil series. The other area lies along the southwest border of the south fork watershed. It is an eroded terrace edge, upon which the Caspar soil series has developed. Both of these areas have been modified by Pleistocene wavecut terracing.

Climate

The climate of the area is dominated by a maritime influence, and is typical of the redwood region of northern coastal California. The summers are warm and dry, with morning and evening coastal fog. The winters are cool and wet. Prolonged periods below -7° C are infrequent. The mean minimum January temperature is 4° C, while the mean maximum July temperature is 18°C. Mean annual precipitation is strongly influenced by orographic effects (Elford and McDonough, 1974). The coast receives 102 cm of rainfall annually, while the eastern rim of the watershed (mean elevation: 274 m) receives 142 cm. Snow only occurs occasionally and never makes a significant contribution to the water budget (interpolated from isopluvial and isothermal maps by Elford, 1970).

Soils

The Mendocino soil series is a moderately well-drained sandy clay loam, with a sandy clay subsoil. It develops on broad ridges and mountainous uplands near the coast, particularly (but not exclusively) on erosionally isolated remnants of Pleistocene wave-cut terraces (U.S. Soil Conservation Service *et al*., 1972). In the Caspar Creek watershed, it is mapped only along the western boundary of the north fork watershed. I have found that the actual extent is much greater, however, occuring along that same ridge, nearly to the site of the Hugo No. 7 soil pit. The Mendocino soils are associated with the Caspar, Hugo, Empire and Goldridge soils, though only with the Caspar and Hugo, within the study area.

The Caspar soil series is a well-drained sandy loam, with a subsoil of clay loam to sandy clay loam (U.S. Soil Conservation

Service *et al.*, 1972) It forms along the brows of coastal wave-cut terraces, where streams that once flowed across the terrace have eroded a valley. This soil is transitional between the younger, colluvial Hugo series, and the ancient, clay-panned Blacklock and Noyo Series of the poorly-drained terrace areas. The Caspar series represents a pedological adjustment of these terrace soils to the improved drainage conditions along the newly eroded terrace edges.

The Hugo soil series is the youngest of the three soils of the study area, in terms of its pedological development. It is a well drained, very gravelly loam, with a gravelly, sandy clay loam subsoil (U.S. Soil Conservation Service *et al.*, 1972). It occurs mostly on mountainous slopes, and develops upon graywacke parent material. It is not limited to coastal areas, as are the Caspar and Mendocino series. As such, it has an extensive regional occurrence and is one of the most common soils of mountainous areas in the redwood region. Colluvial movement, good drainage and steep slopes preclude its attaining an old age, pedologically.

Vegetation

The vegetation of the Caspar Creek drainage (Appendix A) is characteristic of that of the redwood region in general. The overstory is dominated by second-growth redwood and the understory by a sword-fern community. The overstory averages 30 to 60 meters in height and is up to 90 years old. This pattern varies considerably with slope aspect and recency of timber harvest. Douglas-fir is quite common, but never dominant. Madrone, tanoak and chinquapin occur as scattered individuals, but can be the dominant trees on xeric south-facing slopes which have been heavily selection-cut within the last eight to twenty years.[2] More recently selection-cut areas have a crown density ranging from ten to thirty percent, consisting solely of redwoods. The understory at these sites consists of moisture-stressed swordferns and scattered brush species. These areas have favorable slope aspects and are showing good regeneration of redwood by stump sprouting, though the long dry season still takes a heavy toll of seedlings. The stream banks support red alder, particularly in the more open areas.

All recent timber harvesting has occurred in the south fork watershed, since the north fork watershed is being used as a control in an ongoing paired watershed study of the hydrologic effects of road building and timber harvesting in the south fork basin (Krammes and Burns, 1973).

[2]The area around the Hugo No. 2 soil pit shows a dominance of these hardwoods. Seedling mortality is high. The soil was almost too dry to core sample, even during the winter of 1977-78, which was a year of normal rainfall.

METHODS AMID MATERIALS

The purpose of this study was to examine certain hydrologic properties of three forest soils of the redwood region. Each hydrologic parameter was analyzed to determine the extent that it varied between soil series, with depth, and between pits within each soil series. In addition, the parametric differences between the north and south fork watersheds and between slope positions were analyzed. No extensive study of the hydraulics of these soils had previously been done, but the work of Harr and Yee (1975), and Rankin (1974) on certain soils of the Oregon Coast Range were used as models.

Site Selection Criteria

Criteria used in selecting the study area were accessibility, extensive previous research, a variety of soils typical of the redwood region, and the existence of logged and unlogged areas.

A reconnaissance tour of the watershed was given to Dr. Yee and myself by the staff of the Jackson State Forest in the summer of 1976. The Caspar watershed fulfilled all the selection criteria.

Soil Sampling

Soil Pits

Soil samples were taken from a total of 12 soil pits on the two study watersheds (Figure 3 and Table 1). The soil pits were located so as to take into consideration the variations of topography and aspect for the three soil series as they occurred within the study area, rather than using a randomized design.

Table 1. Soil pit location data

Soil Pit	Elevation (m)	Map Distance From Ridge (km)	Map Distance From Creek (km)	Slope Position	Aspect	Local Slope (%)	Sampled Pit Depth (cm)	Vegetation Type
Hugo No. 1	219	0.1	0.5	upper	N	50	150	selection cut redwood
Hugo No. 2	152	0.4	0.4	upper-middle	S	50	150	hardwoods
Hugo No. 3	122	0.3	0.1	lower	S	100	20	redwood (mature)
Hugo No. 4	73	0.9	0.1	lower	N	20	100	selection cut redwood
Hugo No. 5	122	0.9	0.1	lower	E	60	10	redwood (mature)
Hugo No. 6	244	0.1	0.7	upper	E	20	150	" "
Hugo No. 7	268	0.2	0.1	upper	SW	75	30	" "
Hugo No. 8	122	0.6	0.1	lower	W	80	50	" "
Mendocino No. 1	146	0.4	0.2	upper	S	30	150	"
Mendocino No. 2	122	0.5	0.1	upper	N	20	50	" "
Caspar No. 1	146	0.6	0.5	upper-middle	N	30	150	selection cut redwood
Caspar No. 2	122	0.6	0.4	upper-middle	NE	20	150	selection cut redwood

The Hugo soil series is the only one of the three series which occurred in both the south and north fork watersheds of Caspar Creek. This series also possesses the greatest variation in topography, aspect, and soil disturbance. In addition, because the Hugo series is one of the most common soils of the redwood region and within the study area, I decided to sample the Hugo soil more intensively. Four pits in each watershed (for a total of eight) were dug in the Hugo soil. Two soil pits were dug for each of the other two series.

The Caspar soil series is located only along the brow of the southwest rim of the south fork watershed. The, two pits from which Caspar soil samples were taken were located at differing aspects and elevations, as much as this soil's limited occurrence permitted.

The Mendocino soil series is derived from the remnants of marine terrace deposits and is limited to a few broad ridge tops near the coast. Within the study area, it occurs mostly near the top of a small tributary of the north fork, on the westernmost edge of the watershed. The topography here permitted a greater degree of variation in sampling, as to aspect and elevation, than was possible with the Caspar series.

The maximum investigation depth of each soil pit was set at 150 cm. In six of the pits (Hugo 3, 4, 5, 7, 8, and Mendocino 2), the soil was either so stoney or so shallow that core sampling was not possible to the maximum depth. In these cases, visual estimates of the rock content below the lowest sampling depth were made and lab analysis was restricted to the sampleable levels. The Soil Survey Manual (U.S. Soil Conservation Service, 1967) was used as a guide for sampling and describing the soil profiles. Previous descriptions of each soil series were used as a guide in describing each profile.

Soil Sampling

Two types of soil samples were taken from each pit. Representative bulk samples from each level were placed in double plastic bags, sealed and labeled. These bulk samples are each representative of the depth and soil pit from which they were derived. A shovel was used to obtain soil from the entire width of each soil pit, at the specified depth. All bulk samples weighed at least 5 kg. These bulk samples were used to determine the particle-size distribution and aggregate stability of the soils.

In addition, relatively undisturbed core samples were also obtained. These core samples were used to determine the saturated hydraulic conductivity, pore-size distribution, moisture retention characteristics, and bulk density. The sampler was of the impact type. The head of the sampler held two cylindrical 3 cm (dia.) x 5.4 cm (ht.) sample rings. Cores were sampled in the vertical plane for all determinations of hydraulic conductivity. While most of the other cores were taken in a vertical plane, some were taken in a horizontal plane to avoid obstructions.

Once a good quality core had been obtained, its ends were each covered with a double layer of cheesecloth which was secured in place with rubber bands. The core was then marked with indelible ink on its upper end (vertically oriented cores only). The core was then wrapped in a plastic sandwich bag and placed in a carrying tray. The sample rings were numbered to facilitate future identification. Any samples which appeared to have been disturbed by rocks or roots were discarded and resampled.

Samples were taken at depths of 10, 20, 30, 50, 100, and 150 cm, where possible. Due to the common occurrence of large rocks and roots, no systematic sampling arrangement was utilized. Samples were merely taken wherever it was feasible at each sampling depth. From two to four cores were taken from each sample level for moisture retention work plus three to six cores for saturated hydraulic conductivity determination. Any cores which produced anomalous data were resampled (from the same pit) during the next field session.

A total of 707 core samples were used in this work and Table 2 illustrates the final distribution of samples by laboratory test. The disproportionately high number of cores used for permeability determination within the Caspar series is due to the difficulty of achieving consistent results at all sampling levels in this soil.

Table 2. Distribution of core samples by laboratory test.

Soil Series	Cores Used For Tension Work	Cores Used for Permeability Work
Hugo	230	233
Mendocino	40	54
Caspar	66	84
Totals	336	371

Laboratory Analyses of Soils

Particle Density

The particle density (γ_s) of each pit was determined by using a composite sample made up of equal soil weights from each of the pit's sampling levels. The water displacement - pycnometer method was used in determining γ_s. Blake (1965), among others, adequately describes the procedure.

Particle-size Determination

Particle-size distributions were determined for all depth intervals sampled in each soil pit. Because the particles in most of the sample pits varied in diameter from greater than 4 cm down through the clay-size particles (<.0002 mm), a modified, combined sieve-hydrometer method was used. For each determination, approximately 800 g of field-moist soil was used. The 800 g samples could not be oven-dried, since the cohesion of the clays would have made it impossible to differentiate between the aggregates and the clasts of relatively~soft parent material. Dry-weight equivalents were therefore determined through the use of 50 g gravimetric moisture subsamples. If a sample was quite moist, it was permitted to air-dry until it reached a point where the aggregates would easily crumble between the fingers, while not being so moist as to be sticky. Excessively dry bulk samples were sprinkled with distilled water, then dried to this same moisture state.

The samples were then disaggregated and hand shaken through a 2 mm sieve. Primary disaggregation was accomplished by pressure from a rubber stopper. The amount of pressure used was adjusted for each sample, so that no freshly broken particle faces appeared.

When a minimum of 200 g of material had passed the 2 mm sieve, it was collected, labeled, oven-dried (105° C), and saved for hydrometer analysis and aggregate stability determination. The retained coarse fraction was cleaned and wet sieved by alternately submerging the sieve and its contained particles in a dispersing solution for 10 minutes and then flushing the fines away using a strong stream of hot tap water. This process was continued until all clay had been dispersed, and no further fines passed the sieve. The retained coarse fraction was then quantitatively transfered to an evaporating pan, oven-dried at 105° C overnight, weighed to the nearest 0.01 g, and stored for later dry sieving.

The total amount of soil particles passing the sieve in both the above operations represented the portion of soil particles less than 2 mm in size. These particles will be collectively termed the "fines" henceforth. The total weight of fines (W_1) was obtained by subtracting the oven-dry weight of the coarse fraction (W_c) from the equivalent oven-dry weight of the total sample (W_s).

To determine the particle sizes present in the fine fraction, a slight modification of Day's (1965) hydrometer method was used. Dispersion of the clays was accomplished by combining a 50 g sample with 100 ml of a 5% Calgon solution and 300 ml of distilled water, in a 500 ml container. The samples were then shaken on a reciprocating table for 12 hours at 120 cycles per minute. This extensive disaggregation period was used due to the noted difficulty of dispersing western forest soils (Youngberg, 1957). The rotary mixer method of dispersion was avoided, due to the fact that the parent rock (Franciscan graywacke) could often be easily broken by hand. Rotor blades would have broken up many primary particles, skewing the distribution toward the fines.

Because of the insensitivity of the hydrometer method in defining particle diameters in the sand-size class (0.074 mm to 1.99 mm), a wet sieving of the hydrometer samples was done subsequent to the hydrometer analyses. A pair of small (8 cm diameter) sieves with mesh openings of 0.5 mm and 1.0 mm were used. Each dispersed sample was poured through the sieve nest and carefully wet sieved under flowing tap water. The particles trapped on each of the sieves were then washed out onto tared filter paper, held under suction in a Buchner funnel. Oven drying and weighing to the nearest 0.001 g completed the procedure. The total weight of sand-size particles less than 2 mm was then extrapolated from these subsample weights.

Since 15 sedimentation samples were run at a time, logistics required an adjustment of the normal hydrometer reading times. Hydrometer and temperature readings were taken at 35 sec, 45 sec, 2 min, 10 min, 1 hr, 6 hr, 12 hr, and 24 hr. A matched pair of A.S.T.M. 152-H hydrometers were used. The effective diameter, D, of the particles left in suspension at each of the measuring times throughout the hydrometer analyses was computed by

$$D = ((1.8 \times 10^{-3}\mu)\ (\gamma_s - \gamma_w)^{-1})^{1/2} \quad ((Z_r)(t)^{-1})^{1/2}, \qquad (11)$$

where: μ = the viscosity of water at the temperature of the test (Newton seconds meter^{-2})

γ_s = unit mass of the soil grains (g cc^{-1})

γ_w = unit mass of water at the temperature of the test (mm)

Z_r = the distance from the surface of the suspension to the center of volume of the hydrometer (mm)

t = the total elapsed time (min).

The percentage-finer of the fine fraction, N_f, was computed by

$$N_f = (G_s\ V'\gamma_c\ (r-r_w)\ 100)(G_s - 1)^{-1}, \qquad (12)$$

where: G_S = the specific gravity of solids

V' = the volume of the suspension (1000 cc)

γ_c = the unit mass of water at the temperature of calibration of the hydrometer (g cc-1)

r = the hydrometer reading in the suspension

r_w = the hydrometer reading in water (at the same temperature as the suspension)

The coarse particles larger than 2 mm, which were previously cleaned and dried, were hand sieved through 25.4, 12.5, and 8 mm sieves. The material in the "pan" was considered 2 mm in size. Visual inspection was used to assure thoroughness of sieving. The resulting fractions were weighed to the nearest 0.01 g.

In order to combine the data for the fine and coarse fractions, the percent-finer value of each of the hydrometer fractions had to be adjusted so that it represented its relative percent of the total sample. Only the percent-finer values of the fines needed to be corrected, since the coarse fraction values already represented the total sample weight.

The following formula was used to achieve this adjustment:

$$N' = (N_f\ W_l)\ (W_s)^{-1}. \qquad (13)$$

where N' = the corrected percent-finer based upon the total soil dry mass (%)

N_f = the percent finer than a specified size within the fines fraction, based upon the fines fraction only (%)

W_1 = the equivalent dry mass of the total soil sample passing the 2 mm sieve (g)

W_s = equivalent dry mass of the total soil sample (g)

Aggregate Stability

Aggregate stability was determined by combining 50 g of oven-dried fines with enough distilled water to make a one liter suspension. The sedimentation cylinder containing this was then turned end for end 20 times in 30 seconds. After the last inversion, 35 and 45 second readings were taken with the hydrometer. A reading was also taken in a control cylinder containing only distilled water, at the same temperature. The resulting percent finer values were averaged to yield a 40 second value, and compared with the 40-second value of the same sample in a dispersed condition. By the time 40 seconds had passed, all sand-size particles had settled past the detection depth of the hydrometer. The aggregates in the distilled water tended to settle out with the sand, so the hydrometer measured the disaggregated particles of silt and clay.

All aggregates which had survived the 20 inversions were labeled "water-stable aggregates". The aggregate stability value (percent by weight) was obtained by subtracting the 40 second percent-finer value of the undispersed sample from that of the dispersed sample. It can be seen that sand grains that were not incorporated into aggregates were canceled out during this subtraction, so that the resulting value represented only water-stable aggregates.

Saturated Hydraulic Conductivity

Saturated hydraulic conductivity measurements were made using undisturbed core samples. From two to six replicate determinations were made for each level sampled in each pit. Three-centimeter high core rings were used throughout. Most pits were sampled under barely moist as well as quite moist conditions. Final output represents the mean permeability in these two moisture states. The samples selected were saturated by placing them in a large, deep pan and slowly siphoning in deaired, distilled water. When the water level neared the top of the cores, the flow was interrupted until the water level in the cores had also reached this level. This procedure was used to help prevent air pockets from becoming entrapped by overlying water. The water level was then raised to a depth of 2 cm above the top of the cores.

The actual testing was done using a constant-head permeameter. My particular apparatus incorporated the sample core ring as part of the containing structure of the permeameter (Figure 4). This eliminated the need for further soil disturbance resulting from transference of the soil cord from the retaining ring to the permeameter. The permeameter, consisted of two chambered endplates, four bolts, a constant-head reservoir, and connecting plastic tubing. The four bolts connected the

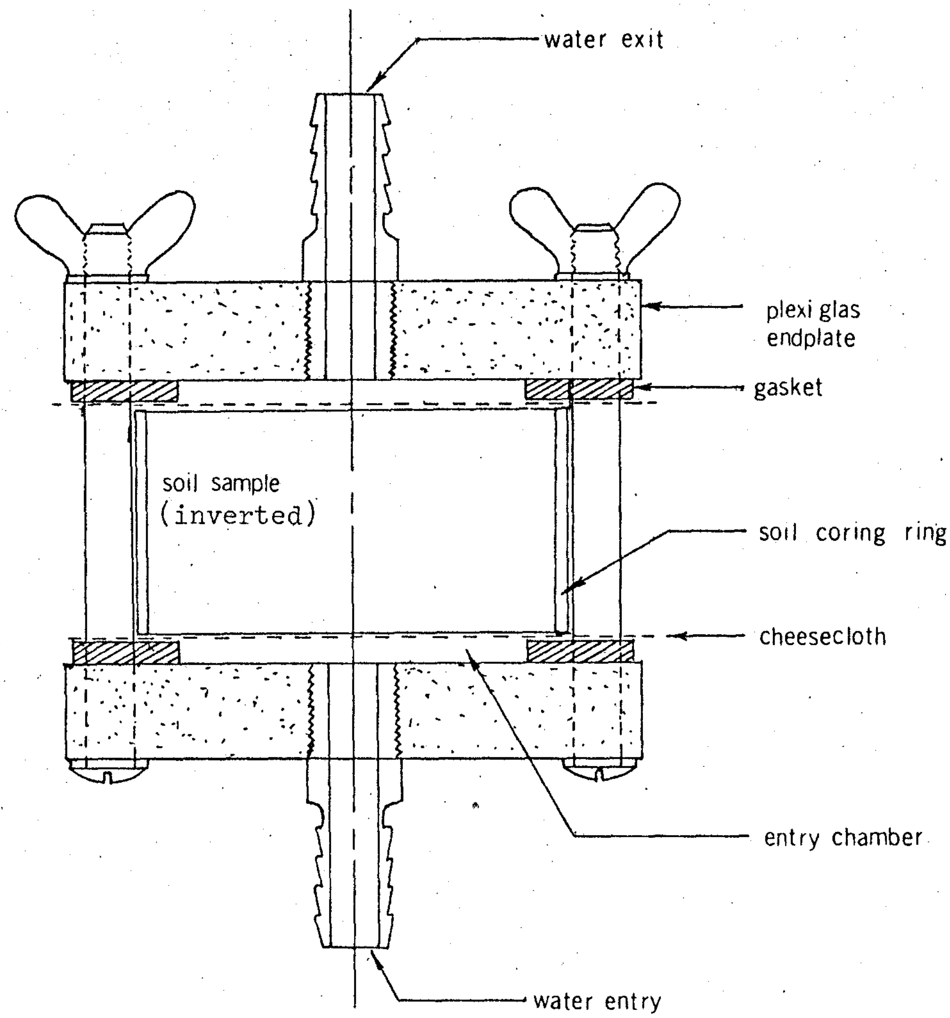

Figure 4. Constant-head permeameter, with inverted core in place. The sample was placed inverted in the permeameter so that the water would flow from the sample top to the sample bottom, thus duplicating the normal flow direction of rain water in the soil.

two endplates, and provided the confining pressure necessary to force them against the ends of the core ring. Rubber gaskets, attached to each of the endplates, provided a seal when mated to the core ring. A screen was attached across the chamber of each endplate to provide full support for the soil samples.

The core ring and endplates were assembled under water to prevent the introduction of air into the system. The four wingnuts were then tightened. The clamp on the plastic tubing from the reservoir was released until the flowing water had expelled any air bubbles from the tubing. The free end was then submerged, reclamped and connected to the assembled permeameter.

The assembly was then lifted from the water. The piece of plastic tubing extending from the exit end of the permeameter assembly was connected to a 3-way plastic tubing connector, which served as the water outlet. The two coaxial ends of the connector were mounted vertically such that the one attached to the permeameter was on the bottom. The open top end served as an ambient air inlet. The remaining end was horizontal and served as the water outlet. The open top-end permitted a free water surface to form within the 14 mm diameter trunk of the connector. All measurements of hydraulic head were made relative to this free water surface, rather than the small (4 mm diameter) outlet orifice. Preliminary testing of the equipment showed that variations in the meniscus across the necessarily small outlet orifice could cause up to a 1 cm error in the true hydraulic head if the measurements were made relative to the outlet.

Once the assembly was affixed to its ringstand, the clamp was released once more, permitting flow through the sample. The outlet was lowered until a flow rate of about two drops per second was achieved. This flow rate was induced by a hydraulic head of from 1 to 30 cm, depending upon the sample. Some of the samples yielded only a drop every 10 seconds, with 30 cm of head. This rate, which is equivalent to a K_s value of 0.3 cm/hr, was taken as the slowest the equipment was capable of measuring. Any samples slower than this were assigned a K_s value of 0 cm/hr.

After each run, the soil sample was removed from its core ring to check for indications of piping or excessive rock content. If the sample passed this visual test, then its saturated hydraulic conductivity was computed using the Darcy equation. Samples used for this test were not reused for other types of tests because of the destructive nature of the piping check and because the small amount of fines which passed from the sample during the initial portion of each run indicated structural changes that could have had an effect on other physical properties.

Each core was loaded in the permeameter such that the through-flowing water passed from its top to its bottom, relative to its position in the field (Figure 4).

Drainage Characteristics

The moisture-retention characteristics of each soil was determined for capillary pressures ranging from 0 to 15 bars. This data was used to estimate the unsaturated hydraulic conductivity at various capillary tension levels as well as the pore-size distribution of each soil. Each soil was analysed at all levels sampled, using from two to four undisturbed cores per sampling level. Tension tables (Vomocil, 1965) were used for tensions up to 60 cm, while Soiltest Model 1500 pressure chambers were used for the higher tension levels.

The normal testing routine called for the application of steadily increasing increments of tension, beginning with a saturated core sample. The cores were initially saturated by slowly immersing them in a bath of deaired, distilled water. After an overnight soaking period, each core's saturated weight was determined by locking it, while submerged, in a special C-clamp which prevented water loss once the core was withdrawn from the water (Rankin, 1974). The apparatus was then wiped off prior to weighing. The saturated weight of each core was recorded after subtracting the standard tare weight of the C-clamp. After weighing, the samples were partially submerged once more on a tension table.

The tension table (Figure 5) was similar to that used by Harr and Yee (1975) and Rankin (1974), but incorporated several changes in design. Each tension table was prepared for use by pouring in deaired, distilled water to a depth of 3 cm, then flushing all air bubbles from the Tygon drain tube, by raising and lowering the overflow reservoir above and below the level of the table. The reservoir was then brought to the same level as that of the water in the table and clamped in position. Next, a 23.8 cm diameter fast filter paper, a 30 cm square piece of construction paper with razor-beveled edges, and a 35 cm square piece of blotter paper were saturated in distilled water, under a vacuum, to remove any internal air pockets. A 19 cm diameter piece of plastic window screening with razor-beveled edges was then submerged directly over the drain hole. Entrapped bubbles in the screen were then removed. The saturated papers were carefully lowered on top of the window screen, in the order mentioned above. The saturated cores were placed on top of this stack and the overflow reservoir lowered

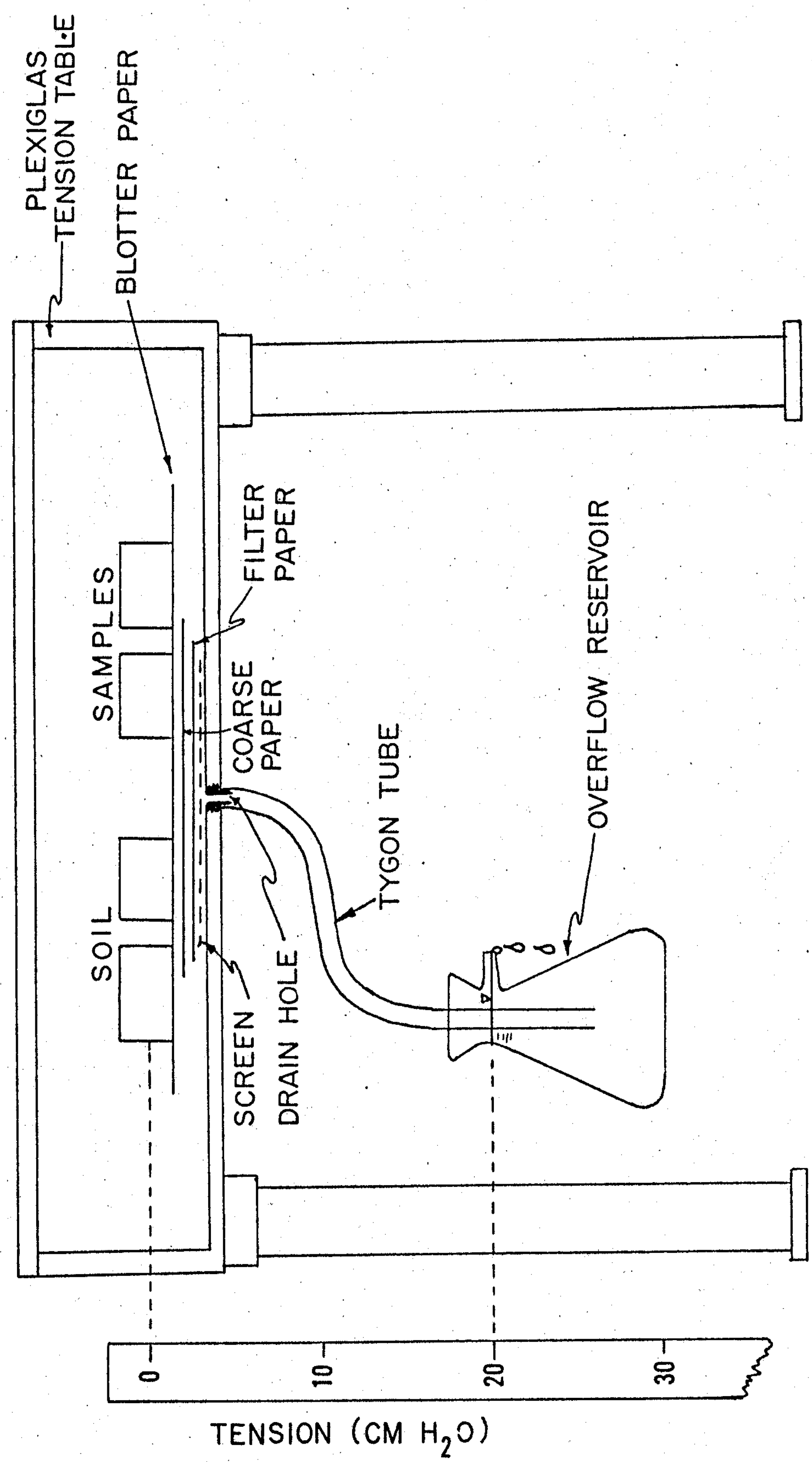

Figure 5. Tension table apparatus for determining drainage characteristics of soil samples.

until its outlet was 10 cm below the center of the cores. The water overflow rate stabilized within a few seconds to about a drop per second, indicating that the flexible filter paper had sealed any direct lateral flow channels. All flow was thus assured of passing only vertically through the filter paper and not underneath the edge of it. Because the filter paper had no pores large enough to allow desorption at capillary pressures less than 60 cm, the filter paper acted as an air block. The blotter paper permitted lateral migration of the water from any cores that were not directly over the filter paper. The window screen facilitated lateral migration of the water to the drain hole, once it had passed the filter. With a good seal assured, excess water was relatively rapidly siphoned off. Finally the table was covered, to prevent evaporation.

The cores were assumed to have come to equilibrium with the 10 cm of tension[3] once flow had ceased from the overflow reservoir. They were removed for weighing and the overflow reservoir was raised to the level of the blotter paper. After weighing, the cores were placed back on the tension table and sprayed with distilled water until water could be seen flowing from the bottom of each core. This assured a good hydraulic contact with the blotter paper. This process was repeated for tensions of 20, 30, 40, and 60 cm.

To calculate the volumetric water content (θ), a core's dry weight was subtracted from its moist weight at each tension level. This weight in grams, when divided by the core volume, yielded theta[4] values for each core.

Evaluation of the soil's response to 1/10 bar[5], 1 bar, 3 bar, and 15 bar P_c' levels were made using the method described by Klute (1965). This entailed the moist-sieving of material from a bulk sample, using a 2 mm diameter sieve. The moist material which passed the sieve was placed into 1 cm high rubber retaining rings on a pressure plate rated for the degree of P_c' which was to be applied. Each sample was represented by two of these rings. The pressure plate was then placed in a pressure chamber, after thoroughly moistening the samples. The pressure in the chamber was then increased to the prescribed level.

Once water ceased flowing from the chamber outlet (within 2 days) the plate of samples was removed and each sample was weighed, then oven-dried, then reweighed. The equilibrium moisture content (w%) of each sample was then determined by dividing its water content, in grams, by its dry weight and multiplying the quotient by 100. Each soil's equivalent volumetric water content (θ) was obtained by multiplying its w% value by the soil's bulk density and dividing by 100 times the unit mass of water.

---

[4]The term "volumetric water content" represents the proportion of the total soil volume which is taken up by water, and is signified by the Greek letter theta (θ).

[5]Bars are normally used for large capillary tension values to avoid large numerical values when expressed in centimeters of water. One bar is equal to 1020 cm of water.

Once the majority of the field and lab work was done, preliminary moisture characteristic curves were drawn up using each soil's, mean θ values for the 10 cm P_c to 15 bar P_c' range. In every case, the mean θ values derived from the intact cores plotted nicely, while those derived from the sieved bulk samples showed a high degree of scatter along the θ axis. Moisture characteristic curves tend to be steep at low P_c levels, but have very low slopes at higher P_c levels. The scatter in the high tension range (P_c') data was particularly vexing since the low-slope in this section of the moisture characteristic, curves required low scatter data in order to be meaningful. In many cases the data would indicate that a soil held more water at 15 bars than at 3 bars of P_c' . This led me to throw out all θ data in the 1/10 to 15 bar P_c' range. The scatter may have been caused by any of several factors, such as small sample size, in relation to the 3 cm high core samples, difficulty in determining when the small samples had come into equilibrium with the pressure in the chamber, or loss of material during the transfers from the pressure plate.

To counter the above problems, an alternate method of obtaining this data was developed. This method produces data which plots consistently across the entire range of P_c. One merely used the same core samples for the high pressure work as for the low pressure range. This eliminates variation caused by switching methods and samples halfway through the capillary pressure range and by working with small samples. All resultant data is in terms of θ directly, so no dubious conversion from w% to θ is necessary. Unfortunately this method could only be applied to samples from a few sampling levels in a couple of pits, since the other pits had all been completely processed and their cores destroyed (in order to free the limited supply of core rings for further sampling). Fortunately, the majority of water flow relations can be adequately described using only the low capillary pressure range (0 cm to 60 cm) data, so the loss of the P_c' range data is not a great impediment.

Bulk Density and Porosity

The bulk density and porosity (n) of the soils were calculated from the desaturation data, rather than making these determinations from separate groups of samples. The dry weight of each core was determined as part of the procedure for calculating its volumetric water content (θ) in response to various applied tensions. This weight was divided by the core volume to obtain the bulk density.

The value of total porosity for each core (in percent) was obtained by multiplying the saturation value of theta by 100. Originally, an Eley volumeter was used to determine the bulk density of all soils. This tool works well on soils that have a low gravel content, but tends, to greatly underestimate the true overall value of bulk density for gravelly soils, because of its small cross-sectional area (24.6 cm^2 as opposed to 68.7 cm^2 for the sampling cores). The data obtained from the Eley sampler was not used for this reason, and also because of the fact that the overall variation of the data would be lowered if as many parameters as possible were obtained from a single set of samples.

RESULTS AND DISCUSSION

Drainage Characteristics

Scope of the Analysis

This section delineates and compares the drainage characteristics of three soil series for capillary pressures of 0 cm, 10 cm, 20 cm, 30 cm, 40 cm, and 60 cm of water. The majority of water movement through soils occurs in this range. The saturation, volumetric moisture content, and pore-size distribution data for each pit are presented in Appendix B.

The Mendocino and Caspar soil series tend to make a gradual transition downs slope into the Hugo series. The areal extent of the Mendocino and Caspar series, within the Caspar Creek watershed, is so small that the pits representing them are in all cases quite close to the boundary with the Hugo series (Figure 3). Since the width of the Hugo-Mendocino and Hugo-Caspar boundaries were not determined in this study, it is difficult to estimate the degree to which the pits within the Mendocino and Caspar series represent their respective series. These two series are represented by only two pits each, while the Hugo series has eight pits. The pits were located so as to maximize within-series variation, rather than by any randomization scheme. Thus from a statistical standpoint, the data from the plots cannot be extrapolated to the Caspar Creek watershed or to the geographic range of the series they represent. A thorough analysis of these soil series would necessarily cover a wide geographic range and include perhaps hundreds of soil pits. The present study is, however, a good beginning. Further studies of these series in other geographic areas would be valuable in helping to establish their series-wide variation.

Volumetric Water Content

The average volumetric water content (θ) at each depth and capillary pressure level is given in Table 3, for the Hugo, Mendocino, and Caspar soil series. Individual soil pit results are given in Appendix B.

A graphic representation of the change in water content with increasing capillary pressure is known as a soil moisture characteristic or moisture release curve. Figure 6 contains moisture release curves for the combined pits of each of the three series. The reclining J-shape of the curves is typical, but the exact shape of any particular curve is a function of the soil's structure and texture. This report uses θ, rather than the gravimetric water content (w), because of the convenience with which it can be applied to hydrologic problems regarding fluxes and the addition or subtraction of water to or from the soil.

Table 3 shows that all three series show some change in θ, with increasing depth. The Hugo series shows the smallest change in θ, with depth of the three series, while the Mendocino shows the largest. The Caspar series tends to yield slightly higher θ values than the other two series. In addition, the Caspar series can be divided into two groups of sampling depths which exhibit distinctly different responses to capillary pressure (the 0 to 30 and 50 to 150 cm depth intervals). The other two series tend to vary more gradually with depth.

The within-series variation of θ was greatest for the Hugo series. No two pits in this series showed exactly the same responses to capillary pressure, even when pits of similar depth were compared. This variability between pits did not occur within either the Mendocino or the Caspar series, in spite of the fact that the two Mendocino pits were of greatly different depths (50 and 150 cm).

Table 3. Average soil moisture, as a decimal fraction of total soil volume (θ), for increasing capillary pressure.

Depth Interval (cm)	Capillary pressure (cm of water) 0	10	20	30	40	60	No. Cores/ No. pits
Hugo Soil Series (soil pits 1-8)							
0-10	.561	.446	.395	.371	.358	.341	38/8
10-20	.523	.439	.389	.366	.352	.336	34/7
20-30	.515	.458	.424	.402	.388	.369	30/6
30-50	.516	.461	.429	.408	.388	.369	26/5
50-100	.545	.482	.455	.440	.427	.400	16/3
100-150	.549	.486	.455	.442	.430	.407	16/3
Caspar Soil. Series (soil pits 1-2)							
0-10	.597	.441	.408	.389	.372	.340	8/2
10-20	.562	.454	.418	.395	.378	.349	8/2
20-30	.540	.443	.423	.406	.391	.364	8/2
30-50	.550	.505	.487	.471	.457	.432	8/2
50-100	.603	.520	.489	.474	.461	.436	8/2
100-150	.582	.529	.506	.494	.483	.455	8/2
Mendocino Soil Series (soil pits 1-2)							
0-10	.588	.400	.339	.315	.304	.289	13/2
10-20	.500	.455	.417	.395	.379	.364	8/2
20-30	.534	.487	.441	.411	.393	.370	8/2
30-50	.525	.492	.451	.427	.402	.390	8/2
50-100	.546	.528	.498	.480	.458	.451	4/1
100-150	.518	.467	.434	.414	.398	.390	4/1

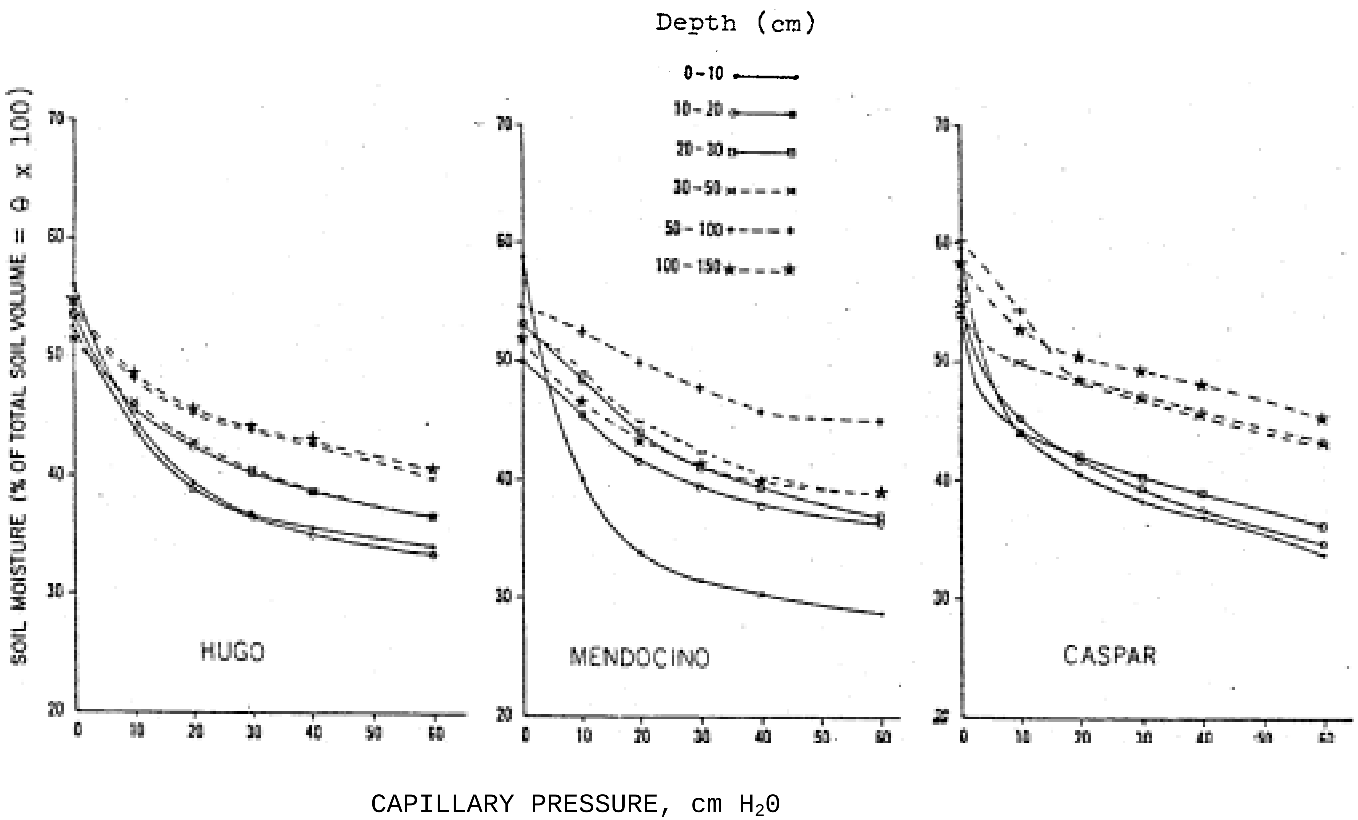

Figure 6. Moisture release curves for the Hugo, Mendocino, and Caspar soil series.

Colluvial movement helps to explain the great variation in soil depth exhibited by the Hugo series. Colluvial movement events are not uniform in time or space. Some areas may receive a minimum of movement and at widely spaced time intervals. Other areas may be constantly moving or accepting colluvial material from upslope. Thus, the soil depth and degree of development can be expected to vary more in this soil than in the other two series. Both the Caspar and Mendocino series occur at or near the break on slope, where the slope is less steep, while the Hugo series occurs only on the steeper portions of the slope. Since colluvial movement occurs as a response to unstable (high angle) slope conditions, the Hugo series can be expected to sustain the greatest amount of movement.

The pits of the Hugo series exhibit the most variation in hydrologic response to capillary pressure, as well as having the greatest variation in depth. More extensive sampling in the Caspar and Mendocino series may have revealed more variation than was found in the limited sampling used (2 pits each).

Pore-size Distribution

Pore-size distribution was obtained from the θ data, for capillary pressures of from 0 to 60 cm of water. Bubbling pressure (P_b) and pore-size distribution index (λ) were obtained from logarithmic plots of the data in Appendix B. Figure 7 is a series of plots of the effecttive saturation (S_e) versus capillary pressure (P_c), for all the depths of Hugo pit No. 2. This figure illustrates how P_b and λ are derived from such plots. The value of P_b is the X-axis intercept at the point where S_e has a value of 1. The value of λ is the absolute value of the slope. Effective saturation (S_e) is that portion of the pore space

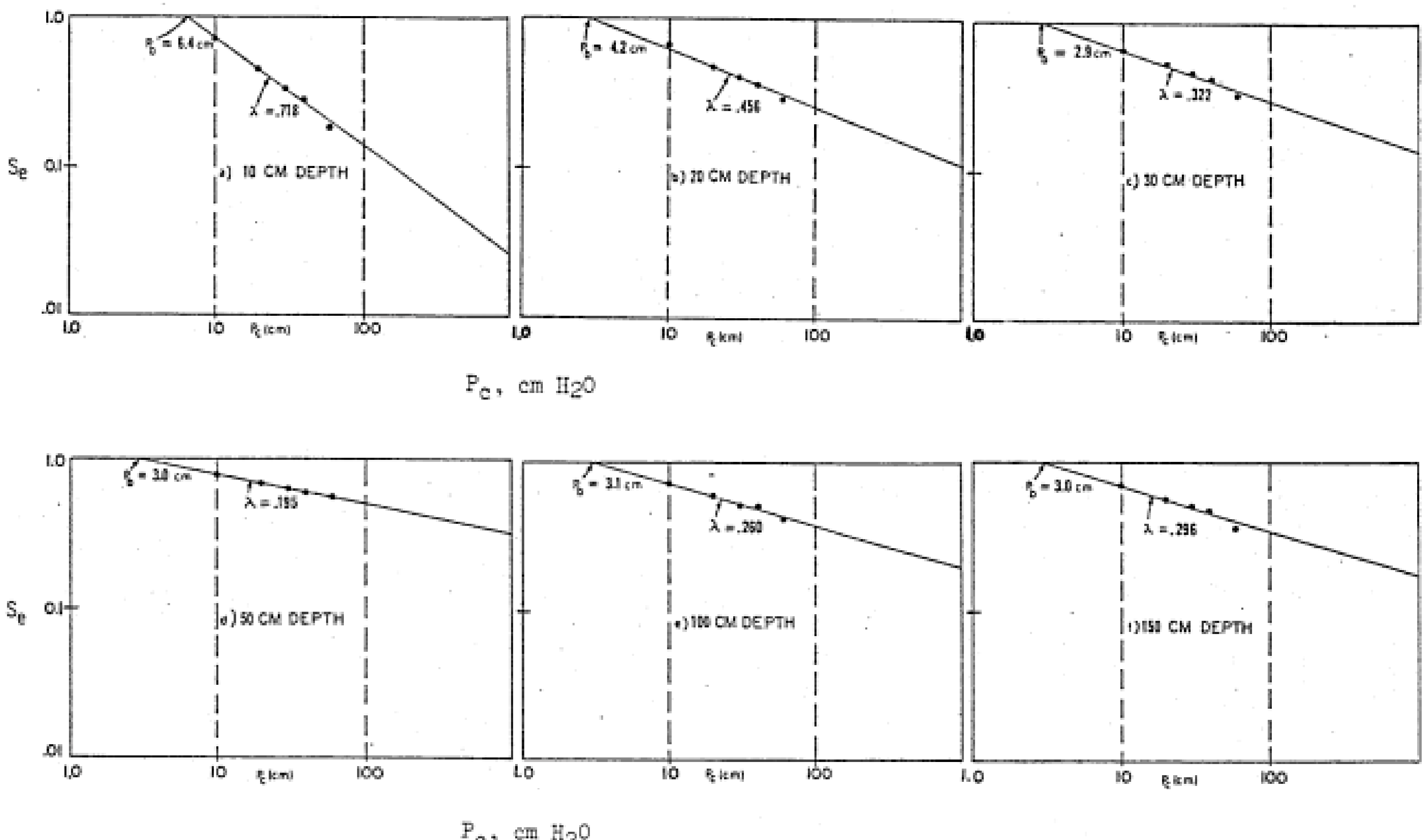

Figure 7. Effective saturation (S_e) versus capillary pressure (P_c) plots for each depth of Hugo pit No. 2, where P_b is the bubbling pressure and λ is a pore-size distribution index.

which is potentially available for active water transport. That portion of the pore volume that is composed of pores so small that practically no flow of water occurs through them is termed the residual saturation (S_r). In addition to being inactive in water transport, these small pores have very small increments of water yield in response to large increments of applied capillary pressure. This causes any plot of total saturation (S_a) versus P_c to be non-linear, especially at the higher tension levels. ("Total" in this case refers to the fact that all soil water is considered, not that the soil is totally saturated.) In order to produce values for P_b and λ, the plot must be reasonably linear. Total saturation is related to the effective saturation and residual saturation by

$$S_e = \frac{S_a - S_r}{1 - S_r},\ for\ Sr < Sa < 1.0 \qquad (14)$$

The value of S_r may be obtained by several methods, but that of Brooks and Corey (1964) is the simplest (Harr and Yee, 1975). This is essentially a process of successive approximations, using the coefficient of determination (R^2) of each successive linear regression of S_e against P_c as an indicator of nearness to the correct S_r value. Highly structured soils quite often yield values of S_r equal to zero. The soils sampled in this work all had S_r values greater than zero. This indicates that all of the soils have a significant amount of micropore space. Table 4 summarizes the mean values of porosity (n), bulk density, bubbling pressure (P_b), pore-size distribution index (λ), and residual saturation (S_r) for all soil pits.

Table 4. Mean Porosity (n), Bulk Density (B.D.), Bubbling Pressure (P_b), Pore-size Distribution Index (λ), and Residual Saturation (S_r) Obtained From Capillary Pressure-Desaturation Data for Three Soils of the Redwood Region (by pit)

Depth Interval (cm)	n (%)	B.D. (gm/cm^3)	P_b (cm)	λ	S_r
HUGO SOIL					
Pit No. 1					
0-10	61.4	1.06	4.1	0.562	0.537
10-20	57.4	1.17	5.0	0.691	0.503
20-30	54.8	1.24	6.6	0.475	0.532
30-50	53.3	1.28	10.9	0.585	0.589
50-100	49.0	1.40	2.5	0.316	0.466
100-150	50.4	1.36	2.5	0.270	0.502
Pit No. 2					
0-10	73.1	0.78	6.4	0.718	0.590
10-20	53.4	1.35	4.2	0.456	0.650
20-30	53.4	1.35	2.9	0.322	0.555
30-50	55.1	1.30	3.0	0.195	0.476
50-100	60.0	1.16	3.1	0.260	0.538
100-150	58.9	1.19	3.0	0.296	0.524
Pit No. 3					
0-10	62.1	1.09	4.4	0.874	0.549
10-20	60.3	1.14	4.0	0.904	0.487
20-30	58.2	1.20	1.0	0.697	0.291
30-50	53.3	1.34	0.6	0.543	0.282
Pit No. 4					
0-10	49.7	1.45	1.7	0.171	0.351
10-20	49.7	1.45	1.6	0.108	0.345
20-30	52.8	1.36	2.2	0.439	0.266
30-50	52.1	1.38	3.0	0.063	0.072
50-100	49.4	1.46	2.8	9.83E-5	---
Pit No. 5					
0-10	55.6	1.29	4.4	0.825	0.556
Pit No. 6					
0-10	67.1	0.87	6.4	1.088	0.648
10-20	48.6	1.36	7.0	0.801	0.720
20-30	47.9	1.38	10.1	1.094	0.839
30-50	51.3	1.29	8.1	0.966	0.801
50-100	52.8	1.25	5.8	0.380	0.692
100-150	49.0	1.35	7.0	0.403	0.782

Table 4. (continued)

Depth Interval (cm)	n (%)	B.D. (gm/cm^3)	P_b (cm)	λ	s_r
HUGO SOIL (continued)					
Pit No. 7					
0-10	63.6	0.98	5.7	1.124	.609
10-20	57.7	1.14	7.3	1.046	.638
20-30	51.0	1.32	8.6	0.867	.741
Pit No. 8					
0-10	62.0	1.02	2.7	0.668	.540
10-20	62.7	1.00	6.8	1.121	.493
20-30	57.1	1.15	5.8	1.230	.540
30-50	57.1	1.15	5.3	1.064	.497
MENDOCINO SOIL					
Pit No. 1					
0-10	58.4	1.12	1.1	0.617	0.499
10-20	49.9	1.35	7.3	0.450	0.663
20-30	53.6	1.25	4.5	0.350	0.615
30-50	55.8	1.19	10.8	0.842	0.795
50-100	57.3	1.15	9.2	0.803	0.784
100-150	55.1	1.21	6.5	0.816	0.709
Pit No. 2					
0-10	66.8	0.91	6.3	1.019	0.344
10-20	59.5	1.11	6.0	0.670	0.616
20-30	62.1	1.04	8.0	0.606	0.519
30-50	60.2	1.09	7.3	0.603	0.568
CASPAR SOIL					
Pit No. 1					
0-10	62.8	1.03	1.7	0.314	0.295
10-20	59.9	1.11	3.1	0.370	0.427
20-30	49.8	1.39	2.0	0.233	0.524
30-50	44.3	1.54	2.5	0.257	0.689
50-100	50.9	1.36	3.7	0.348	0.625
100-150	48.0	1.44	2.3	0.166	0.440
Pit No. 2					
0-10	57.7	1.19	1.0	0.191	0.444
10-20	52.7	1.33	2.1	0.218	0.396
20-30	55.6	1.25	1.6	0.210	0.391
30-50	59.5	1.14	4.8	0.276	0.375
50-100	54.9	1.27	0.1	0.276	0.341
100-150	53.4	1.31	1.9E-2	0.222	0.418

The percentage of pores in each diameter class was computed using the relationship between pore diameter and capillary pressure (Equation 4). Equation 4 was easily solved for the equivalent pore diameter of each positive capillary pressure level shown in Table 3 (10 cm, 20 cm, ..., 60 cm), since T_s and ϕ are essentially constants. These pore diameter values were used to define the pore-size diameter classes in Table 5. The .050 - .073 mm pore-size range values of total porosity in Table 5, for example, represent the difference in θ values between the 40 and 60 cm capillary pressure levels (Table 3) divided by the saturation θ value. Table 5 lists the decimal fraction of pores, by diameter class, for the three soil series. This data represents the mean value for each series and depth (combined pits). Values for each pit are given in Appendix B. Figure 8 compares the pore-size distribution of the three soil series. In this figure, the pore-size classes from 0.050 mm to 0.295 mm have been combined so that only three classes are presented.

Figure 8 shows that the Mendocino series has a lower proportion of pores greater than 0.295 mm in diameter than the other two series, at depths of from 20 to 100 cm. Evidence from inspected roadcuts through the Mendocino soil plus the profile descriptions for its two pits indicates that this series has a much better developed B_t horizon than either of the other two series. The Mendocino's B_t horizon is most strongly developed within the 50 to 120 cm depth range (ref. the soil profile descriptions in Appendix E). This zone tends to be clogged with illuviated fine particles and can be expected to have a lower proportion of larger pore sizes. The data presented in Table 5 and Figure 8 support these observations. The 150 cm depth of the

Mendocino series was below the bottom of the B_t horizon in both pits (only pit No. 1 was sampled to this depth, however) and this is reflected in the increase in the proportion of greater than 0.295 mm pores at that depth, compared to that of the 50 and 100 cm depth. The proportion of pores in the 0.050 to 0.295 mm size range is quite small at all depths for the three series, in comparison with the abundance of pores smaller than 0.050 mm.

Table 5. Mean Values of Pore-size Distribution as Fractions of Total Porosity, by Soil Series.

Depth Interval (cm)	Pore-size Diameter Classes (mm) <.050	.050-.073	.074-.098	.099-.148	.149-.295	>.295
Hugo Soil Series (pits 1-8)						
0-10	.608	.030	.025	.042	.089	.206
10-20	.649	.031	.026	.044	.091	.159
20-30	.721	.037	.028	.042	.065	.107
30-50	.719	.037	.040	.040	.062	.102
50-100	.739	.050	.025	.026	.049	.113
100-150	.747	.042	.021	.023	.057	.110
Caspar Soil Series (pits 1-2)						
0-10	.578	.053	.029	.033	.052	.256
10-20	.625	.053	.031	.040	.061	.191
20-30	.673	.050	.028	.032	.033	.179
30-50	.786	.045	.026	.029	.033	.083
50-100	.724	.041	.021	.025	.053	.137
100-150	.780	.049	.019	.021	.039	.093
Mendocino Soil Series (pits 1-2)						
0-10	.487	.028	.020	.045	.112	.310
10-20	.731	.031	.033	.043	.074	.089
20-30	.696	.044	.033	.054	.085	.089
30-50	.745	.024	.047	.046	.079	.061
50-100*	.826	.013	.040	.033	.055	.033
100-150*	.752	.015	.031	.039	.064	.099

* The 50-100 cm and 100-150 cm depth interval values of the Mendocino soil series are based on only one pit, as soil pit no. 2 was too stoney to permit sampling at depths greater than 50 cm.

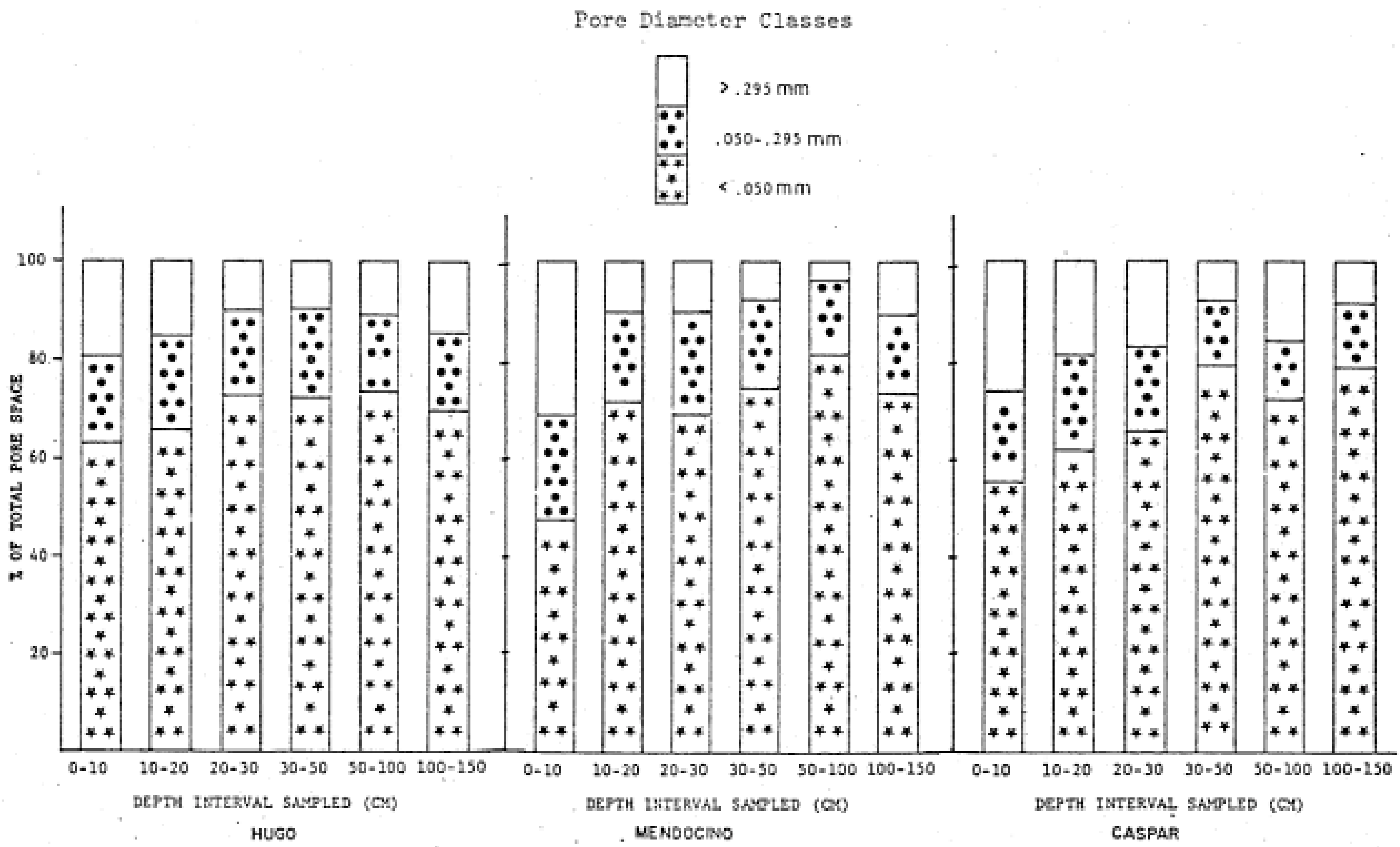

Figure 8. Change in pore-size distribution with depth for the Hugo, Mendocino, and Caspar soil series (from pit means).

Table 6 represents the soil water content, in terms of degree of saturation, for each of the three series, at all six capillary pressure levels and depths. Appendix B contains the saturation values of each individual pit. This data was derived from the tabulated θ values and is merely another way of expressing the same relationship.

Physical Properties of the Soils

The physical properties of each soil series are given in Table 7. This table shows the mean value of all the pits, at each depth, and for each of the parameters. The tabulated parameters include: bulk density, particle-size distribution, total porosity, Soil Conservation Service soil class, vertical hydraulic conductivity (K_s), and percent water-stable aggregates. The values of sand, silt and clay are organized by two systems. The values in parentheses represent the particle-size fraction's percent by weight in the soil, excluding gravel. The particle-size fraction values not in parentheses represent the fraction's overall value including gravel as part of the particle-size distribution. Appendix B contains similar tables for each pit separately. Appendix B also contains a table which gives the specific gravity of the soil particles (G_s) from each pit.

Bulk Density

The bulk densities of all three series tend to increase sharply between the 10 and 20 cm depth (Table 7), then increase gradually or remain fairly constant. In terms of trends, the Hugo and Mendocino series increase greatly in bulk density between the 10 and 20 cm depths then remain relatively constant. The Caspar series' bulk density increases gradually within the first 30 cm of depth, then remains

Table 6. Saturation Values For Soils at 0-60 cm of Water Capillary pressure.

Depth Interval (cm)	Capillary Pressure (cm of Water) 0	10	20	30	40	60	No. of Pits
Hugo Soil Series (pits 1-8)							
0-10	1.00	.795	.704	.661	.638	.608	8
10-20	1.00	.839	.744	.700	.673	.343	7
20-30	1.00	.889	.823	.781	.753	.717	6
30-50	1.00	.893	.831	.791	.752	.715	5
50-100	1.00	.884	.835	.807	.784	.734	4
100-150	1.00	.885	.829	.805	.783	.741	3
Caspar Soil Series (pits 1-2)							
0-10	1.00	.739	.693	.652	.623	.570	2
10-20	1.00	.808	.744	.703	.673	.621	2
20-30	1.00	.820	.783	.752	.724	.674	2
30-50	1.00	.918	.886	.856	.831	.785	2
50-100	1.00	.862	.811	.786	.765	.723	2
100-150	1.00	.909	.869	.849	.830	.782	2
Mendocino Soil Series (pits 1-2)							
0-10	1.00	.680	.576	.536	.517	.492	2
10-20	1.00	.910	.834	.790	.758	.728	2
20-30	1.00	.912	.826	.769	.736	.693	2
30-50	1.00	.937	.859	.813	.766	.743	2
50-100*	1.00	.967	.912	.879	.839	.826	1
100-150*	1.00	.902	.838	.799	.768	.753	1

* The 50-100 cm and 100-150 cm depth intervals of this soil represent the values of only one pit.

Table 7. Mean Values for All Pits of Bulk Density, Particle-Size Classes, Porosity, Soil Conservation Service Soil Class, K_{sat}, and % Water-Stable Aggregates

Depth (cm)	Bulk DensiSy (g/cm^3)	% Gravel (≥5 mm)	% Sand (4.99-.074 mm)	% Silt (.073-.002 mm)	% Clay (< .002 mm)	Total Porosity (%)	S.C.S. Soil Class	Vertical K_S (cm/hr)	Water-stable Aggregates (% by wt.)
			( ) = % without gravel						
Hugo Soil Series - Pits 1-8 (mean values)									
0-10	1.07	22.9	33.2 (43.3)	33.1 (42.8)	10.9 (13.9)	56.1	gl	266.6	35.8
10-20	1.23	17.2	34.0 (41.1)	35.7 (43.1)	13.2 (15.9)	52.3	gl	131.5	34.4
20-30	1.30	14.7* / 31.7	32.1 (37.6)	34.5 (40.5)	18.7 (21.9)	51.5	gl	59.9	36.6
30-50	1.28	21.6 / 44.1	27.2 (34.7)	29.9 (38.1)	21.4 (27.3)	51.6	gcl	45.7	39.6
50-100	1.32	11.5 / 43.9	30.7 (34.7)	35.6 (40.2)	22.3 (26.2)	54.5	gl	11.8	39.2
100-150	1.30	23.8 / 57.1	21.6 (31.1)	35.8 (49.6)	18.8 (19.3)	54.8	gl	12.1	49.9
Hugo Series Average	1.25	18.6 / 36.2	29.8 (36.6)	34.1 (41.9)	17.6 (20.6)	53.5	gl	87.9	39.3

* The numerator represents the mean gravel content of all pits where particle size determinations were done, while the denominator is the mean gravel content of all pits (includes visual estimates). The sand, silt, and clay fractions represent only those pits analyzed by laboratory methods.

Table 7 (continued)

Depth (cm)	Bulk Density (g/cm^3)	% Gravel ($\geq$5 mm)	% Sand (4.99-.074 mm)	% Silt (.073-.002 mm)	% Clay (<.002 mm)	Total Porosity (%)	S.C.S. Soil Class	Vertical K_S (cm/hr)	Water-stable Aggregates (% by wt.)
			( ) = % without gravel						
Mendocino Soil Series - Pits 1 & 2									
0-10	1.02	10.0	39.3 (43.6)	35.6 (39.6)	15.1 (16.8)	58.8	gl	373.8	47.4
10-20	1.23	9.5	35.8 (39.5)	38.4 (42.5)	16.3 (18.0)	50.0	1	117.0	39.7
20-30	1.15	3.5	32.0 (33.2)	41.8 (43.3)	22.7 (23.5)	53.4	1	86.6	39.8
30-50	1.14	4.8	35.2 (37.0)	35.3 (37.1)	24.7 (25.9)	52.5,	cl	50.5	40.6
50-100	1.15	1.2 35.6	23.0 (23.3)	39.9 (40.4)	35.9 (36.3)	54.6	cl	13.4	59.7
100-150	1.21	8.6 39.3	49.8 (54.5)	22.3 (24.4)	19.3 (21.1)	51.8	scl	5.0	35.0
Mendocino Series Average	1.15	6.3 17.2	35.8 (38.2)	35.6 (38.0)	22.3 (23.8)	53.5	1	107.7	43.7

Table 7 (continued)

Depth (cm)	Bulk Density (g/cm^3)	% Gravel ($\geq$5 mm)	% Sand (4.99-.074 mm)	% Silt (.073-.002 mm)	% Clay (<.002 mm)	Total Porosity (%)	S.C.S. Soil Class	Vertical K_S (cm/hr)	Water-stable Aggregates (% by wt.)
			( ) = % without gravel						
Caspar Soil Series -Pits 1 & 2									
0-10	1.11	6.5	42.0 (44.9)	37.7 (40.3)	13.8 (14.8)	59.7	1	362.5	31.6
10-20	1.22	7.1	27.5 (29.6)	44.1 (47.5)	21.3 (22.9)	56.2	1	23.7	50.3
20-30	1.32	19.7	28.5 (35.5)	31.6 (39.4)	20.2 (25.1).	53.4	gl	15.0	46.3
30-50	1.34	14.8	30.7 (36.0)	31.0 (36.4)	23.5 (27.6)	55.0	gcl	3.0	44.5
50-100	1.32	11.7	22.9 (25.9)	37.9 (42.9)	27.6 (31.3)	60.3	gcl	6.8	50.7
100-150	1.38	11.5	31.0 (35.0)	39.0 (44.1)	18.5 (20.9)	58.2	gl	1.7	36.1
Caspar Series Average	1.28	11.9	30.5 (34.6)	36.8 (41.8)	20.8 (23.6)	57.1	gl	68.7	43.2

relatively constant. In terms of actual values, however, the Hugo and Caspar series are very similar. These two series have generally greater bulk density values than the Mendocino series, at most depths.

Saturated Hydraulic Conductivity

Saturated hydraulic conductivity (K_S),is the most variable of all soil parameters. Often the K_S values from repeated measures of the same depth and soil pit are so variable that their standard deviation is greater than their mean. As such; only trends based upon order-of-magnitude relationships in the data can be expected to be of any value in regard to repeatability. All three soil series have very high values of K_S at the 10 cm depth and progressively lower K_S values with increasing depth.

Unsaturated Hydraulic Conductivity

A soil's relative hydraulic conductivity (K_r) is the decimal fraction of its saturated hydraulic conductivity that remains after it has come to equilibrium with a given level of capillary pressure. A soil's unsaturated hydraulic conductivity, $K(P_c)$, is its actual conductivity at a capillary pressure of P_c. Appendix B contains a table of the K_r values of each depth in each pit, at tensions from 10 to 60 cm. A separate table furnishes mean K_r values for each soil series. All values for K_r were obtained by application of equations 8 and 9 to the values of P_b and λ given in Table 4. Mean estimated values of $K(P_c)$ for each of the three soil series are presented in Table 8, in this section.

The hydraulic conductivity of a soil will decrease sharply when the saturation value falls below 100%. This phenomenon occurs because only those pores continuing to contain water can contribute to the flow.

Table 8. Mean Estimated Values of Unsaturated Hydraulic Conductivity ($K(P_c)$) for the Hugo, Mendocino, and Caspar Soil Series, Within the 10 cm to 60 cm Capillary Pressure Range.

Depth (cm)	Mean K_s Value (cm/hr)	$K(P_c)$ (cm/hr) at Capillary Pressure of 10 cm	20 cm	30 cm	40 cm	60cm
Hugo Soil Series (Pits 1-8)						
10	266.6	13.1	6.1E-1	1.2E-1	4.0E-2	9.1E-3
20	131.5	12.8	5.8E-1	l.lE-1	3.8E-2	9.3E-3
30	59.9	19.2	7.8E-1	1.3E-1	4.1E-2	9.0E-3
50	45.7	17.4	1.2E-0	3.0E-1	1.2E-1	3.3E-2
100	11.8	9.3E-1	1.4E-1	5.0E-2	2.5E-2	9.4E-3
150	12.9	1.6	1.8E-1	5.0E-2	2.1E-2	5.6E-3
Mendocino Soil Series (Pits 1-2)						
10	373.8	18.3	5.6E-1	6.7E-2	1.6E-2	2.1E-3
20	117.0	29.3	2.6	6.2E-1	2.3E-1	5.7E-2
30	86.6	22.5	1.8	4.2E-1	1.5E-1	3.6E-2
50	50.5	42.9	2.1	3.6E-1	1.1E-1	1.9E-2
100	13.4	9.1	4.3E-1	7.1E-2	2.0E-2	3.4E-3
150	5.0	7.5E-1	3.5E-2	5.5E-3	1.6E-3	2.6E-4
Caspar Soil Series (Pits 1-2)						
10	362.5	1.5	2.1E-1	6.9E-2	3.1E-2	9.8E-3
20	23.6	5.0E-1	6.6E-2	2.0E-2	9.0E-3	2.8E-3
30	15.0	1.6E-1	2.6E-3	8.3E-3	3.9E-3	1.3E-3
50	3.0	2.3E-1	3.3E-2	9.9E-3	4.5E-3	1.4E-3
100	6.8	1.7E-1	2.0E-2	5.8E-3	2.5E-3	7.5E-4
150	1.7	2.2E-2	3.9E-3	1.4E-3	6.8E-4	2.6E-4

By the law of capillarity, large pores will be the first to drain (Harr and Yee, 1975). The large, interconnected pore spaces are responsible for a large majority of a soil's hydraulic conductivity. In a soil with a pore-size distribution that is skewed towards the larger pore diameters (e.g. sandy soils), the soil's hydraulic conductivity drops very quickly when subjected to a small capillary pressure. A soil with the same porosity, but dominated by micropores (e.g. clay soils), will have a higher relative conductivity at that capillary pressure, since more of its pores will not begin to desorb until a much larger capillary pressure is experienced. Soils midway between these two extremes often exhibit high values of both saturated and unsaturated hydraulic conductivity.

To illustrate how this works under natural conditions, consider the A horizon of a typical forest soil. It will be highly aggregated, exhibiting a loose granular structure with a very low bulk density (perhaps 0.9 g/cc). Its pore-size distribution will cover a wide range of diameters. The small pores will be located within the granules. The larger pores, up to perhaps 6 mm in diameter, will be found between the loosely packed granules. As the first rain of the season filters down through the overlying layers of organic material, the soil's hydraulic conductivity will be very low. This is because only the very smallest pores will still retain water from the last rain. Incoming water will flow into the granules, but not through the large pores between them. The wetting front will pass slowly down through the surface soil profile by passing from granule to granule, at the points where they contact. If the delivery rate of the water is low, only the smaller pore sizes will be available for water passage, since only these pores will be able to resist desorption as a result of the tension exerted by the drier, underlying soil. If the delivery rate is higher than the soil's unsaturated hydraulic conductivity at that degree of wetness, then water. will build up at the surface of the soil, filling larger and larger pores. This has the effect of in-creasing the value of the hydraulic conductivity locally. Should a sudden cloud-burst occur, then even the largest pores will fill, becoming available for flow. The soil's hydraulic conductivity will then be equal to K_S. The unsaturated hydraulic conductivity ($K(P_C)$) thus responds dynamically to variations in the rate of water application.

The total hydraulic gradient inducing the flow across the first 10 cm of depth is a vector summation of the gravitational gradient and the pressure gradient. In this case, since both gradients are inducing downward flow, their effects are directly additive. The gravitational gradient remains constant; regardless of the degree of saturation of the soil. Its value in terms of equivalent hydraulic head is unity. (1 cm of head loss per cm of depth). The pressure gradient is a function of the differences in potential head exhibited at the surface and 10 cm depths. If the surface is saturated and the 10 cm depth is at the wilting point (15 bars, or 15318 cm of water), then the pressure head over the entire 10 cm depth range is 15318 cm or a gradient of 1531.8 cm of head loss per centimeter of depth. Obviously, the pressure head gradient will dominate the total driving force in the initial phase. of wetting. As the wetting front advances to deeper depths, the pressure gradient continually decreases towards zero. Eventually only the gravitational gradient remains as the driving force for infiltration. The just-described phenomenon explains why water infiltration rates decrease toward a constant value as the application of water continues.

A comparison of the expected unsaturated hydraulic conductivities $K(P_C)$, Table 8, for the three soils and expected rainfall events common to the coastal area of the California north coast indicates that unsaturated soil moisture movement dominates in the winter.

Elford and McDonough (1974) indicate that the Mendocino and Humboldt County coastlines receive approximately 100 cm of precipitation per year. A 2 yr-24 hr winter storm will provide intensities of about 0.37 cm hr^{-1}, while a 100 yr-24 hr winter storm will provide an intensity of about 0.74 cm hr^{-1}. If the average value of these two intensities, about 0.5 cm hr^{-1}, is used as the maximum yearly intensity for a typical. winter storm, a comparison of the hydraulic behavior of these three soils can be made.

The Hugo soil will be able to conduct 0.5 cm hr^{-1} through the top 30 cm of soil at a P_C of about 20 cm of water (Table 8). However, below the 50 cm depth, the Hugo soil must attain a greater degree of saturation to accommodate the 0.5 cm hr^{-1} rate. The 50 and 100 cm depths must have a P_C of between 10 cm and 20 cm, while the 150 cm depth must have a P_C of less than 10 cm.

The assumed average rainfall rate can also be easily infiltrated by the Mendocino series, but at different capillary pressure levels. The 10 through 100 cm depth range would equilibriate at about 20 cm of water. The 150 cm depth would be at about 10 cm of water.

While the Hugo and Mendocino series can handle the assumed rainfall value at relatively large capillary pressures (low degrees of saturation), the Caspar series must be much closer to saturation to do so. The 10 cm depth can pass the water at about the same capillary pressure as can the 10 cm depth of the other two series, but the rest of the profile must be at a P_c value at least as low as 10 cm. The 150 cm depth would be close to saturation. Although the Caspar series can be expected to come much closer to saturation during the average storm than the other two series, it still has an ample reserve of carrying capacity before attaining saturation. It should be born in mind that the data for the Mendocino and Caspar series is based upon a very limited sampling. However, the above conclusions appear to be realistic estimates of these soils' responses to typical winter storms, and are consistent with field observations of permeability in these soils.

Zones of positive pore-water pressure can be expected to be the loci of mass movement events (Harr and Yee, 1975). While these three soil series are not likely to attain widespread positive pore-pressures over large areas, because the storms that they must endure cannot be expected to bring the, entire soil profiles to the saturation point, mass movements do occur at localized spots. Many springs and seeps can be found on the Caspar watershed. These areas may become unstable during a normal storm, because they are subjected to positive pore-water pressures due to concentrating subsurface flow patterns.

For the average soil on the Caspar watershed, positive pore-water pressures (a zone of saturated flow) could develop within the first 150 cm of depth if a long-duration, slow, soaking rain was closely followed by a more intense downpour. Some areas, such as at the bottom of declivities, would then be expected to receive a large amount of subsurface flow from upslope. These areas of concentrated subsurface flow would be subjected to higher pore-water pressures than the soils on the surrounding slopes and occasional mass movements would be expected.

In general, the soils of the Caspar Creek watershed appear well suited to withstand the type of storm that usually occurs in the watershed, without developing saturated subsurface flow except in localized areas. It also appears that the B_t horizons, developed to varying degrees in each soil, do not impose a significant barrier to the downward percolation of rainwater. Even the least permeable series-depth combination sampled (the 150 cm depth of the Caspar series) can transmit water at a rate of 1.7 cm hr^{-1}, which is well above the expected maximum rainfall rate.

Particle-size Distribution

One of the most striking features of the soils of the Caspar Creek watershed is their great spatial variation in gravel content. Gravel and other large particles make up the most hydrologically inactive fraction of a soil's particle-size distribution. The sand, silt, and clay fractions are all incorporated into aggregates, which in turn dictate the soil's pore-size distribution. The gravel, cobble, and boulder fractions (hereafter referred to as gravel) take up space and add considerable weight. They do not, however, have any great effect upon the pore-size distribution unless the "soil" resembles a talus slope.

The mean particle-size fraction values for the three soil series are given in Table 7. The value given to each of the finer size-fractions (sand, silt, and clay) is presented in two ways. The values not in parentheses represent each fraction's overall relative abundance in the soil. The values given in parentheses are the relative abundances of the finer fractions only.

The gravel-contents are also presented in two ways. In those cases where the soil was too sparse to sample, relative to the gravel, a visual estimate of the total gravel ($\geq$5 mm) content was made. The values of gravel content in Table 7 are sometimes presented as a fraction. The numerator is the mean percent by weight of gravel found in the pits of a soil series which had a sparse enough gravel content to permit a bulk sample. The denominator is the mean gravel content of all pits in a series, including those that were estimated by visual means.

A single particle-size analysis was done for each sampled depth interval in each pit. Appendix C contains three sets of particle-size distribution curves for these soils. Graph set No. I contains particle-size distribution curves for each series. These curves average the data from all pits and sampled depths within a series and do not include any visual estimate data for gravel size. Graph set No. II contains the curves for each soil pit. Each curve represents the mean of all sampled depths for a pit and contains no visually estimated gravel content data. Graph set No. III presents the mean particle-size distribution of each depth in a series. The curves in this set are drawn without reference to any visual estimates of gravel content, but these estimates are plotted for comparison. Each plot point in the three sets is drawn through the mean percent-finer value of the size fraction it represents. The range about each particle-size fraction mean is indicated by solid vertical lines ending in short, horizontal lines. These horizontal lines indicate the percent-finer values of the samples which deviated the most from the mean value. The number of particle-size determinations used in the preparation of each graph his given in its figure title.

The gravel content seems to follow no particular pattern with depth in these soils, unless the visual estimates are taken into account, in which case a gradual increase with depth is noted in the Hugo and Mendocino series. The Mendocino and Caspar series data indicates that these two series are less gravelly than the Hugo, especially when the visual estimates are taken into account.

The Mendocino and Caspar series both develop on the brows of slopes. The difference in their parent material is not as great as the difference between their degrees of soil profile development. The Hugo series is a colluvial soil. The colluvial mixing it is subjected to apparently causes the broken, underlying clasts of its parent material to be incorporated into the soil profile. The lack of colluvial overturning and burial in the Mendocino and Caspar series perhaps causes them to have a lower gravel content.

Gravel within a soil can be expected to be attacked by chemical weathering to a greater degree than the parent material beneath the soil profile, since the soil's ability to retain water is greater than that of broken rock. This almost continuous attack on the incorporated gravel tends to cause it to break down into soil. This, of course, is the normal way in which soil forms in the first place, but since the gravel is not readily replaced in a non-colluvial soil, it will tend to disappear.

The overall average sand, silt and clay content (given at the bottom of each page of Table 7) is generally similar for each of the three series. The Caspar series tends to have a sharp drop in sand content from the 10 to 20 cm depth. This validates the existence of an albic A horizon in this series. The silt and clay fractions of this series fail to support the existence of the visually obvious B_t horizon (which exists in the 16 to 150 cm depth range of Caspar pit No. 1 and the 37 to 150 cm depth range of pit No. 2). The Mendocino series data shows an abrupt increase in silt and clay between the 50 and 100 cm depths, which seems to support the existence of its well-developed B_t horizon (at 42 to 120 cm of depth in Mendocino pit No. 1 and between 51 and 120 cm of depth in pit No. 2). These variations may, however, be an artifact of the small number of bulk samples which represent these two series. The Hugo series data shows no consistent pattern except that the clay content rises gradually until the 100 cm depth, then begins to fall with increasing depth.

Water-stable Aggregates

The aggregate stability of the three series. show neither an appreciable difference between series, nor a trend with depth (Table 7). This parameter does not seem to vary much across the watershed. Harr and Yee (1975) noted no change in aggregate stability with depth, in their study of two soils of the Oregon Coast Range. Their values of aggregate stability under direct wetting are considerably higher than mine, but their methods were much less energetic in attempting to destroy soil aggregates.

The mean percent of water-stable aggregates for the three series is 43%. Under field conditions, the aggregates will normally be subjected to slow wetting in the tension mode (rather than direct wetting), since the normal rainfall delivery rate in the redwood region is well below the K_S value of the least permeable soil horizon studied. Therefore the actual field aggregate stability under these conditions would probably be considerably higher than 43%.

Subsidiary Comparisons Based Upon the Hugo Series Data

The Hugo soil is the only series of the three which exists in both the north and the south fork watersheds, underlies both logged and unlogged terrain, and occurs on a variety of slope positions. This series is also the most variable in terms of soil properties. The lower variability of the Mendocino and Caspar series may be a function of the sampling pattern, since only two pits were dug in each of these series, and the fact that their limited geographic distribution within the watershed precluded much of a separation between pits. At any rate, the seven Hugo pits do show quite a bit of variation. The following section is devoted to an attempt to delineate the causes of some of this series' great variability.

Comparison of the North and South Fork Watersheds

Most of the south fork drainage of Caspar Creek was logged for the second time between 1970 and 1974. Original old-growth logging took place in the 1890-1900 period. The natural differences in the hydrologic response of the soils of the north and south fork watersheds cannot be separated from whatever effects may have been caused by logging. The following discussion focuses on the differences exhibited by the two watersheds without any attempt to indicate causal factors.

Hugo pits 1, 2, 3, and 4 lie in the south fork watershed, while pits 6, 7, and 8 are in the north fork. (Hugo pit 5 is excluded from discussion, since it had only 13 cm of soil above bedrock). Their relative positions are shown on the location map (Figure 3) and Table 1 gives individual pit information such as elevation, distance from the nearest ridge and creek, slope position, aspect, depth of sampling, and slope steepness.

Table 9 lists the mean values of θ for the two watersheds at depths from 10 to 150 cm and P_C values from 0 to 60 cm of water. No consistent differences are evidenced between the paired values of the two watersheds.

Table 10 lists the mean K_S values of the two watersheds, for all sampling depths. From this data the south fork soils appear to be generally less permeable than those of the north fork, except at the 150 cm depth. The high variance of the data represented by the mean K_S values of Table 10 makes it difficult to draw any realistic conclusions.

The bulk density data for the two watersheds is given in Table 11. While no consistent trend is evident with depth, the north fork soil has the lowest bulk density at five of the six sampling depths. The difference, however, is small in each case and may be due to sampling error.

The mean particle-size distributions of the soils from the two watersheds are fairly similar (Table 12).

Variation of the Hugo Soil With Slope Position

As in the previous analysis, the Hugo pits were divided up into two groups, this time with respect to slope position. The higher slope position pits were numbers 1, 2, 6, and 7, while the lower pits were numbers 3, 4, and 8. The between-watersheds variation did not affect this analysis, since roughly the same number of pits were used from each (Figure 3). No pits had been dug close to the midslope position, so the division was easily made (Table 1).

The first overall difference that was noted was that the lower pits were generally not as deep as the upper ones. Rankin (1974)

Table 9. Mean θ Values (volumetric water content) for the North and South Fork Watersheds

Watershed Depth		θ at Capillary Pressures of 0 cm	10 cm	20 cm	30 cm	40 cm	60 cm
North-10	cm	.611	.478	.434	.405	.393	.383
South-10	cm	.550	.442	.388	.364	.349	.326
North-20	cm	.543	.474	.408	.379	.365	.353
South-20	cm	.509	.412	.375	.356	.343	.324
North-30	cm	.514	.457	.418	.394	.381	.374
South-30	cm	.516	.458	.430	.411	.395	.365
North-50	cm	.527	.445	.400	.378	.365	.357
South-50	cm	.508	.472	.448	.429	.404	.378
North-100	cm	.519	.495	.470	.463	.435	.440
South-100	cm	.553	.477	.449	.432	.418	.398
North-150	cm	.485	.472	.445	.441	.431	.419
South-150	cm	.581	.494	.460	.442	.430	.401

Table 10. Mean Values of Saturated Hydraulic Conductivity (K_S) for the North and South Fork Watersheds

Watershed	K_S (cm/hr) at a Depth of 10 cm	20 cm	30 cm	50 cm	100 cm	150 cm
North Fork	339.0	198.6	104.4	95.4	15.3	3.9
South Fork	221.9	81.3	15.3	12.6	10.6	16.2

Table 11. Mean Bulk Density Values (g cc^{-1}) for the North and South Fork Watersheds

Watershed	Bulk Density at a Depth of					
	10 cm	20 cm	30 cm	50 cm	100 cm	150 cm
North Fork	0.96	1.17	1.28	1.22	1.25	1.35
South Fork	1.10	1.28	1.32	1.32	1.34	1.28

Table 12. Mean Values of Particle-size Fractions for the North and South Fork Watersheds (mean of all pits and depths)

Watershed	Percent by Weight of			
	Gravel	Sand	Silt	Clay
North Fork	19.6	30.6	32.5	17.3
		(38.1)[1]	(40.4)	(21.5)
South Fork	18.5	32.2	34.7	14.6
		(39.5)	(42.6)	(17.9)

[1] The values in parentheses represent the percent of sand, silt, and clay, without gravel.

found that the soil he studied in the H. J. Andrews Experimental Forest (Oregon) became deeper as one progressed upslope. His work was done on a gravelly, steeply sloping colluvial soil. His depth trend data is thus comparable to the Hugo series, and agrees with it in this regard. The deepest pit (No. 4) in the lower group was 100 cm deep, while the other two were only 50 cm to bedrock. Three of the four higher slope position pits were 150 cm deep, while the fourth (Hugo pit No. 7) could be sampled only to a,30 cm depth, due to its high gravel content. However, the B horizon of this pit extends down to the 76 cm depth (Appendix E).

The between-slope-positions differences with regard to θ were considerable (Table 13). Nearly every depth and P_C level of the higher slope-position pits exhibited greater values of θ than did those lower on the slope. This relationship is not consistent at the 0 cm P_C level, but is otherwise consistent. The soil at the higher slope position thus appears to have a pore-size distribution which is skewed toward the finer pore sizes, compared to that of the lower pits.

A comparison of the Hugo soil θ values of the two slope positions in Tabel 13 with those of the Caspar and Mendocino series. (Table 3) reveals an interesting relationship. But for a few exceptions in the data, at the 10 cm depth and at the 0 cm P_c level, the low slope position θ values are all lower than those of the Mendocino and Caspar series. In most cases, the difference is considerable. However, the high slope position θ values are above those of the Mendocino and Caspar series about as often as they are below them. For the most part, the Hugo series is a soil of steep slopes. However, this data indicates that in its upper slope positions, it seems to take on the moisture-retention characteristics of the Mendocino and Caspar series. This

Table 13. Mean θ Values (volumetric water content) for the Hugo Soil by Slope Position

Slope Pos./ Depth	θ at a Capillary Pressure of					
	0 cm	10 cm	20 cm	30 cm	40 cm	60 cm
High 10 cm	0.606	0.496	0.434	0.402	0.388	0.371
Low 10 cm	0.536	0.407	0.372	0.355	0.345	0.324
High 20 cm	0.518	0.449	0.407	0.381	0.361	0.354
Low 20 cm	0.530	0.425	0.365	0.346	0.331	0.313
High 30 cm	0.508	0.467	0.434	0.411	0.397	0.382
Low 30 cm	0.529	0.439	0.404	0.385	0.370	0.344
High 50 cm	0.515	0.483	0.453	0.432	0.409	0.392
Low 50 cm	0.516	0.428	0.392	0.373	0.359	0.335
High 100 cm	0.572	0.502	0.469	0.454	0.442	0.417
Low 100 cm	0.461	0.422	0.410	0.383	0.383	0.348
High 150 cm	0.549	0.486	0.455	0.442	0.430	0.407
Low 150 cm	-----	-----	-----	-----	-----	-----

Table 14. Mean Saturated Hydraulic Conductivity (K_S) Values for the Hugo Soil by Slope Position

Slope Position	K_s (cm/hr) at a Depth of					
	10 cm	20 cm	30 cm	50 cm	100 cm	150 cm
High	310.8	95.1	25.8	11.1	7.6	12.1
Low	220.5	180.1	128.0	97.6	24.3	----

indicates a possible connection between slope position and moisture-retention characteristics, regardless of inherent differences between series.

No consistent trend is evident in the K_s or bulk density data from the two slope positions (Tables 14 and 15).

The particle-size distribution shows a decrease in gravel content from the low to the high slope position, in the Hugo soil (Table 16). In comparing the three soil series, it was found that the two high slope position series (Caspar and Mendocino) tended to contain less gravel than the Hugo series. Earlier in this section, it was hypothesized that there are two main reasons that this relationship exists. First, the lower amount of colluvial activity in the upper slope position brings less broken parent material up into the soil profile. Second, the gravel that once did exist in the profile has been subjected to chemical weathering for a long time, so that it has tended to change to soil. Since this disintegrating gravel is not replaced, the Mendocino and Caspar soils end up with a low gravel content regardless of what they contained previously. This hypothesis seems to be supported by the gravel content variations that the Hugo series shows, with slope position. In fact, the existence of this relationship within the Hugo series offers even greater support for the hypothesis than does the between-series variation, since it cannot be caused by some factor other than slope position (such as a difference in parent material between the soil series). There could, however, be differences between the weathering characteristics of parent material within Hugo series that are also related to slope position. With regard to the parenthesized values in Table 16 (which ignore changes in gravel content) the sand content increases at the expense of silt, from the high to the low slope position, while the clay content remains steady. Perhaps less silt is lost by illuviation from the high slope position soils.

Table 15. Mean Bulk Density Values for the Hugo Soil, by Slope Position

Slope Position	Bulk Density (g cc^{-1})					
	10 cm	20 cm	30 cm	50 cm	100 cm	150 cm
High	0.92	1.26	1.32	.129	1.27	1.30
Low	1.19	1.20	1.26	1.27	1.46	-----

Table 16. Mean Particle-size Distribution Values for the Hugo Soil Series, by Slope Position

Slope Position	Percent by Weight of			
	Gravel*	Sand	Silt	Clay
High	13.9	30.4 (35.3)**	38.1 (44.2)	17.7 (20.5)
Low	25.8	33.0 (44.5)	28.1 (37.9)	13.1 (17.7)

*The gravel values do not include visual estimates.

**The values in parenthesis represent the sand, silt, and clay fraction values excluding gravel.

In summary, the higher up the slope, the less colluvial action can be expected, since the upper slopes are generally convex upward. Thus, the soil at the upper slope position has less of a downslope vector component of gravity. to resist, as well as less material upslope from it which could cover it up. In other words, there is a colluviation gradient from the higher to the lower slope position. The two series in the Caspar Creek watershed which are subjected to little or no colluvial mixing (Caspar and Mendocino) tend to have higher values of θ at most capillary pressures and depths, and lower gravel contents than the Hugo series. This relationship exists wherever a comparison is made (either between or within series) along a slope gradient. It is proposed that the principal cause of this variation is the decreasing amount of colluvial mixing which occurs as one proceeds upslope. This factor appears to cause many of the differences between the three soil series and much of the variation within the Hugo series. The variation of some parameters, such as K_s, do not seem to be related to slope position. However, much of the variation of θ, pore-size distribution, and gravel content within the Caspar Creek watershed seems to be explained by this model. The Hugo series also exhibits a variation in hydrologic properties between the two watersheds, though to a lesser degree than along the colluviation gradient. This series may need to be studied further, to determine whether the range of variation it exhibits within the Caspar watershed is representative of its variation within the redwood region. In the study area the Caspar and Mendocino series only occur in a single watershed each, so comparison between watersheds is not possible. The indication that the pits of these two series show so much less variation than do the Hugo series' pits rests upon a rather sparse sample. However, the profile descriptions of all three series (Appendix E) closely match the Soil Conservation Service's descriptions of each soil's published typical profile. A more detailed study of these three soils in other parts of the redwood region would be very valuable.

CONCLUSIONS

The major conclusions with regard to the hydrologic properties of the Hugo, Mendocino, and Caspar soil series are as follows:

1. The three soils vary in the way their drainage characteristics change with depth. Generally speaking, the Hugo and Caspar series tend to hold a progressively increasing amount of water, against a given capillary pressure, from the surface to the 150 cm depth. The Mendocino series follows a similar pattern down to the 100 cm depth, but then the θ values begin to decrease with depth (however, the 100 and 150 cm depth of this series are represented by only a single pit). This change in moisture characteristics reflects the fact that the B_t horizon has been passed, with a corresponding increase in the proportion of macropores. The moisture characteristic curves of these soils show their greatest initial steepness at the 10 cm depth and this initial slope decreases at each successive depth. This points toward a generally decreasing proportion of macropores with increasing depth, except as noted above for the 100 to 150 cm depth range of the Mendocino soil.

2. The mean porosity of all three soil series is quite high, and the series differ only slightly in this regard. This, plus a generally wide pore-size distribution attest to good structural development throughout the three soil profiles., Of the three soil series, the Caspar series shows the least structural development. The porosity of all three series remains fairly constant with depth.

3. No difference in saturated hydraulic conductivity could be detected between the series. Their values of K_S are quite high,

exhibiting a pronounced drop in value in the first 20 cm of depth, and a slowly decreasing trend thereafter. The unsaturated values of hydraulic conductivity, $K(P_c)$, are high enough within the 5 to 30 cm capillary pressure range to make the development of a zone of saturated flow an unnecessary mechanism for the dispersal of the normally long duration, low intensity rainfall events found in this area. This may not apply to soils near the bottom of declivities, since these soils must transmit not only the rain which falls upon them, but also the concentrated subsurface flow from the soils upslope. Neither does this generalization apply to seepage areas, where positive pore-water pressures may exist even in the dry season.

4. The three soils exhibit fairly low bulk densities, with depth specific mean values ranging from a little under 0.9 g cc^{-1} up to just over 1.35 g cc^{-1}. The Caspar and Hugo series have generally higher bulk densities than the Mendocino series. The bulk density values take a sharp increase within the first 20 or 30 cm of depth, then increase only slightly with depth or remain constant.

5. The Hugo soil shows a large spatial variation in the value of most of its hydrologic parameters. Much of this variation, as well as many of the differences between the Hugo series and the Caspar and Mendocino series appear to be attributable to slope position. The lower the slope position, the higher the degree of colluvial turnover. The only hydrologic parameter which failed to change with slope position was hydraulic conductivity.

REFERENCES CITED

Blake, G.R. 1965. Bulk density. In C.A. Black (Ed.), Methods of Soil Analysis, Part 1, Physical and Mineralogical Properties, Number 9 in the series Agronomy. American Society of Agronomy, Madison, Wisconsin. Pp. 374-390.

Brooks, R.H. and A.T. Corey. 1964. Hydraulic properties of porous media and their relationship to drainage design. Transaction, American Society of Agricultural Engineers, 7(1):26-28.

California Division of Mines. 1960. Geologic map of California, Ukiah, California Sheet. Sacramento, CA.

California Forest and Range Experiment Station. September 11, 1950. Legends and supplemental information to accompany vegetation soil maps of California. 45A-2. 20 pp.

Corey, A.T. 1969. Flow In Porous Media. Colorado State University, Fort Collins, Colorado. 259 pp.

Day, P.R. 1965. Particle fractionation and particle-size analysis. In C.A. Black (Ed.), Methods of Soil Analysis, Part 1, Physical and Mineralogical Properties. Number 9 in the series Agronomy. American Society of Agronomy, Madison, Wisconsin. Pp. 545-566.

Elford, R.C. 1970. Climatology of the U.S.: Climate of California. U.S. Department of Commerce. G.P.O., Wash.,D.C. 20 pp.

Elford, R.C. and M.R. McDonough. 1974. The Climate of Humboldt and Del Norte Counties. Humboldt and Del Norte Counties Agricultural Extension Service, Univ. of Calif., Eureka, CA. 34 pp.

Harr, D.T. and C.S. Yee. 1975. Soil and Hydrologic Factors Affecting the Stability of Natural Slopes in the Oregon Coast Range. Water Resources Institute, Oregon State University, Corvallis, Oregon. 204 pp.

Hillel, D. 1971. Soil and Water Physical Principles and Processes. Academic Press, New York, N.Y. 287 pp.

Hubert, M.K. 1956. Darcy's law and the field equations of the flow of underground fluids. Transaction, American Institute of Mining Methods and Petroleum Engineering. 207:222-239.

Jenny, H. 1973. Pygmy forest ecological staircase. Unpubl. report, University of California, Berkeley. 31 numb. leaves.

Klute, A. 1965. Water capacity. In C.A. Black (Ed.), Methods of Soil Analysis, Part 1, Physical and Minerological Properties. Number 9 in the series Agronomy. American Society of Agronomy, Madison, Wisconsin. pp. 273-278.

Krammes, J.S. and D.M. Burns. 1973. Road construction on Caspar Creek watersheds... 10-year report on impact. Pacific Southwest Forest and Range Experiment Station, Berkeley, CA. Research Paper PSW-93. 10 p.

Laliberte, G.E., R.H. Brooks, and A.T. Corey. 1968. Permeability calculated from desaturation data. ASCE, Journal of Irrigation and Drainage. IR 1:55843, pp. 57-71

Lambe, T.W. 1951. Soil Testing for Engineers. John Wiley & Sons, New York, N.Y. 165 pp.

Page, B.M. 1966. Geology of the coast ranges of California. In E.H. Bailey (Ed.), Geology of Northern California. California Division of Mines and Geology Bulletin 190. Pp. 255-275.

Rankin, D.W. 1974. Hydrologic Properties of Soil and Subsoil on a Steep, Forested Slope. M.S. Thesis. Corvallis, Oregon State University, 117 pp.

Rice, R.M., F.B. Tilley, and P.A. Datzman. 1979. A watershed's response to logging and roads: South Fork of Caspar Creek, California, 1967-1976. Pacific Southwest Forest and Range Experiment Station, Berkeley, CA. Research. Paper PSW-146. 12 pp.

Sowers, G.B. and G.F. Sowers. 1951. Introductory Soil Mechanics and Foundations. MacMillan, New York, N.Y. 248 pp.

Terrell, E.E. 1977. A checklist of names for 3,000 vascular plants of economic importance. (Agricultural Handbook No. 505). Agricultural Research Service, U.S.D.A. Washington, D.C. 201 pp.

U.S. Soil Conservation Service. 1967. Supplement to soil classification system (7th approximation). U.S. Dept. of Agriculture. G.P.O., Wash., D.C. 207 pp.

U.S. Soil Conservation Service, U.S. Forest Service, and U.C. Agricultural Experiment Station. 1972. Soil Survey of Sonoma County. G.P.O., Wash., D.C. 187 pp.

Vomocil, J.A. 1965. Porosity. In C.A. Black (Ed.), Methods of Soil Analysis, Part 1. Physical and Mineralogical Properties. Number 9 in the series Agronomy. American Society of Agronomy, Madison, Wisconsin. Pp. 299-314.

Wu, T.H. 1970. Soil Mechanics. Allyn and Bacon, Boston, Mass. 431 pp.

Youngberg, C.T. 1957. A modification of the hydrometer method of mechanical analysis for certain western forest soils. Proceedings Soil Science Society of America, 21:655-656.

APPENDIX A

COMMON AND SCIENTIFIC NAMES OF SPECIES FOUND IN THE STUDY WATERSHED (CALIFORNIA FOREST AND RANGE EXPERIMENT STATION, 1950, and Terrell, 1977)

Common Name	Scientific Name
	OVERSTORY TREES
grand fir	Abies grandis, (Dougl.) Lindl.
red alder	Alnus rubra, Bong.
Douglas-fir	Pseudotsuga menziesii, (Mirbal) Franco
redwood	Sequoia sempervirens,(D. Don) Endl.
western hemlock	Tsuga heterophylla, (Raf.) Sarg.
	SHRUBS AND SMALLER TREES
Pacific madrone	Arbutus menziesii, Pursh.
hairy manzanita	Arctostaphylos columbiana, Piper
eastern manzanita	Arctostaphylos glandulosa, Estw.
glossyleaf manzanita	Arctostaphylos numularia, Gray
golden chinquapin	Castanopsis chrysophylla, (Doubl.) A. DC.
blue blossom	Ceanothus thyrsiflorus, Eseh.
Mendocino cypress	Cupressus pygmaea, (Lemmon) Sarg.
scotch broom	Cytisus scoparius, (L.) Link
salal	Gualtheria shallon, Pursh.
tanoak	Lithocarpus densiflora, (H. & A.) Rehd.
Pacific wax-myrtle	Myrica californica, Cham. & Schlect.
coast rhododendron	Rhododendron macrophyllum, D. Don.
thimbleberry	Rubus Parviflorus, Nutt.
Pacific poison oak	Toxicondendron diversilobum, (T. &G.) Greene
California huckleberry	Vaccinium ovatum, Pursh.
	HERBACEOUS SPECIES
Oregon oxalis	Oxalis oregana, Nutt.
grasses	Poeceae family
sword-fern	Polystichum munitum, (Kaulf.) Presl.
bracken fern	Pteridium aquilinum pubescens, Underw.
western trillium	Trillium ovatum, Pursh.

APPENDIX B

Table 1. Soil moisture values for each pit, as decimal fractions of total soil volume (θ), for increasing capillary pressures.

Depth Interval	Capillary pressure (cm of water)						Number of cores used per depth
(cm)	0	10	20	30	40	60	
Hugo Soil Series (soil pit 1)							
0-10	.615	.505	.447	.421	.412	.387	10
10-20	.550	.441	.384	.354	.338	.318	10
20-30	.499	.452	.409	.380	.360	.337	10
30-50	.467	.461	.423	.397	.351	.337	10
50-100	.565	.455	.420	.400	.385	.358	4
100-150	.566	.476	.444	.427	.415	.386	4
Hugo Soil Series (soil pit 2)							
0-10	.572	.473	.378	.340	.321	.294	4
10-20	.483	.425	.392	.377	.370	.353	4
20-30	.550	.467	.435	.419	.407	.383	4
30-50	.569	.504	.477	.461	.447	.416	4
50-100	.634	.555	.518	.500	.487	.455	4
100-150	.596	.511	.476	.457	.444	.415	4
Hugo Soil Series (soil pit 3)							
0-10	.545	.411	.360	.342	.327	.317	4
10-20	.537	.378	.329	.309	.293	.283	4
Hugo Soil Series (soil pit 4)							
0-10	.467	.382	.368	.351	.334	.307	4
10-20	.464	.405	.395	.383	.369	.342	4
20-30	.500	.455	.446	.434	.419	.374	4
30-50	.488	.451	.443	.429	.415	.380	4
50-100	.461	.422	.410	.398	.383	.348	4
Hugo Soil Series (soil pit 5)							
0-10	.457	.359	.307	.298	.286	.275	4
Hugo Soil Series (soil pit 6)							
0-10	.634	.535	.487	.451	.437	.428	4
10-20	.486	.445	.417	.393	.380	.371	4
20-30	.483	.475	.449	.430	.420	.415	4
30-50	.510	.485	.459	.439	.429	.423	4
50-100	.519	.495	.470	.463	.453	.440	4
100-150	.485	.472	.445	.441	.431	.419	4

Table 1. Theta (θ) values (continued)

Depth Interval (cm)	0	Capillary pressure (cm of water) 10	20	30	40	60	Number of cores used per depth
Hugo Soil Series (soil pit 7)							
0-10	.603	.470	.425	.394	.381	.373	4
10-20	.553	.484	.436	.399	.383	.373	4
20-30	.500	.475	.444	.415	.401	.393	4
Hugo Soil Series (soil pit 8)							
0-10	.595	.429	.391	.372	.362	.348	4
10-20	.590	.493	.372	.346	.331	.314	4
20-30	.558	.423	.361	.336	.321	.314	4
30-50	.544	.404	.341	.316	.300	.290	4
Caspar Soil Series (soil pit 1)							
0-10	.655	.456	.402	.380	.362	.322	4
10-20	.628	.501	.446	.421	.406	.373	4
20-30	.551	.468	.443	.429	.418	.392	4
30-50	.542	.492	.473	.463	.456	.439	4
50-100	.577	.513	.481	.466	.454	.433	4
100-150	.566	.495	.471	.456	.443	.410	4
Caspar Soil Series (soil pit 2)							
0-10	.538	.426	.414	.397	.381	.357	4
10-20	.495	.406	.389	.369	.350	.324	4
20-30	.528	.418	.402	.382	.363	.335	4
30-50	.558	.517	.500	.479	.458	.425	4
50-100	.629	.527	.496	.481	.468	.439	4
100-150	.598	.562	.541	.532	.523	.500	4
Mendocino Soil Series (soil pit 1)							
0-10	.662	.406	.376	.361	.359	.346	9
10-20	.456	.429	.401	.386	.365	.352	4
20-30	.499	.449	.420	.405	.393	.373	4
30-50	.509	.495	.462	.447	.422	.417	4
50-100	.546	.528	.498	.480	.458	.451	4
100-150	.518	.467	.434	.414	.398	.390	4
Mendocino Soil Series (soil pit 2)							
0-10	.513	.394	.302	.268	.249	.231	4
10-20	.544	.480	.433	.404	.393	.375	4
20-30	.568	.524	.461	.417	.393	.366	4
30-50	.540	.489	.439	.406	.382	.362	4

Table 2. Mean Values of Pore-size Distribution for Each Pit, as Fraction of Total Porosity.

	Diameter Class of Pores (mm)					
Depth Interval (cm)	<.050	.050-.073	.074-.098	.099-.148	.149-.295	>.295
Hugo Soil Series (soil pit 1)						
0-10	.629	.041	.015	.042	.094	.179
10-20	.578	.036	.029	.055	.104	.198
20-30	.675	.046	.040	.058	.086	.094
30-50	.722	.030	.099	.056	.081	.013
50-100	.633	.048	.027	.035	.062	.195
100-150	.682	.051	.021	.030	.057	.159
Hugo Soil Series (soil pit 2)						
0-10	.514	.047	.033	.066	.166	.173
10-20	.731	.035	.015	.031	.068	.120
20-30	.696	.044	.022	.029	.058	.151
30-50	.731	.055	.025	.028	.048	.114
50-100	.718	.050	.021	.028	.058	.125
100-150	.696	.049	.022	.032	.059	.143
Hugo Soil Series (soil pit 3)						
0-10	.581	.018	.028	.033	.094	.246
10-20	.527	.019	.030	.037	.091	.295
Hugo Soil Series (soil pit 4)						
0-10	.657	.058	.036	.036	.030	.182
10-20	.737	.058	.030	.026	.022	.127
20-30	.748	.090	.030	.024	.018	.090
30-50	.779	.072	.029	.029	.016	.076
50-100	.755	.076	.033	.026	.026	.085
Hugo Soil Series (soil pit 5)						
0-10	.702	.024	.026	.020	.114	.214
Hugo Soil Series (soil pit 6)						
0-10	.675	.014	.022	.057	.076	.156
10-20	.763	.019	.027	.049	.058	.084
20-30	.859	.010	.021	.039	.054	.017
30-50	.829	.012	.020	.039	.051	.049
50-100	.848	.025	.019	.014	.048	.046
100-150	.864	.025	.021	.008	.056	.027

Table 2. (cont.) Mean Values of Pore-size Distribution for Each Pit, as Fraction of Total Porosity.

Depth Interval (cm)	Diameter Class of Pores (mm) .050	.050-.073	.074-.098	.099-.148	.149-.295	.295
Hugo Soil Series (soil pit 7)						
0-10	.619	.013	.022	.051	.075	.220
10-20	.675	.018	.029	.067	.087	.125
20-30	.786	.016	.028	.058	.062	.050
Hugo Soil Series (soil pit 8)						
0-10	.585	.024	.017	.032	.064	.279
10-20	.532	.029	.025	.044	.205	.164
20-30	.563	.013	.027	.045	.111	.242
30-50	.533	.018	.029	.046	.116	.257
Caspar Soil Series (soil pit 1)						
0-10	.492	.061	.028	.034	.082	.304
10-20	.594	.053	.024	.040	.088	.202
20-30	.711	.047	.020	.025	.045	.151
30-50	.810	.031	.013	.019	.035	.092
50-100	.750	.036	.021	.026	.056	.111
100-150	.724	.058	.023	.027	.042	.125
Caspar Soil Series (soil pit 2)						
0-10	.664	.045	.030	.032	.022	.208
10-20	.655	.053	.038	.040	.034	.180
20-30	.635	.053	.036	.039	.030	.208
30-50	.762	.059	.038	.038	.030	.073
50-100	.698	.046	.021	.024	.049	.162
100-150	.836	.039	.015	.015	.035	.060
Mendocino Soil Series (soil pit 1)						
0-10	.523	.020	.003	.023	.045	.387
10-20	.772	.029	.046	.033	.061	.059
20-30	.748	.040	.024	.030	.058	.100
30-50	.819	.010	.049	.030	.065	.028
50-100	.826	.013	.040	.033	.055	.033
100-150	.752	.015	.031	.039	.064	.099
Mendocino Soil Series (soil pit 2)						
0-10	.450	.035	.037	.066	.179	.232
10-20	.689	.033	.020	.053	.086	.118
20-30	.644	.048	.042	.078	.111	.078
30-50	.670	.037	.044	.061	.093	.094

Table 3. Saturation Values for Each Pit for Increasing Capillary Pressures

Depth Interval (cm)	Capillary pressure (cm of water) 0	10	20	30	40	60
Hugo Soil Series (soil pit 1)						
0-10	1.00	.821	.727	.685	.670	.629
10-20	1.00	.802	.698	.644	.615	.578
20-30	1.00	.906	.820	.762	.721	.675
30-50	1.00	.987	.906	.850	.752	.722
50-100	1.00	.805	.743	.708	.681	.634
100-150	1.00	.841	.785	.754	.733	.682
Hugo Soil Series (soil pit 2)						
0-10	1.00	.827	.661	.594	.561	.514
10-20	1.00	.880	.812	.781	.766	.731
20-30	1.00	.849	.791	.762	.740	.696
30-50	1.00	.886	.838	.810	.786	.731
50-100	1.00	.875	.817	.789	.768	.718
100-150	1.00	.857	.799	.767	.744	.696
Hugo Soil Series (soil pit 3)						
0-10	1.00	.754	.661	.627	.580	.582
10-20	1.00	.704	.613	.575	.506	.527
Hugo Soil Series (soil pit 4)						
0-10	1.00	.818	.788	.752	.715	.657
10-20	1.00	.873	.851	.825	.795	.737
20-30	1.00	.910	.892	.868	.838	.848
30-50	1.00	.924	.908	.879	.850	.779
50-100	1.00	.915	.889	.863	.831	.755
Hugo Soil Series (soil pit 5)						
0-10	1.00	.786	.672	.652	.626	.602
Hugo Soil Series (soil pit 6)						
0-10	1.00	.844	.768	.711	.689	.675
10-20	1.00	.916	.858	.809	.782	.763
20-30	1.00	.921	.930	.890	.870	.859
30-50	1.00	.950	.899	.860	.841	.829
50-100	1.00	.954	.906	.892	.872	.848
100-150	1.00	.973	.918	.909	.889	.864
Hugo Soil Series (soil pit 7)						
0-10	1.00	.779	.704	.653	.632	.619
10-20	1.00	.875	.788	.722	.693	.675
20-30	1.00	.950	.888	.830	.802	.786

Table 3. (cont.)

Depth Interval (cm)	0	Capillary pressure (cm of water) 10	20	30	40	60
Hugo Soil Series (soil pit 8)						
0-10	1.00	.721	.657	.625	.608	.595
10-20	1.00	.836	.631	.586	.561	.532
20-30	1.00	.758	.647	.602	.575	.562
30-50	1.00	.743	.627	.581	.552	.533
Caspar Soil Series (soil pit 1)						
0-10	1.00	.696	.614	.580	.553	.492
10-20	1.00	.780	.710	.670	.647	.594
20-30	1.00	.849	.804	.779	.759	.711
30-50	1.00	.908	.873	.854	.841	.810
50-100	1.00	.889	.834	.808	.787	.750
100-150	1.00	.877	.832	.806	.783	.724
Caspar Soil Series (soil pit 2)						
0-10	1.00	.792	.770	.738	.708	.664
10-20	1.00	.820	.786	.746	.707	.655
20-30	1.00	.792	.761	.724	.688	.635
30-50	1.00	.927	.896	.858	.821	.762
50-100	1.00	.838	.789	.765	.743	.698
100-150	1.00	.940	.905	.890	.874	.836
Mendocino Soil Series (soil pit 1)						
0-10	1.00	.613	.568	.545	.542	.523
10-20	1.00	.941	.879	.847	.800	.772
20-30	1.00	.900	.842	.812	.788	.748
30-50	1.00	.973	.908	.878	.829	.819
50-100	1.00	.967	.912	.879	.839	.826
100-150	1.00	.902	.838	.799	.768	.753
Mendocino Soil Series (soil pit 2)						
0-10	1.00	.768	.589	.522	.485	.450
10-20	1.00	.882	.796	.743	.722	.689
20-30	1.00	.923	.812	.734	.692	.644
30-50	1.00	.906	.813	.752	.707	.670

APPENDIX B

Table 4 Mean Saturation Values for the Hugo, Mendocino and Caspar Soil Series, for Increasing Capillary Pressures.

Depth Interval (cm)	Capillary pressure (cm of water) 0	10	20	30	40	60	No. of pits
Hugo Soil Series (pits 1-8)							
0-10	1.00	.795	.704	.661	.638	.608	8
20-30	1.00	.839	.744	.700	.673	.643	7
30-40	1.00	.889	.823	.781	.753	.717	6
40-50	1.00	.893	.831	.791	.752	.715	5
50-100	1.00	.884	.835	.807	.784	.734	4
100-150	1.00	.885	.829	.805	.783	.741	3
Caspar Soil Series (pits 1-2)							
0-10	1.00	.739	.693	.652	.623	.570	2
10-20	1.00	.808	.744	.703	.673	.621	2
20-30	1.00	.820	.783	.752	.724	.674	2
30-50	1.00	.918	.886	.856	.831	.785	2
50-100	1.00	.862	.811	.786	.765	.723	2
100-150	1.00	.909	.869	.849	.830	.782	2
Mendocino Soil Series (pits 1-2)							
0-10	1.00	.680	.576	.536	.517	.492	2
10-20	1.00	.910	.834	.790	.758	.728	2
20-30	1.00	.912	.826	.769	.736	.693	2
30-50	1.00	.937	.859	.813	.766	.743	2
50-100	1.00	.967	.912	.879	.839	.826	1
100-150	1.00	.902	.838	.799	.768	.753	1

APPENDIX B.

Table 5. Mean Values of Relative Hydraulic. Conductivity (K_r) For Each Pit Within the Hugo, Mendocino, and Caspar Soil Series, Within the 10 cm to 60 cm Tension Range.

Depth (cm)	K_S (cm/hr)	K_r at applied tensions of 10 cm	20 cm	30 cm	40 cm	60 cm
Hugo Soil Series (Pit No. 1)						
10	315.0	3.7E-2	2.9E-3	6.5E-4	2.3E-4	5.1E-5
20	185.8	5.9E-2	3.5E-3	6.7E-4	2.1E-4	4.0E-5
30	36.9	2.4E-1	2.2E-2	5.6E-3	2.1E-3	5.2E-4
50	19.3	1.4E-0	1.0E-1	2.2E-2	7.6E-3	1.7E-3
100	3.9	1.7E-2	2.2E-3	6.6E-4	2.8E-4	8.5E-5
150	31.9	2.0E-2	2.9E-3	9.3E-4	4.1E-4	1.3E-4
Hugo Soil Series (Pit No. 2)						
10	234.5	1.5E-1	7.3E-3	1.3E-3	3.7E-4	6.5E-5
20	3.0	5.4E-2	5.2E-3	1.3E-3	5.1E-4	1.3E-4
30	4.0	2.5E-2	3.3E-3	9.8E-4	4.2E-4	1.3E-4
50	3.9	4.5E-2	7.4E-3	2.6E-3	1.2E-3	4.3E-4
100	3.6	3.9E-2	5.6E-3	1.8E-3	8.2E-4	2.7E-4
150	0.4	3.1E-2	4.2E-3	1.3E-3	5.6E-4	1.8E-4
Hugo Soil Series (Pit No. 3)						
10	314.4	2.3E-2	9.1E-4	1.4E-4	3.7E-5	5.7E-6
20	127.4	1.3E-2	5.1E-4	7.5E-5	1.9E-5	2.9E-6
Hugo Soil Series (Pit No. 4)						
10	23.5	1.2E-2	2.0E-3	7.4E-4	3.6E-4	1.3E-4
20	8.8	1.4E-2	2.8E-3	1.1E-3	5.6E-4	2.2E-4
30	5.0	6.6E-3	6.6E-4	1.7E-4	6.6E-5	1.7E-5
50	14.5	7.2E-2	1.6E-2	6.5E-3	3.5E-3	1.4E-3
100	24.3	7.8E-2	2.0E-2	8.7E-3	4.9E-3	2.2E-3
Hugo Soil Series (Pit No. 5)						
10	228.6	2.5E-2	1.1E-3	1.9E-4	5.1E-5	8.4E-6
Hugo Soil Series (Pit No. 6)						
10	134.0	9.5E-2	2.5E-3	2.9E-4	6.5E-5	7.7E-6
20	74.1	2.1E-1	9.8E-3	1.7E-3	4.7E-4	7.8E-5
30	31.9	l.lE-0	2.7E-2	3.2E-3	7.0E-4	8.2E-5
50	10.0	3.6E-1	1.2E-2	1.6E-3	4.0E-4	5.5E-5
100	15.3	1.8E-1	2.1E-2	5.7E-3	2.3E-3	6.5E-4
150	3.9	3.2E-1	3.4E-2	9.4E-3	3.7E-3	1.0E-3
Hugo Soil Series (Pit No. 7)						
10	558.9	4.9E-2	1.2E-3	1.3E-4	2.9E-5	3.2E-6
20	117.6	2.0E-1	5.6E-3	7.0E-4	1.6E-4	2.0E-5
30	30.3	5.0E-1	2.1E-2	3.2E-3	8.5E-4	1.3E-4

Table 5. (continued)

Depth (cm)	K_S (cm/hr)	K_r at applied tensions of 10 cm	20 cm	30 cm	40 cm	60 cm
Hugo Soil Series (Pit No. 8)						
10	323.6	5.3E-3	3.3E-4	6.5E-5	2.1E-5	4.1E-6
20	404.0	1.3E-1	3.1E-3	3.5E-4	7.5E-5	8.5E-6
30	251.0	4.5E-2	8.7E-4	8.7E-5	1.7E-5	1.7E-6
50	180.7	3.7E-2	1.0E-3	1.2E-4	2.8E-5	3.4E-6
Mendocino Soil Series (Pit No. 1)						
10	383.1	1.8E-4	1.2E-5	2.6E-6	8.5E-7	1.8E-7
20	100.0	3.6E-1	3.5E-2	9.0E-3	3.4E-3	8.8E-4
30	45.2	8.8E-2	1.1E-2	3.1E-3	1.3E-3	3.7E-4
50	54.6	1.4E-0	6.2E-2	9.8E-3	2.7E-3	4.3E-4
100	13.4	6.8E-1	3.2E-2	5.3E-3	1.5E-3	2.5E-4
150	5.0	1.5E-1	6.9E-3	1.1E-3	3.2E-4	5.2E-5
Mendocino Soil Series (Pit No. 2)						
10	364.4	9.7E-2	2.9E-3	3.7E-4	8.7E-5	l.lE-5
20	134.0	1.3E-1	8.0E-3	1.6E-3	5.0E-4	9.8E-5
30	127.9	4.3E-1	3.0E-2	6.4E-3	2.2E-3	4.6E-4
50	46.3	3.0E-1	2.2E-2	4.6E-3	1.5E-3	3.3E-4
Caspar Soil Series (Pit No. 1)						
10	403.3	5.5E-3	7.1E-4	2.2E-4	9.2E-5	2.8E-5
20	12.6	2.6E-2	3.0E-3	8:6E-4	3.5E-4	1.0E-4
30	19.4	1.3E-2	2.0E-3	6:7E-4	3.1E-4	1.0E-4
50	2.6	2.2E-2	3.1E-3	1.0E-3	4.6E-4	1.5E-4
100	8.6	4.9E-2	5.9E-3	1.7E-3	7.1E-4	2.1E-4
150	0.2	2.5E-2	4.5E-3	1.6E-3	8.0E-4	2.9E-4
Caspar Soil Series (Pit No. 2)						
10	321.6	2.5E-3	4.2E-4	1.5E-4	7.0E-5	2.5E-5
20	34.6	1.6E-2	2.5E-3	8.6E-4	4.0E-4	1.4E-4
30	10.5	8.1E-3	1.3E-3	4.5E-4	2.1E-4	7.3E-5
50	3.3	1.3E-1	1.8E-2	5.6E-3	2.5E-3	7.9E-4
100	4.9	2.2E-6	3.1E-7	9.9E-8	4.4E-8	1.4E-8
150	3.1	5.6E-8	8.8E-9	3.0E-9	1.4E-9	4.7E-10

APPENDIX B

Table 6. Mean Values of Relative Hydraulic Conductivity (K_r) for the Hugo, Mendocino, and Caspar Soil Series (mean values of all pits in each series).

Depth (cm)	K_S (cm/hr)	K_r at applied tensions of 10 cm	20 cm	30 cm	40 cm	60 cm
Hero Soil Series (Pits 1-8)						
10	266.6	4.9E-2	2.3E-3	4.4E-4	1.5E-4	3.4E-5
20	131.5	9.7E-2	4.4E-3	8.4E-4	2.9E-4	7.1E-5
30	59.9	3.2E-1	1.3E-2	2.2E-3	6.9E-4	1.5E-4
50	45.7	3.8E-1	2.7E-2	6.6E-3	2.6E-3	7.2E-4
100	11.8	7.9E-2	1.2E-2	4.2E-3	2.1E-3	8.0E-4
150	12.9	1.2E-1	1.4E-2	3.9E-3	1.6E-3	4.4E-4
Mendocino Soil Series (Pits 1-2)						
10	373.8	4.9E-2	1.5E-3	1.8E-4	4.4E-5	5.6E-6
20	117.0	2.5E-1	2.2E-2	5.3E-3	2.0E-3	4.9E-4
30	86.6	2.6E-1	2.1E-2	4.8E-3	1.8E-3	4.2E-4
50	50.5	8.5E-1	4.2E-2	7.2E-3	2.1E-3	3.8E-4
100	13.4	6.8E-1	3.2E-2	5.3E-3	1.5E-3	2.5E-4
150	5.0	1.5E-1	6.9E-2	1.1E-3	3.2E-4	5.2E-5
Caspar Soil Series (Pits 1-2)						
10	362.5	4.0E-3	5.7E-4	1.9E-4	8.1E-5	2.7E-5
20	23.6	2.1E-2	2.8E-3	8.6E-4	3.8E-4	1.2E-4
30	15.0	1.1E-2	1.7E-4	5.6E-4	2.6E-4	8.7E-5
50	3.0	7.6E-2	1.1E-2	3.3E-3	1.5E-3	4.7E-4
100	6.8	2.5E-2	3.0E-3	8.5E-4	3.6E-4	1.1E-4
150	1.7	1.3E-2	2.3E-3	8.0E-4	4.0E-4	1.5E-4

<u>APPENDIX B</u>

Table 7. Mean Values of Bulk Density, Particle-size Classes, Porosity, S.C.S. Soil Class, K_s, and % Water-stable Aggregates for Each Pit

Depth (cm)	Bulk Density (g/cm^3)	Gravel (≥5 mm)	% Sand (4.99-.074 mm)	% Silt (4.73-.002 mm)	% Clay (<.002 mm)	Total Porosi-ty (%)	S.C.S. Soil S Class	Vertical K_S (cm/hr)	Water-Stable Aggregates (% by wt.)
			( ) = wt. % sans gravel						
<u>Hugo Soil Series - Pit No. 1</u>									
0-10	1.06	26.0	14.0 (18.9)	50.0 (67.6)	10.0 (13.5)	61.5	gsil	315.0	28.1
10-20	1.17	27.0	17.0 (23.3)	42.0 (57.5)	14.0 (19.2)	55.0	gsil	185.8	33.9
20-30	1.24	22.0	36.0 (46.2)	32.0 (41.0)	10.0 (12.8)	49.9	gl	36.9	23.5
30-50	1.28	26.0	32.4 (43.7)	31.2 (42.2)	10.4 (14.1)	46.7	gl	19.3	30.0
50-100[1]	1.40	6.0	49.0 (52.1)	35.0 (37.2)	10.0 (10.6)	56.5	sl	3.9	19.3
100-150[1]	1.36	14.0	30.0 (34.9)	46.0 (53.5)	10.0 (11.6)	56.5	gsil	31.9	40.6
Pit Average	1.25	20.2	29.7 (36.5)	39.4 (49.8)	10.7 (13.6)	54.4	gl	98.8	29.2

1) The 100 cm and 150 cm depths of this pit consist mainly of punky rock, thus the particle size distribution is questionable, particularly with regards to the gravel fraction, which is probably underestimated.

Table 7. (cont.)

Depth (cm)	Bulk Density (g/cm^3)	% Gravel (≥5 mm)	% Sand (4.99-.074 mm)	% Silt (.073-.002 mm)	% Clay (< .002mm	Total Porosity (%)	S.C.S. Soil Class	Vertical K_S (cm/hr)	Water-Stable Aggregates (% by wt.)
			( ) = wt. % sans gravel						
Hugo Soil Series - Pit No. 2									
0-10	0.78	12.9	41.3 (47.4)	36.2 (41.6)	9.6 (11.0)	57.2	gl	234.5	39.6
10-20	1.35	8.4	39.2 (42.8)	42.4 (46.3)	10.0 (10.9)	48.3	1	3.0	33.9
20-30	1.35	6.0	32.3 (34.4)	39.7 (42.2)	22.0 (23.4)	55.0	1	4.0	42.0
30-50	1.30	10.2	23.8 (26.5)	36.0 (40.1)	30.0 (33.4)	56.9	gcl	3.9	56.5
50-100	1.16	5.7	21.3 (22.6)	38.9 (41.3)	34.1 (36.1)	63.4	cl	3.6	62.5
100-150[1]	1.19	50.0	9.3 (18.6)	18.7 (37.4)	22.0 (44.0)	59.6	gc	0.4	59.7
Pit Average	1.19	15.5	27.9 (33.0)	35.3 (41.8)	21.3 (25.2)	56.7	gl	41.6	49.0

----

[1] The gravel to cobble size rocks at this depth were too numerous to practically sample, some single rocks being larger than the entire normal sample size (5 kg).

Table 7. (cont.)

Depth (cm)	Bulk Density (g/cm^3)	% Gravel (≥5 mm)	% Sand (4.99-.074 mm)	% Silt (.073-.002 mm)	% Clay . (< .002mm	Total Porosity (%)	S.C.S. Soil Class	Vertical K_S (cm/hr)	Water-Stable Aggregates (% by wt.)
			( ) = wt. % sans gravel						
Hugo Soil Series - Pit No. 3									
0-10	1.09	22.0	41.0 (52.6)	29.0 (37.2)	8.0 (10.2)	54.5	gs1	314.4	27.7
10-20	1.14	17.6	38.2 (46.4)	33.9 (41.1)	10.3 (12.5)	53.7	gl	127.4	33.7
20-150[1]	2.50	90.0	---	---	---	---	---	---	
Pit Average[2]	1.12	19.8	39.6 (49.4)	31.5 (39.2)	9.1 (11.4)	54.1	gl	220.9	30.7

----

[1]Below the 20 cm depth, this pit's profile changes to broken rock (90%) mixed with well-aggregated surface soil (10%), and grades gradually into broken rock at the 150 cm level.

[2]Averages'reflect only the first 20 cm of depth.

Table 7. (cont.)

Depth (cm)	Bulk Density (g/cm^3)	%Gravel (≥ 5 mm)	% Sand (4.99-.074 mm)	% Silt (.073-.002 mm)	% Clay (<.002 mm)	Total Porosity (%)	S.C.S. Soil Class	Vertical K_S (cm/hr)	Water-Stable Aggregates (% by wt.)
			( ) =	wt. % sans	gravel				
Hugo Soil Series - Pit No. 4									
0-10	1.45	32.3	31.8 (46.9)	22.2 (32.7)	13.8 (20.4)	46.7	gl	23.5	39.3
10-20	1.45	13.8	40.2 (46.6)	30.3 (35.2)	15.7 (18.2)	46.4	gl	8.8	33.1
20-30	1.36	10.2	32.8 (36.5)	35.4 (39.4)	21.6 (24.1)	50.0	gl	5.0	39.1
30-50	1.38	15.7	30.7 (36.5)	35.6 (42.2)	18.0 (21.4)	48.8	gl	14.5	39.3
50-100	1.46	20.7	22.3 (28.1)	40.0 (50.4)	17.0 (21.4)	46.1	gsl	24.3	32.7
100-150[1]	---	80.0	---	---	---	---	---	---	
Pit Average	1.42	18.5	31.6 (38.8)	32.7 (40.1)	17.2 (21.1)	47.6	gl	15.2	36.7

----
[1]Profile changes to 60% boulders and 20% gravel below the 100 cm level. Pit averages exclude this level.

Table 7. (cont.)

Depth (cm)	Bulk Density (g/cm^3)	% Gravel (≥5 mm)	% Sand (4.99-.074 mm)	% Silt (.073-.002 mm)	% Clay (<.002 mm)	Total Porosity (%)	S.C.S. Soil Class	Vertical K_S (cm/hr)	Water-Stable Aggregates (% by wt.)
			( ) = wt. % sans gravel						
Hugo Soil Series - Pit No. 5									
0-10	1.29	30.0	36.9 (52.7)	23.1 (33.0)	10.0 (14.3)	45.7	gsl	228.6	28.9
10-150[1]	---	75.0	---	---	---	---	---	---	
Pit Average[2]	1.29	30.0	36.9 (52.7)	23.1 (33.0)	10.0 (14.3)	45.7	gsl	228.6	28.9

----

[1]This pit is on a fault and has soil developed in only the first 10 cm of depth, below which is rocky fault gouge. The 10-150 cm depth range contains 50% boulders and 30% gravel.

[2]Pit average 0-10 cm.

Table 7. (cont.)

Depth (cm)	Bulk Density (g/cm^3)	Gravel (≥5 mm)	%Sand (4.99-.074 mm)	% Silt (.073-.002 mm)	% Clay (< .002mm)	Total Porosity (%)	S.C.S. Soil Class	Vertical K_S (cm/hr)	Water-Stable Aggregates (% by wt.)
			( ) = wt. % sans gravel						
Hugo Soil Series - Pit No. 6									
0-10	0.87	17.6	38.4 (46.6)	36.1 (43.8)	7.9 (9.6)	63.4	gl	134.6	36.5
10-20	1.36	8.1	39.9 (43.4)	40.0 (43.5)	12.0 (13.1)	48.6	1	74.1	23.7
20-30	1.38	1.8	32:3 (32.9)	40.1 (40.8)	25:8 (26.3)	48.3	cl	31.9	35.3
30-50	1.29	1.2	25.8 (26.1)	33.4 (33.8)	39.6 (40.1)	51.0	c	10.0	54.2
50-100	1.25	13.4	30.1 (34.8)	28.5 (32.9)	28.0 (32.3)	51.9	gcl	15.3	42.3
100-150	1.35	7.4	25.6 (27.6)	42.6 (46.0)	24.4 (26.4)	48.5	cl	3.9	49.5
Pit Average	1.25	8.2	32.0 (35.3)	36.8 (40.1)	23.0 (24.6)	52.0	1	45.0	40.3

Table 7. (cont.)

Depth (cm)	Bulk Density (g/cm^3)	% Gravel (≥5 mm)	% Sand (4.99-.074 mm)	% Silt (.073-.002 mm)	% Clay (<.002mm)	Total Porosity (%)	S.C.S. Soil Class	Vertical K_S (cm/hr)	Water-Stable Aggregates (% by wt.)
			( ) = wt. % sans gravel						
Hugo Soil Series - Pit No. 7									
0-10	0.98	10.0	30.0 (33.3)	46.0 (51.1)	14.0 (15.6)	60.3	sil	558.9	52.2
10-20	1.14	10.4	34.8 (38.8)	39.6 (44.2)	15.2 (17.0)	55.3	gl	117.6	50.0
20-30	1.32	14.4	30.6 (35.7)	36.8 (43.0)	18.2 (21.3)	50.0	gl	30.3	47.8
30-150[1]	---	80.0	---	---	---	---	---	---	
Pit Average	1.15	11.6	31.8 (36.0)	40.8 (46.0)	15.8 (18.0)	55.2	gl	235.6	50.0

[1]Soil pit Hugo #7 changes abruptly to 80% gravel below the 30 cm level. This pit may actually be in soil that is transitional to the Mendocino soil series, since it is located on the brow of a broad ridge that is a Pleistocene wave cut terrace remnant. The site is mapped as Hugo.

[2]This average reflects the first 30 cm of depth only.

Table 7 (cont.)

Depth (cm)	Bulk Density (g/cm^3)	% Gravel (≥5 mm)	% Sand (4.99-.074 mm)	% Silt (.073-.002 mm)	% Clay (<.002 mm)	Total Porosity (%)	S.C.S. Soil Class	Vertical K_S (cm/hr)	Water-Stable Aggregates (% by wt.)
			( ) = wt. % sans gravel						
Hugo Soil Series - Pit No. 8									
0-10	1.02	32.2	31.8 (46.9)	22.2 (32.7)	13.8 (20.4)	59.5	gl	323.6	34.1
10-20	1.00	35.1	28.5 (43.9)	21.5 (33.1)	14.9 (23.0)	59.0	vgl	404.0	32.7
20-30	1.15	33.9	28.7 (43.4)	23.0 (34.8)	14.4 (21.8)	55.8	gl	251.0	31.7
30-50	1.15	54.8	23.2 (51.3)	13.1 (29.0)	8.9 (19.7)	54.4	vgl	180.7	18.0
50-150[1]	---	60.0	---	---	---	---	---	---	
Pit Average[2]	1.08	39.0	28.1 (46.4)	20.0 (32.4)	13.0 (21.2)	57.2	vgl	289.8	29.1

----

[1]The soil at this pit site has had an exceptional amount of colluvial movement in its history, as reflected in its high K_S for all sampled depths. At the 50 cm level, the gravel percentage was high (54.8%), but its small size still permitted sampling. Below the 50 cm depth, cobbles and gravel made up 40% and 20% of the volume, respectively.

[2]This average reflects the first 50 cm of depth only.

Table 7. (cont.)

Depth (cm)	Bulk Density (g/cm^3)	% Gravel (≥5 mm)	% Sand (4.99-.074 mm)	% Silt (.073-.002 mm)	% Clay (<.002 mm)	Total Porosity (%)	S.C.S. Soil Class	Vertical K_S (cm/hr)	Water-Stable Aggregates (% by wt.)
			( ) = wt. % sans gravel						
Mendocino Soil Series - Pit No. 1									
0-10	1.12	2.0	35.6 (36.3)	44.2 (45.1)	18.2 (18.6)	66.2	1	383.1	60.3
10-20	1.35	5.0	30.0 (31.6)	45.0 (47.4)	20.0 (21.1)	45.6	1	100.0	48.6
20-30	1.25	0.4	19.0 (19.1)	48.4 (48.6)	32.2 (32.3)	49.9	sicl	45.2	39.1
30-50	1.19	0.3	11.6 (11.6)	47.8 (47.9)	40.3 (40.4)	50.9	sic	54.6	54.2
50-100	1.15	1.2	23.0 (23.3)	39.9 (40.4)	35.9 (36.3)	54.6	cl	13.4	59.7
100-150	1.21	8.6	49.8 (54.5)	22.3 (24.4)	19.3 (21.1)	51.8	scl	5.0	35.0
Pit Average	1.21	2.9	28.2 (29.4)	41.3 (42.3)	27.7 (28.3)	53.2	cl	100.2	49.5

Table 7. (cont.)

Depth (cm)	Bulk Density (g/cm³)	% Gravel (≥5 mm)	% Sand (4.99-.074 mm)	% Silt (.073-.002 mm)	% Clay (< .002mm)	Total Porosity (%)	S.C.S. Soil Class	Vertical K_S (cm/hr)	Water-Stable Aggregates (% by wt.)
			( ) = wt. % sans gravel						
Mendocino Soil Series - Pit No. 2[1]									
0-10	0.91	18.0	43.0 (52.4)	27.0 (33.0)	12.0 (14.6)	51.3	gsl	364.4	34.5
10-20	1.11	14.0	41.6 (48.4)	31.9 (37.1)	12.5 (14.5)	54.4	gl	134.0	30.8
20-30	1.04	6.6	45.0 (48.2)	35.2 (37.7)	13.2 (14.1)	56.8	1	127.9	40.5
30-50	1.09	9.2	58.8 (64.8)	23.0 (25.3)	9.0 (9.9)	54.0	sl	46.3	27.0
50-150	---	70.0	---	---	---	---	---	---	
Pit Average[2]	1.04	12.0	47.0 (53.4)	29.3 (33.3)	11.7 (13.3)	54.1	gsl	168.2	33.2

[1]This soil pit is near the bottom of a small declivity and is atypical of the standard profile. The first 50 cm of the profile is a colluvial mixture of granular, well-aggregated Al horizon material from upslope, and gravel. This has subsequently undergone a slight modification toward the more typical Mendocino profile. Below the 50 cm depth, cobbles make up 50% and gravel 20% of the total volume. The pit average for gravel content applies only to the first 50 cm.

[2]Pit average reflects the first 50 cm of depth only.

Table 7. (.cont.)

Depth (cm)	Bulk Density (g/cm^3)	% Gravel (≥5 mm)	% Sand (4.99-.074 mm)	% Silt (.073-.002 mm)	% Clay (< .002mm)	Total Porosity (%)	S.C.S. Soil Class	Vertical K_S (cm/hr)	Water-Stable Aggregates (% by wt.)
			( ) = wt. % sans gravel						
Caspar Soil Series - Pit No. 1									
0-10	1.03	12.5	36.0 (41.1)	39.5 (45.1)	12.0 (13.7)	65.5	gl	403.3	32.8
10-20	1.11	12.0	35.1 (39.9)	39.3 (44.7)	13.6 (15.5)	62.8	gl	12.6	45.0
20-30	1.39	11.9	31.9 (36.2)	38.8 (44.0)	17.4 (19.8)	55.1	gl	19.4	33.0
30-50	1.54	14.6	23.4 (27.4)	37.5 (43.9)	24.5 (28.7)	54.2	gcl	2.6	46.7
50-100	1.36	21.4	16.2 (20.6)	35.6 (45.3)	26.8 (34.1)	57.7	gcl	8.6	40.7
100-150	1.44	19.0	32.4 (40.0)	29.5 (36.4)	19.1 (23.6)	56.6	gl	0.2	34.0
Pit Average	1.31	15.2	29.2 (34.3)	36.7 (43.2)	18.9 (22.6)	58.7	gl	74.5	38.7

Table 7. (cont.)

Depth (cm)	Bulk Density (g/cm^3)	% Gravel (≥5 mm)	% Sand (4.99-.074 mm)	% Silt (.073-.002 mm)	% Clay (< .002mm)	Total Porosity (%)	S.C.S. Soil Class	Vertical K_S (cm/hr)	Water-Stable Aggregates (% by wt.)
			( ) = wt. % sans gravel						
Caspar Soil Series - Pit No. 2									
0-10	1.19	0.4	47.9 (48.1)	36.1 (36.2)	15.6 (15.7)	53.8	1	321.6	30.3
10-20	1.33	2.2	19.9 (20.4)	48.9 (50.0)	29.0 (29.7)	49.5	cl	34.8	55.5
20-30	1.25	27.4	25.0 (34.4)	24.6 (33.9)	23.0 (31.7)	52.8	gcl	10.5	59.5
30-50	1.14	15.0	38.0 (44.7)	24.6 (28.9)	22.4 (26.4)	55.8	gl	3.3	42.2
50-100	1.27	2.0	29.5 (30.1)	40.2 (41.0)	28.3 (28.8)	62.9	cl	4.9	60.7
100-150	1.31	3.9	29.5 (30.7)	48.4 (50.4)	18.2 (18.9)	59.8	sil	3.1	38.2
Pit Average	1.25	8.5	31.6 (34.7)	37.1 (40.1)	22.8 (25.2)	55.8	1	63.0	47.7

APPENDIX B

Table 8. Specific Gravity of the Soil Solids (G_S) From Each Soil Pit and Series

Series	Pit	GS
Hugo	1	2.743
"	2	2.896
"	3	2.872
"	4	2.883
"	5	2.907
"	6	2.648
"	7	2.693
"	8	2.683
Mendocino	1	2.694
"	2	2.741
Caspar	1	2.767
"	2	2.813

Hugo	mean of all pits except no. 5	2.774
Mendocino	mean of all pits	2.718
Caspar	mean of all pits	2.790

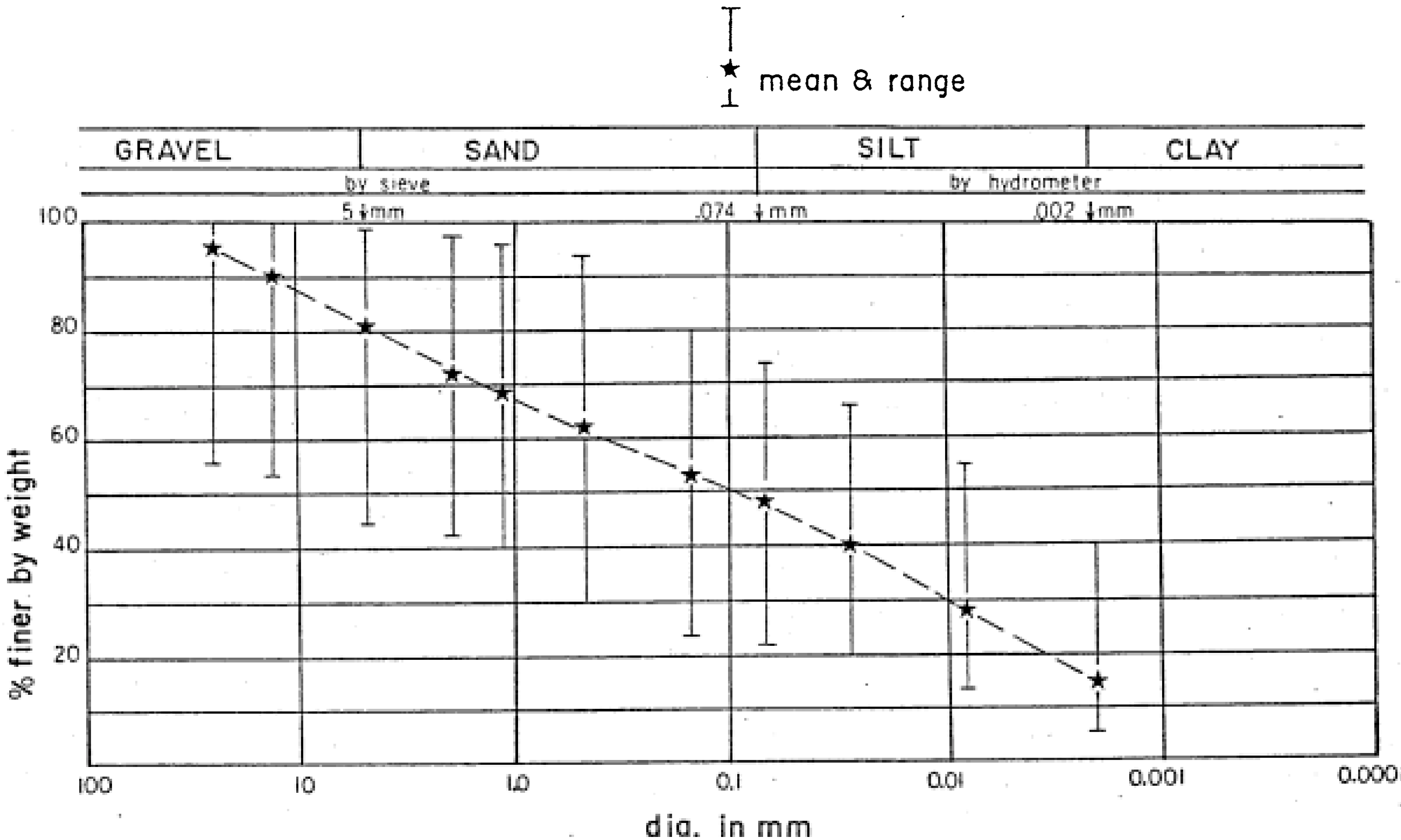

Figure I-1. Particle-size distribution of the Hugo soil series (representing 31 bulk samples).

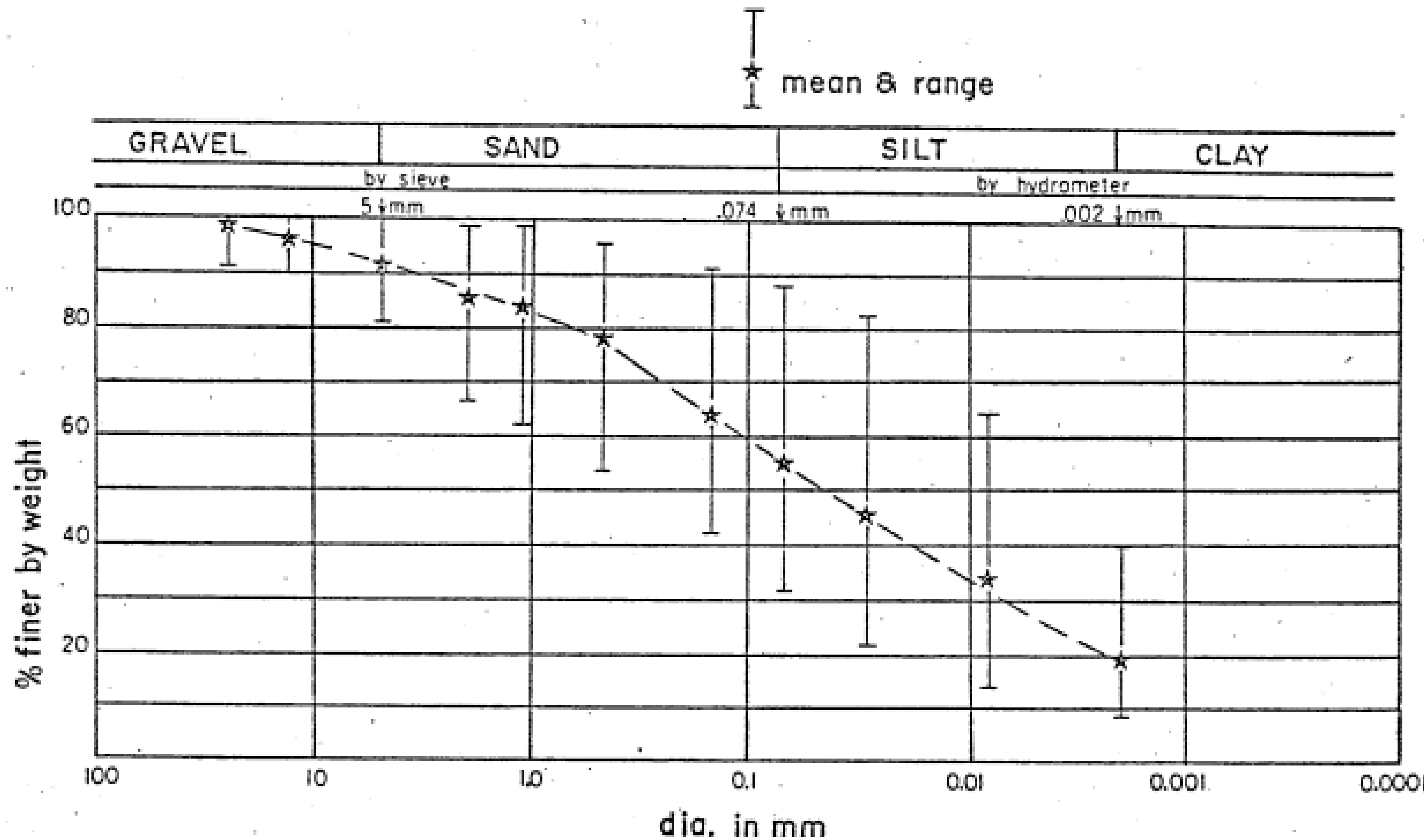

Figure I-2. Particle-size distribution of the Mendocino soil series (representing 10 bulk samples)

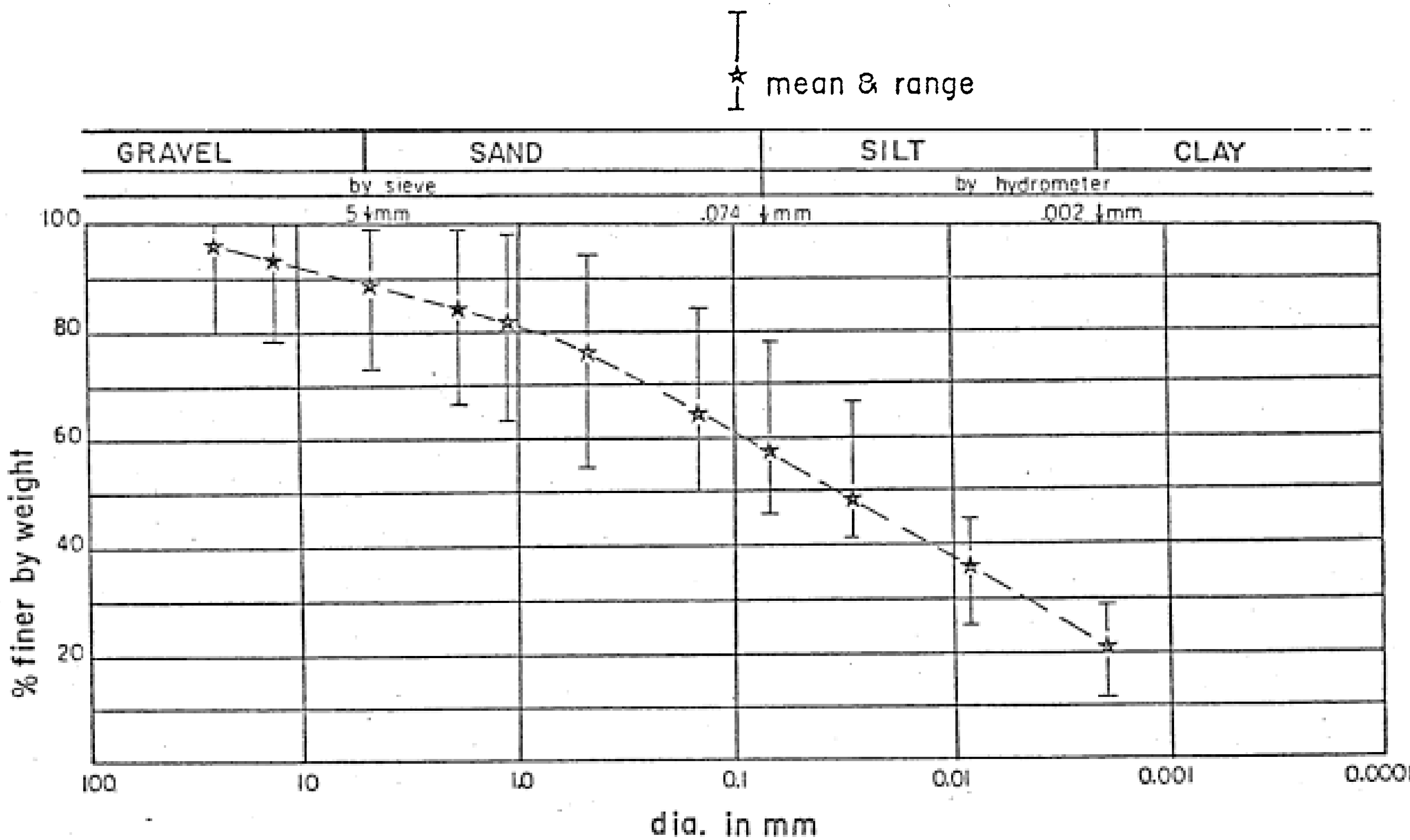

Figure I-3. Particle-size distribution for the Caspar soil series (representing 12 bulk samples).

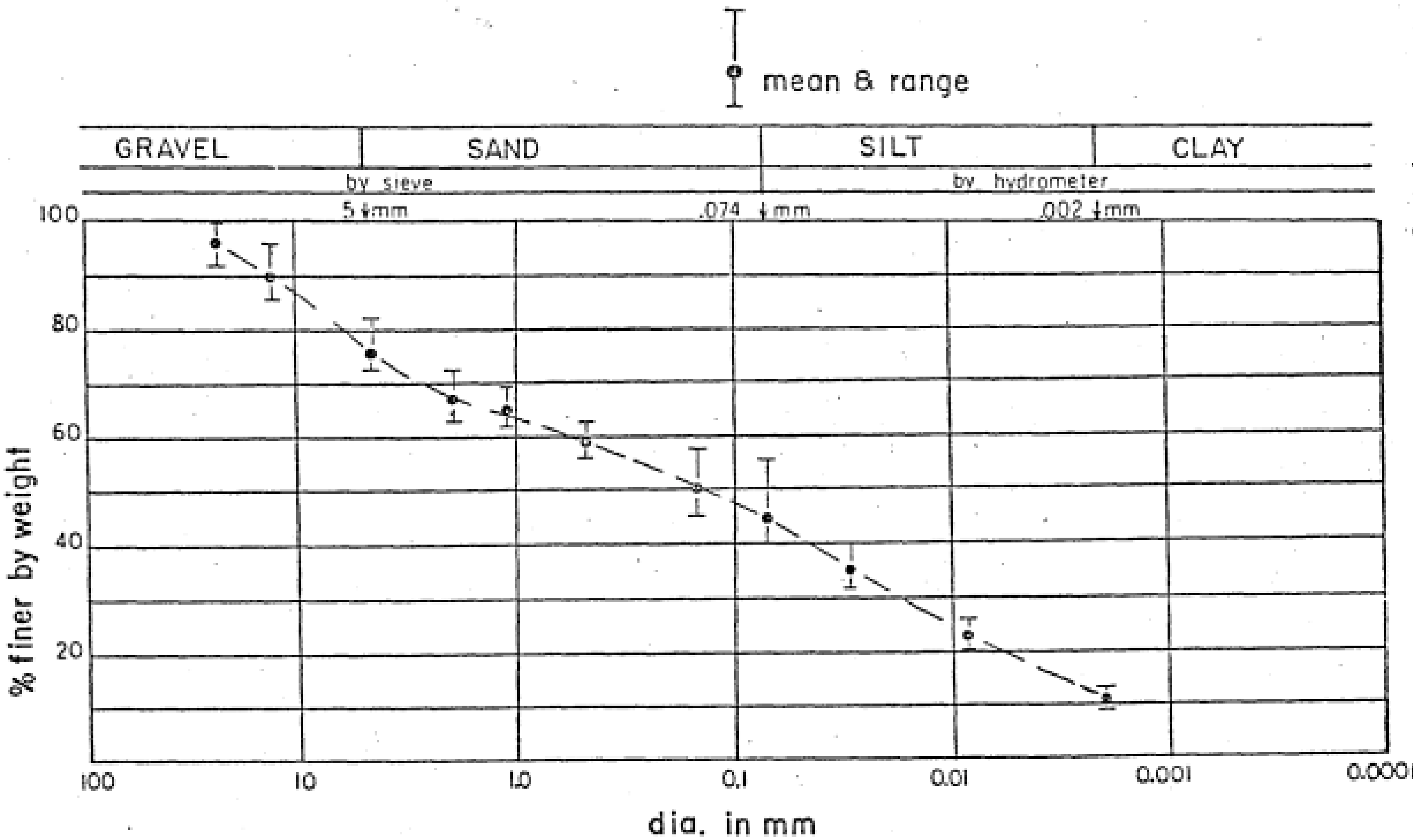

Figure II-1. Particle-size distribution for Hugo pit No, 1 (10 through 100 cm depths, represented by 5 bulk samples).

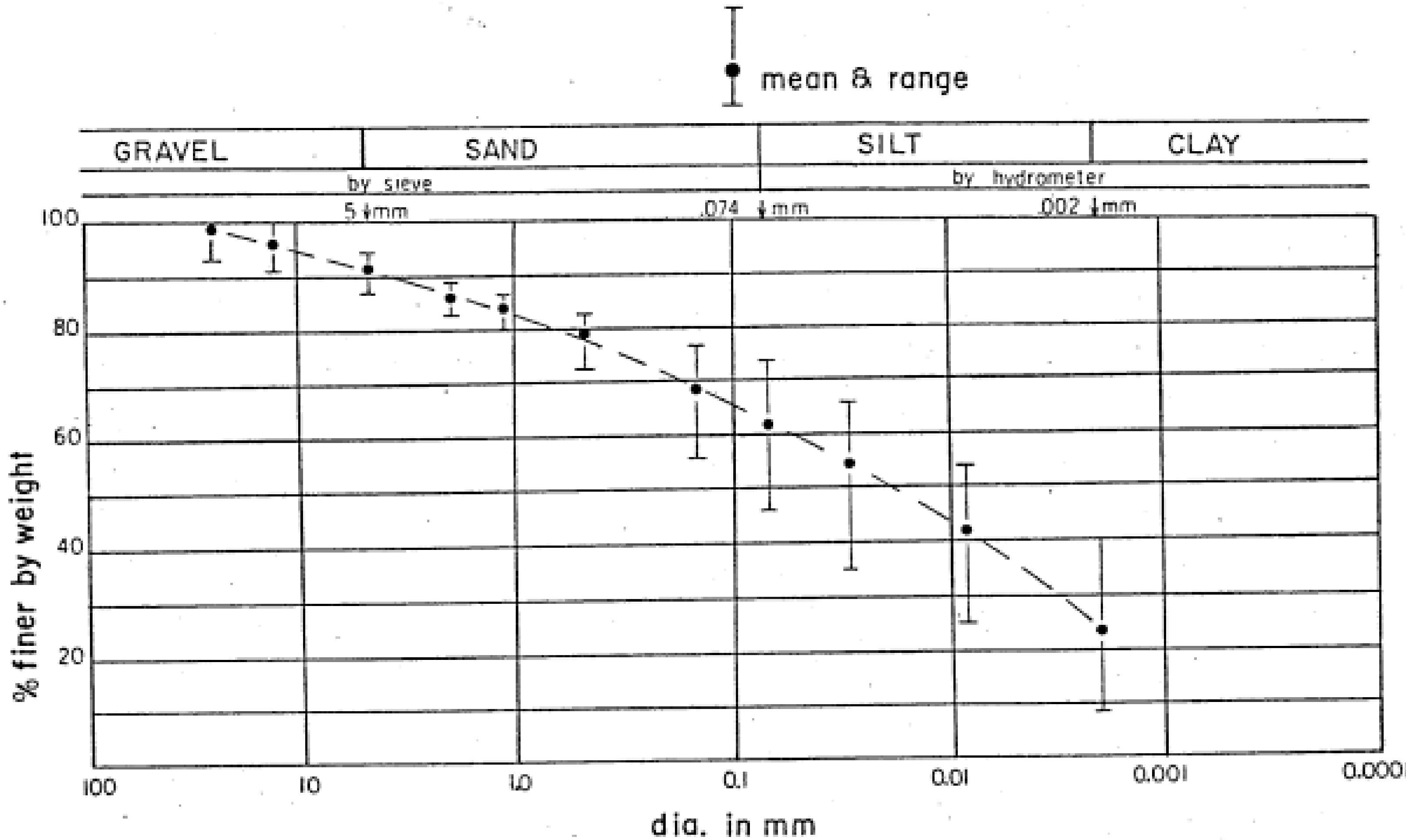

Figure II-2. Particle-size distribution for Hugo pit No. 2 (10 through 150 cm depths, represented by 6 bulk samples).

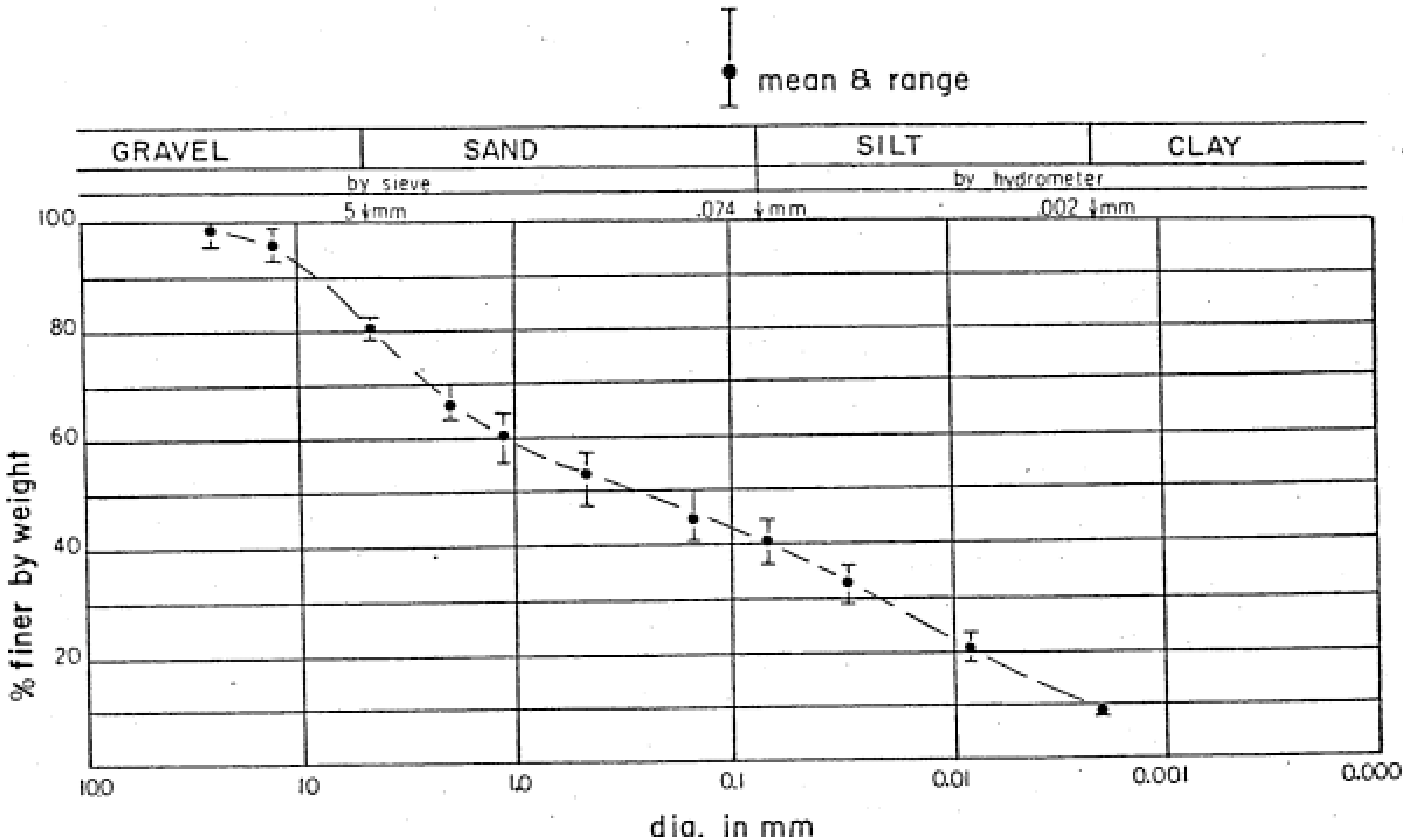

Figure II-3. Particle-size distribution for Hugo pit No. 3 (10 and 20 cm depth, represented by 2 bulk samples).

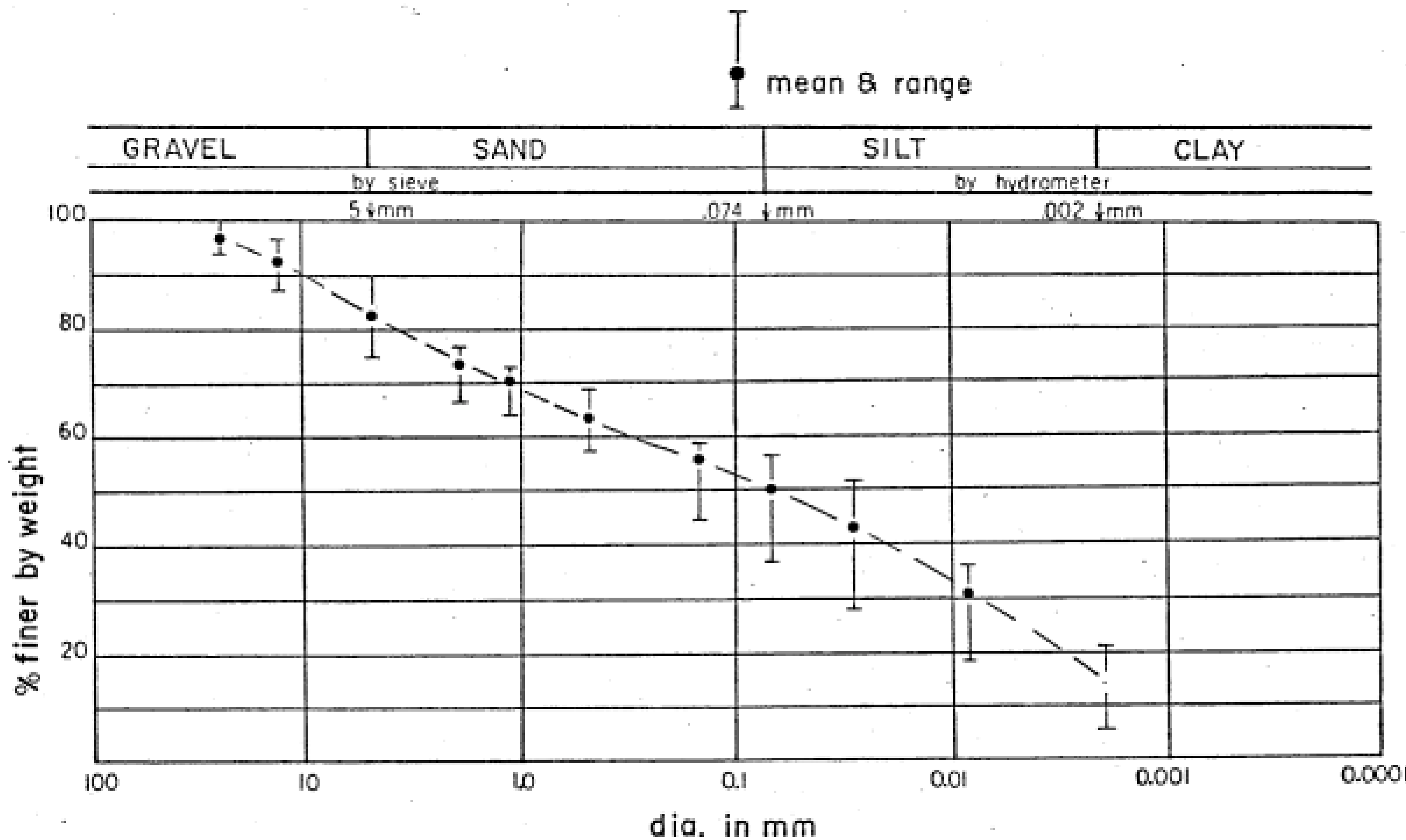

Figure II-4. Particle-size distribution for Hugo pit No. 4 (10 through 100 cm depths, represented by 5 bulk samples).

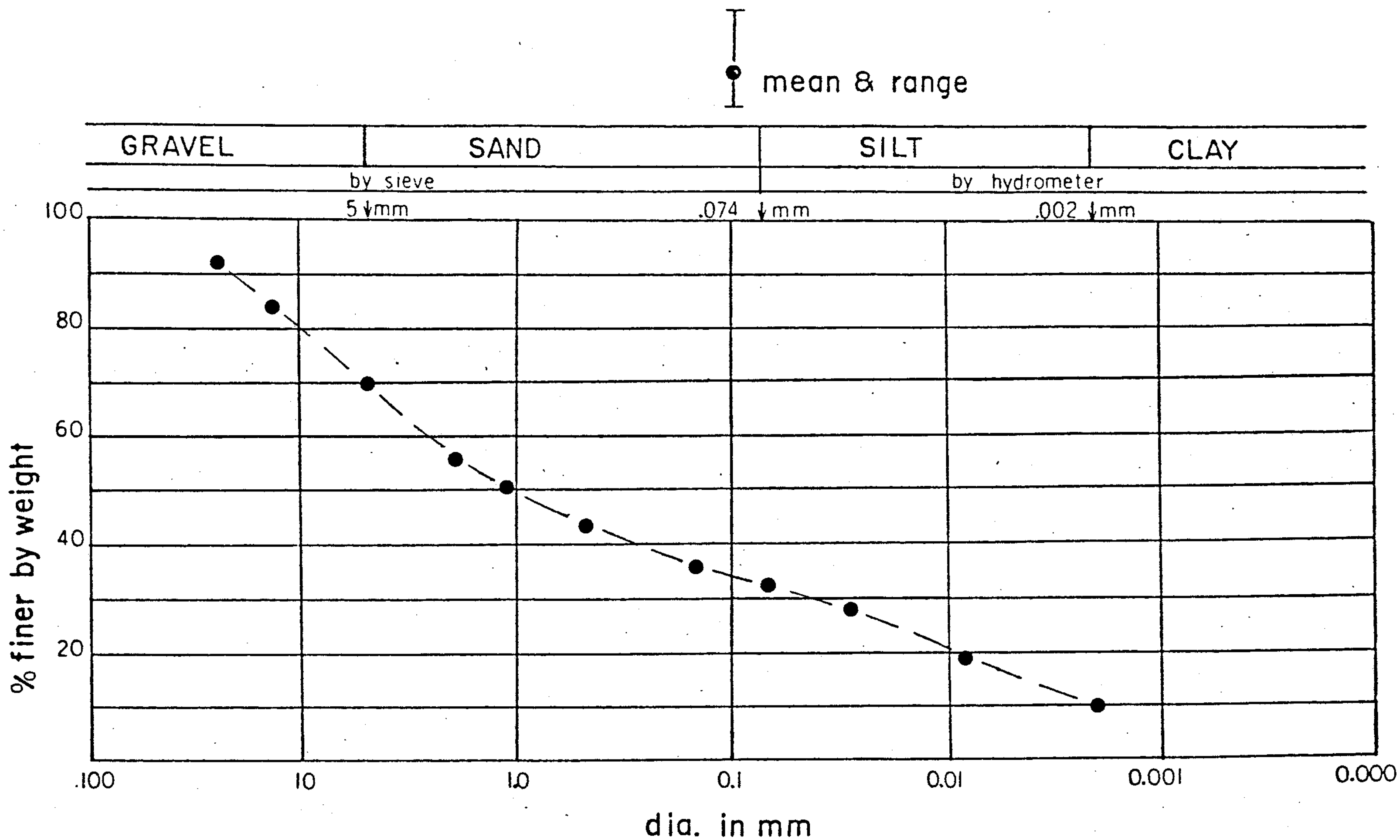

Figure II-5. Particle-size distribution for Hugo pit No. 5 (10 cm depth only, represented by 1 bulk sample).

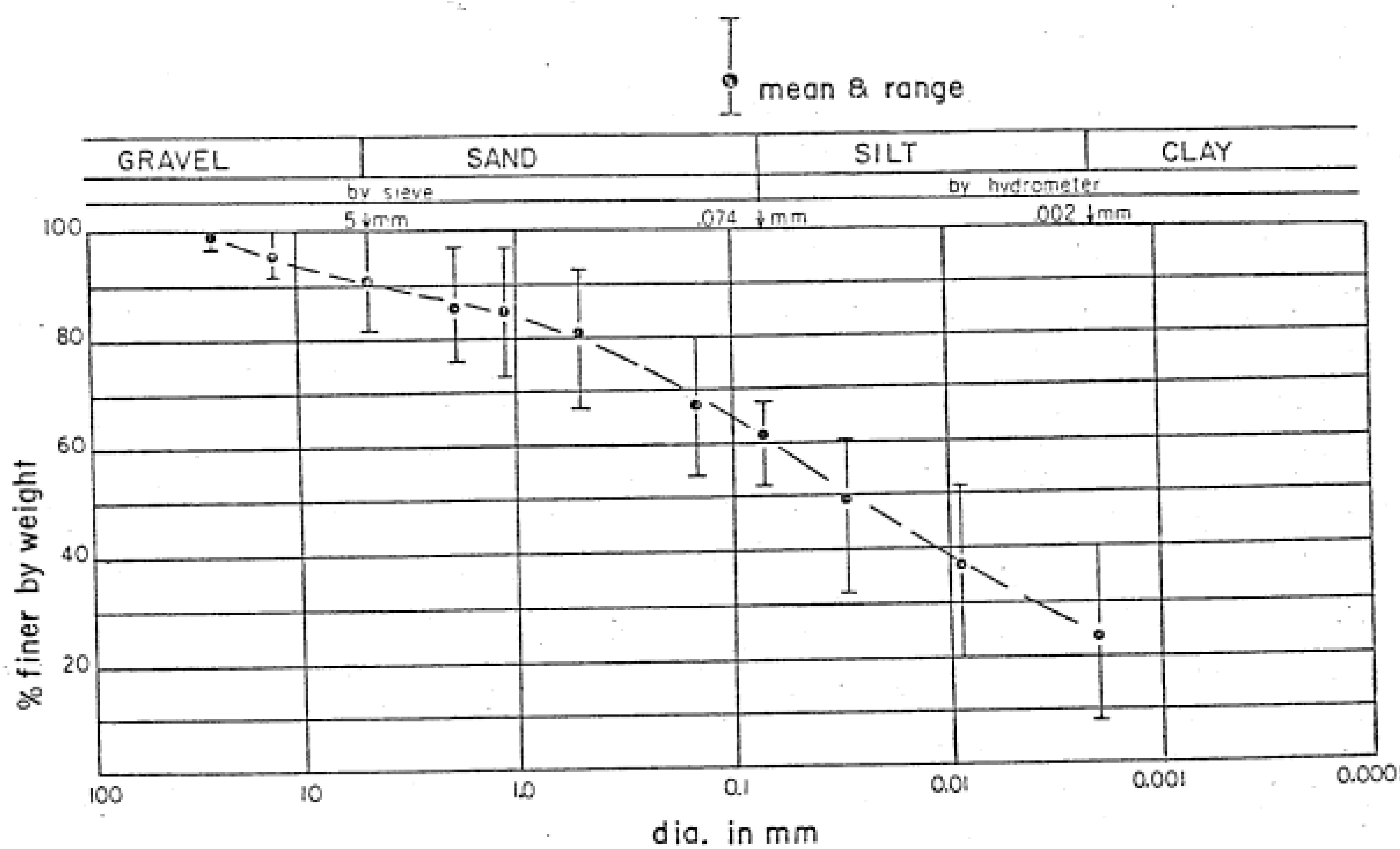

Figure II-6. Particle-size distribution for Hugo pit No. 6 (10 through 150 cm depths, represented by 6 bulk samples).

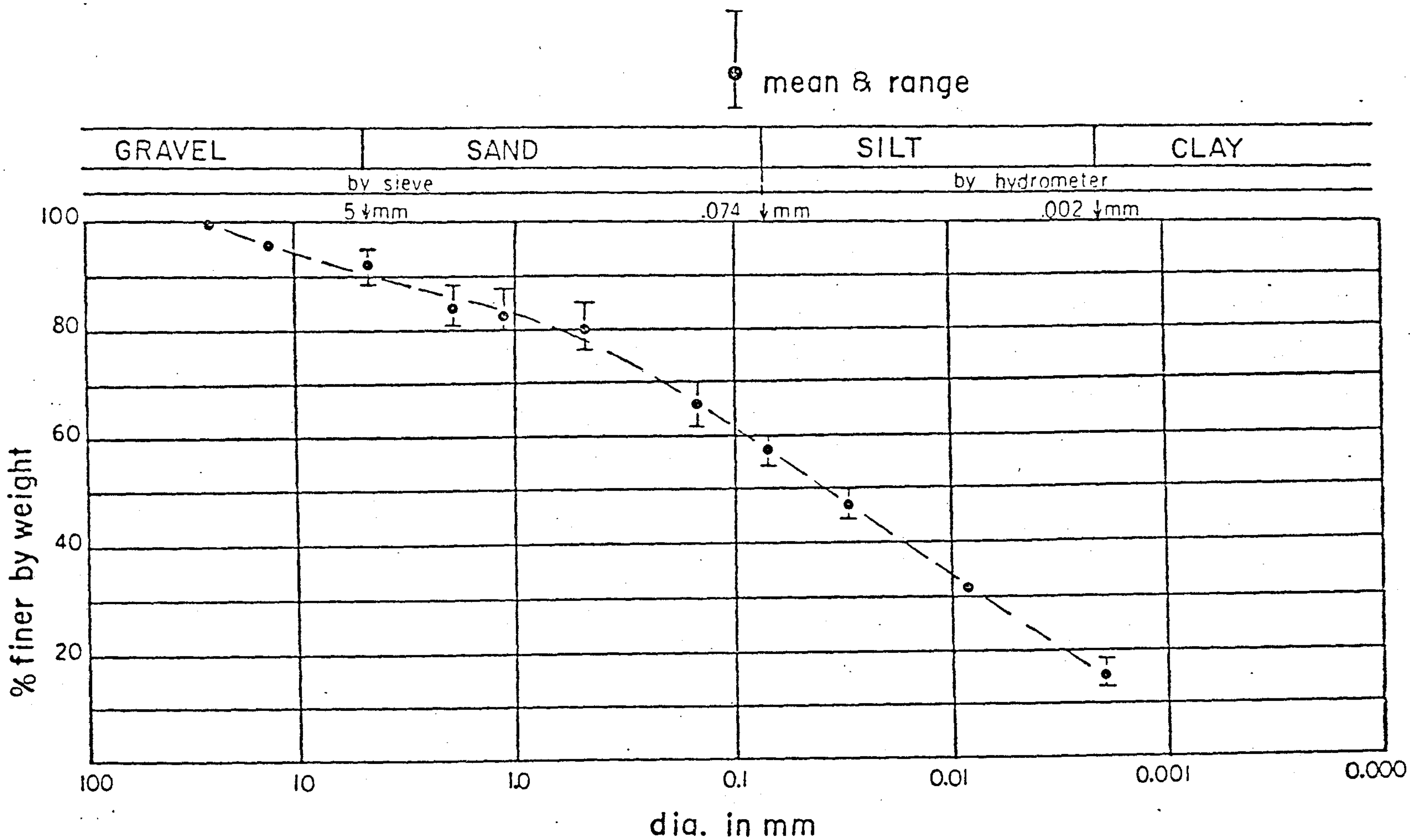

Figure II-7. Particle-size distribution for Hugo pit No. 7 (10 through 30 cm depths, represented by 3 bulk samples).

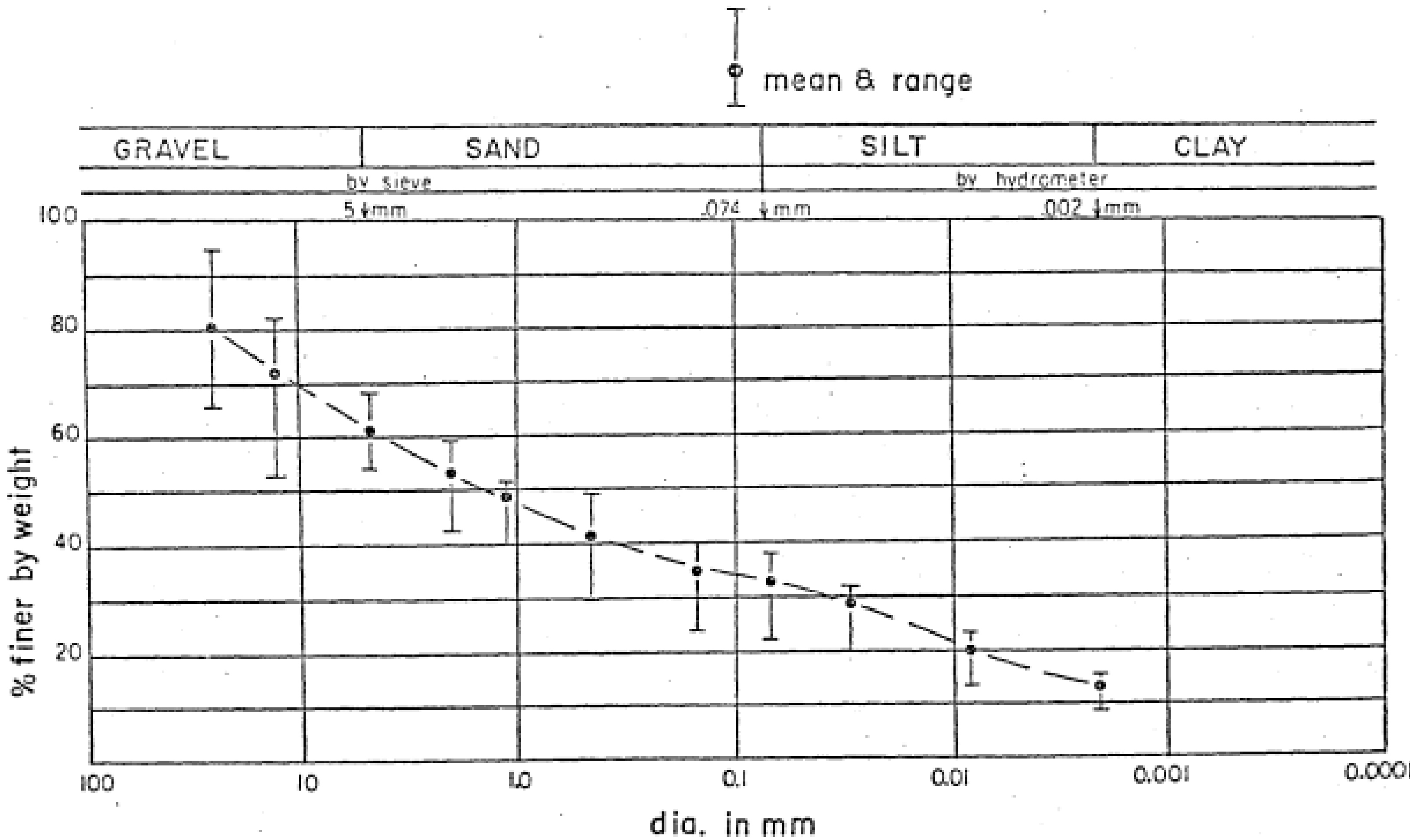

Figure II-8. Particle-size distribution for Hugo pit No. 8 (10 through 50 cm depths, represented by 4 bulk samples),

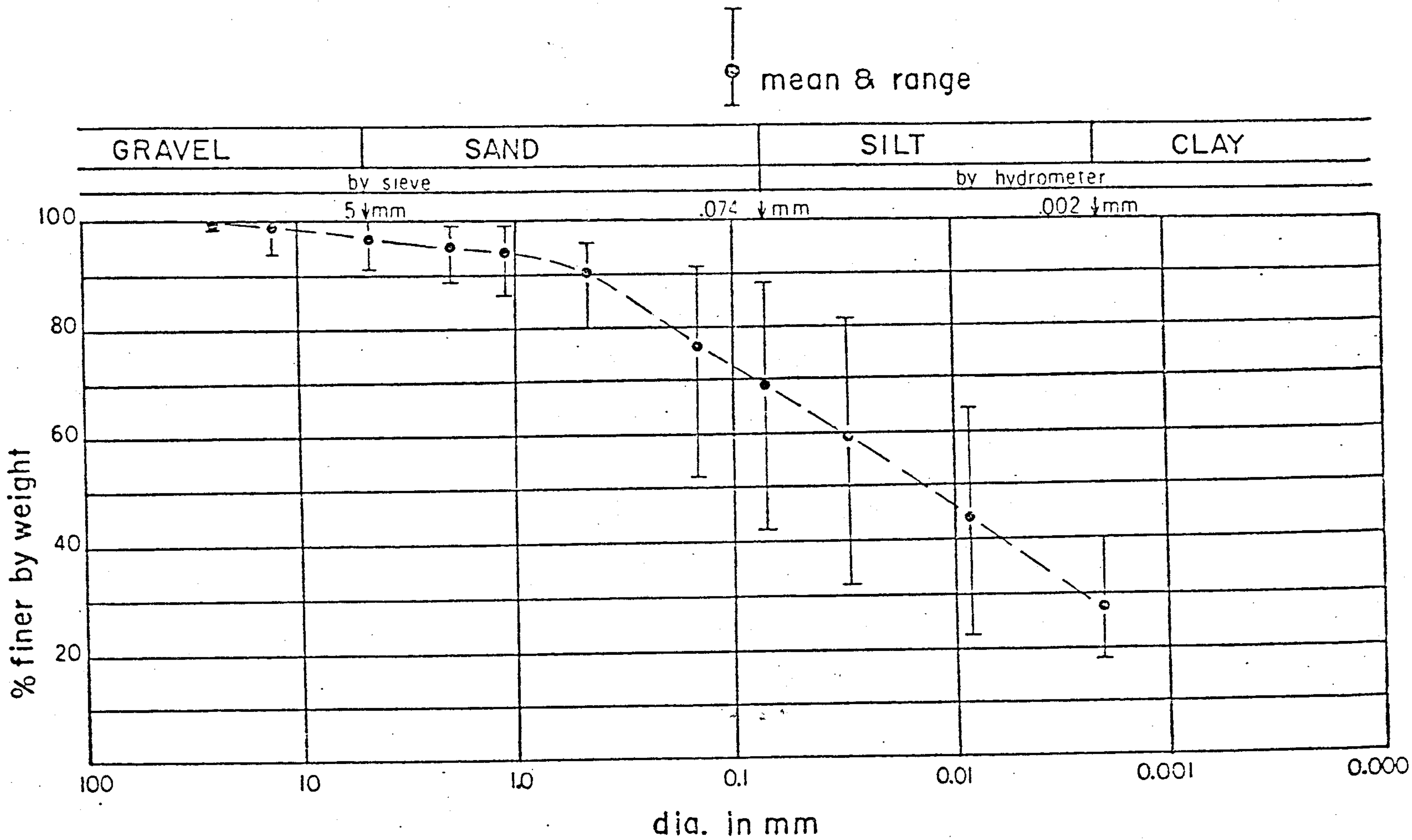

Figure II-9. Particle-size distribution for Mendocino pit No. 1 (10 through 150 cm depths, represented by 6 bulk samples).

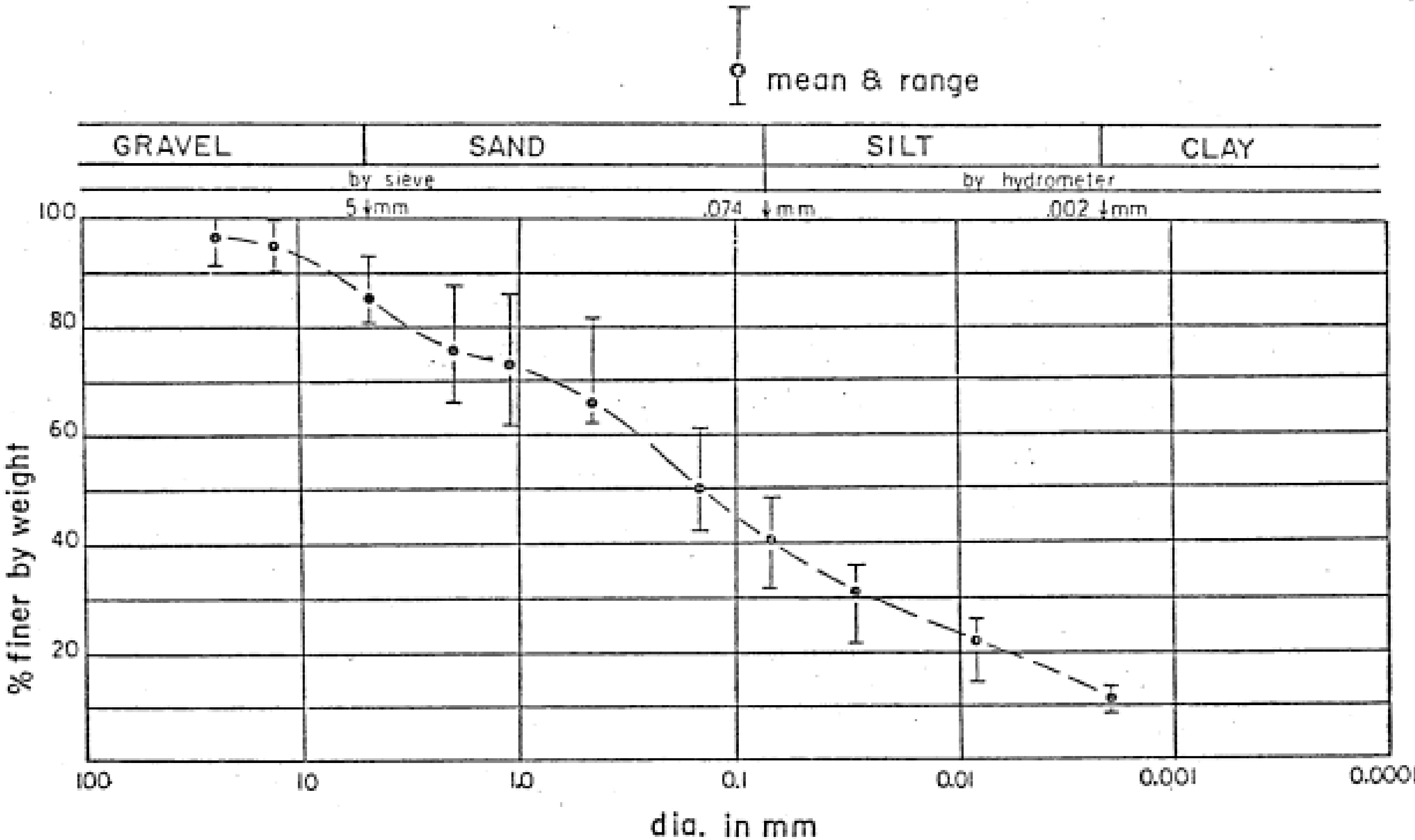

Figure II-10. Particle-size distribution for Mendocino pit No. 2 (10 through 50 cm depths, represented by 4 bulk samples).

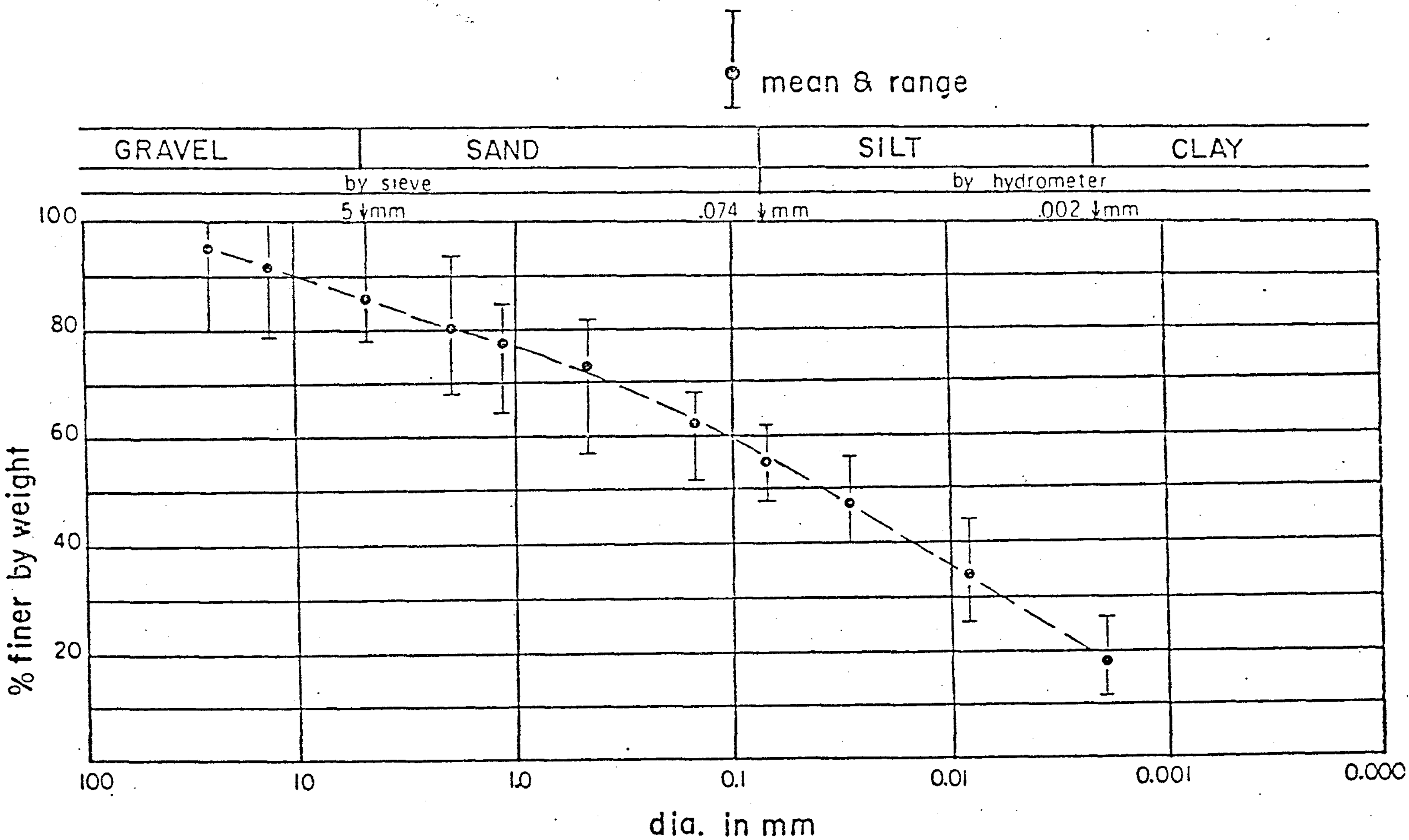

Figure II-11. Particle-size distribution for Caspar pit No. 1 (10 through 150 cm depths, represented by 6 bulk samples).

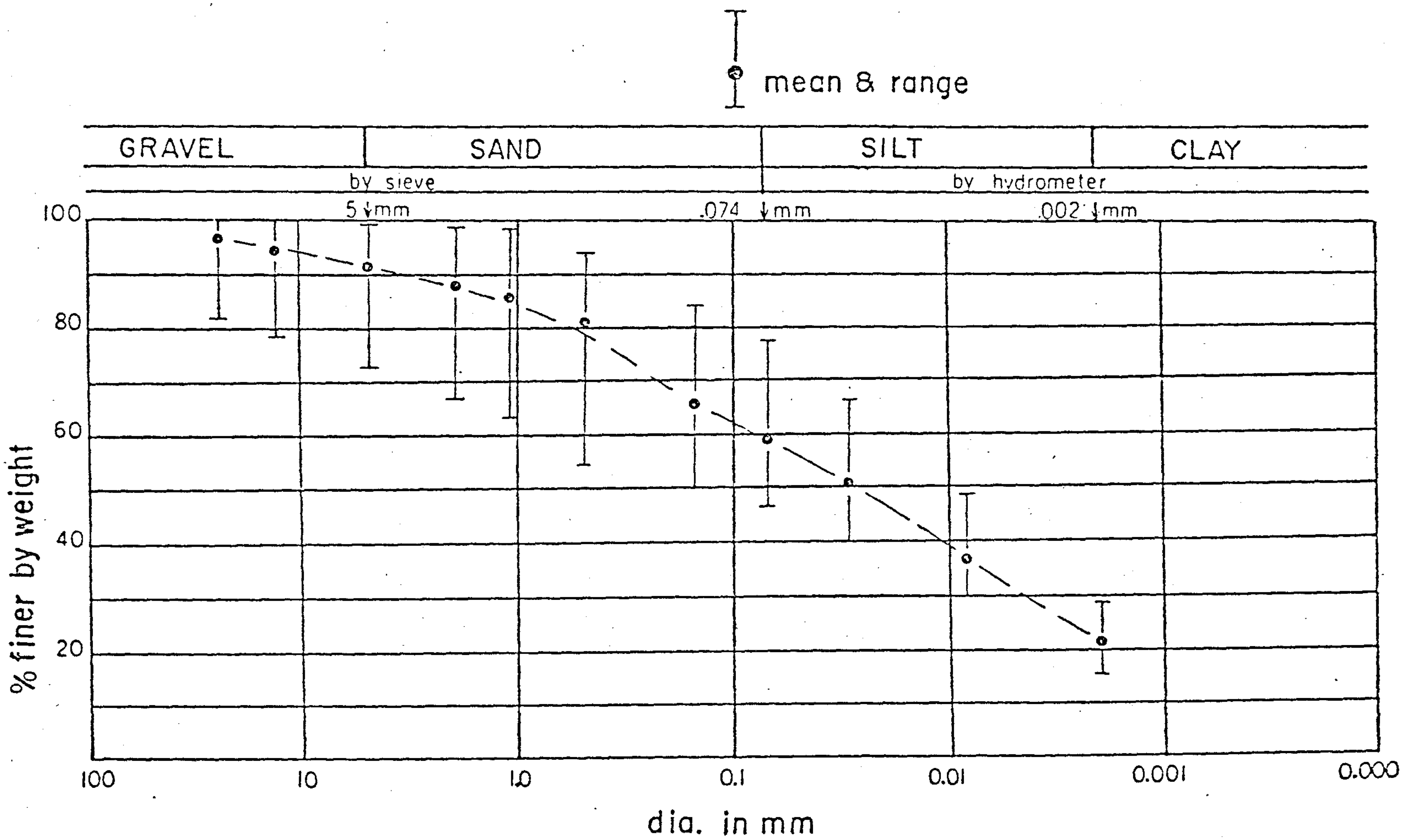

Figure II-12. Particle-size distribution for Caspar pit No. 2(10 through 150 cm depths, represented by 6 bulk samples).

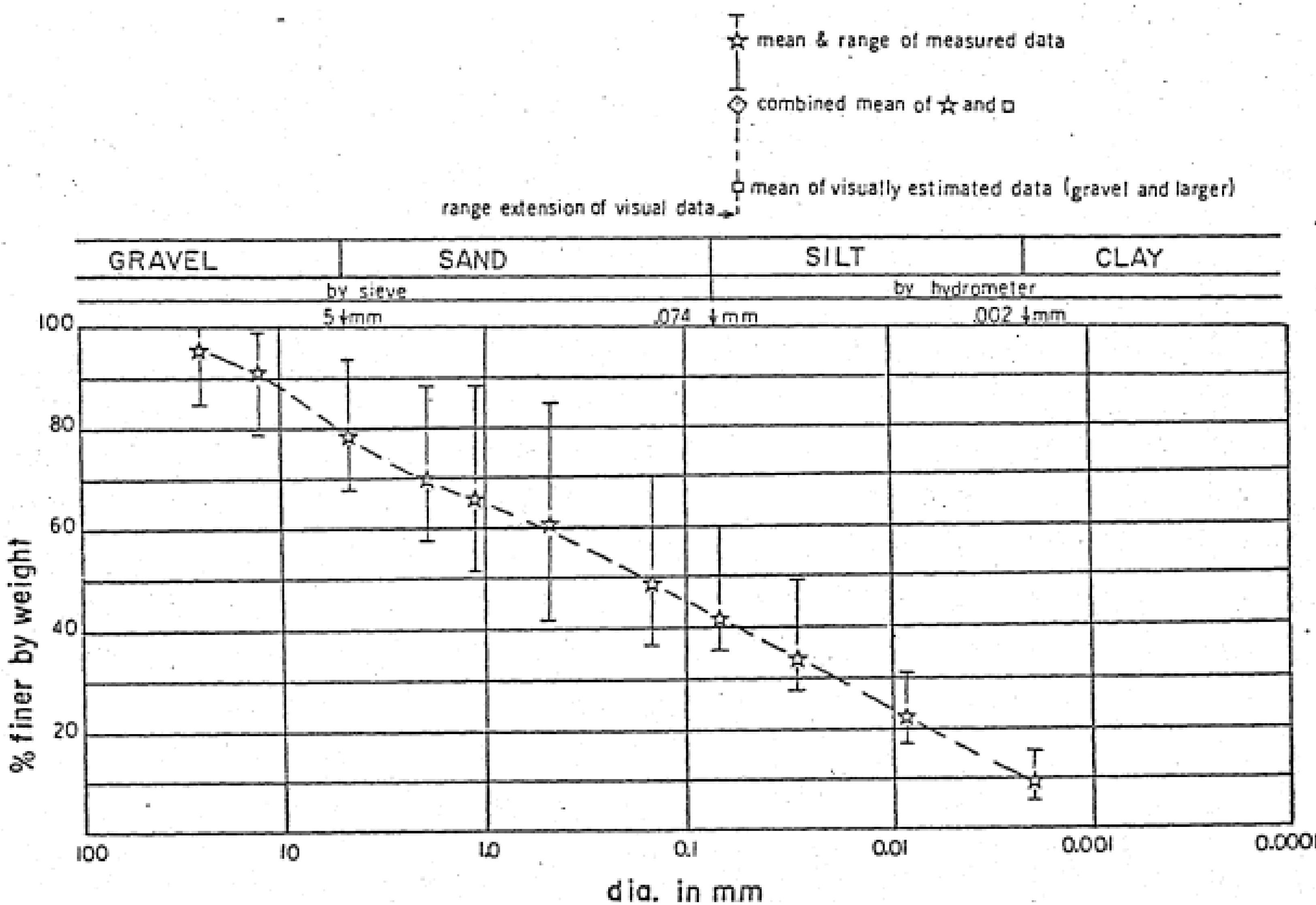

Figure III-1. Particle-size distribution for the 10 cm depth of the Hugo soil series (represented by 7 bulk samples and 0 visual estimates).

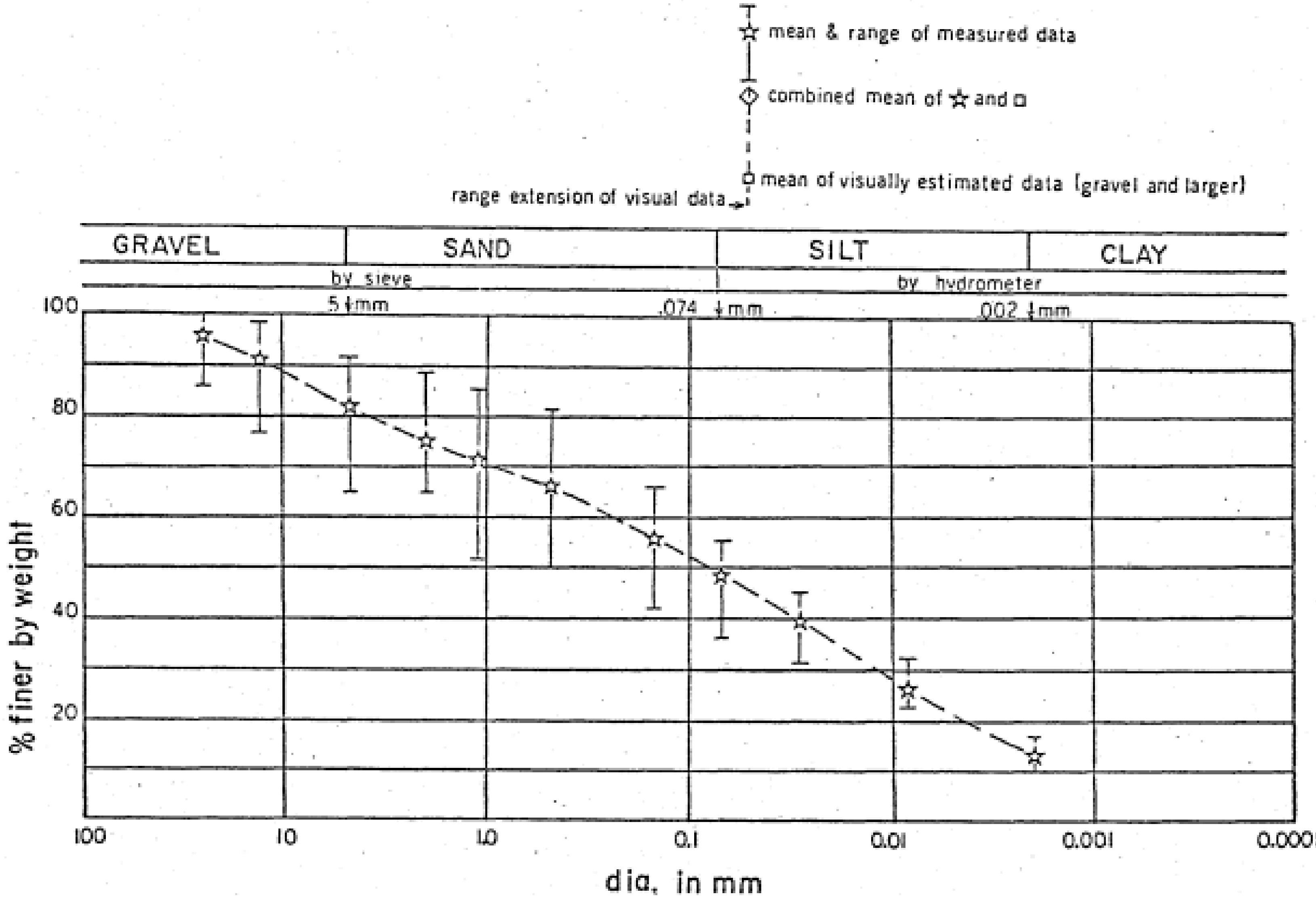

Figure III-2. Particle-size distribution for the 20 cm depth of the Hugo soil series (represented by 7 bulk samples and 0 visual estimates).

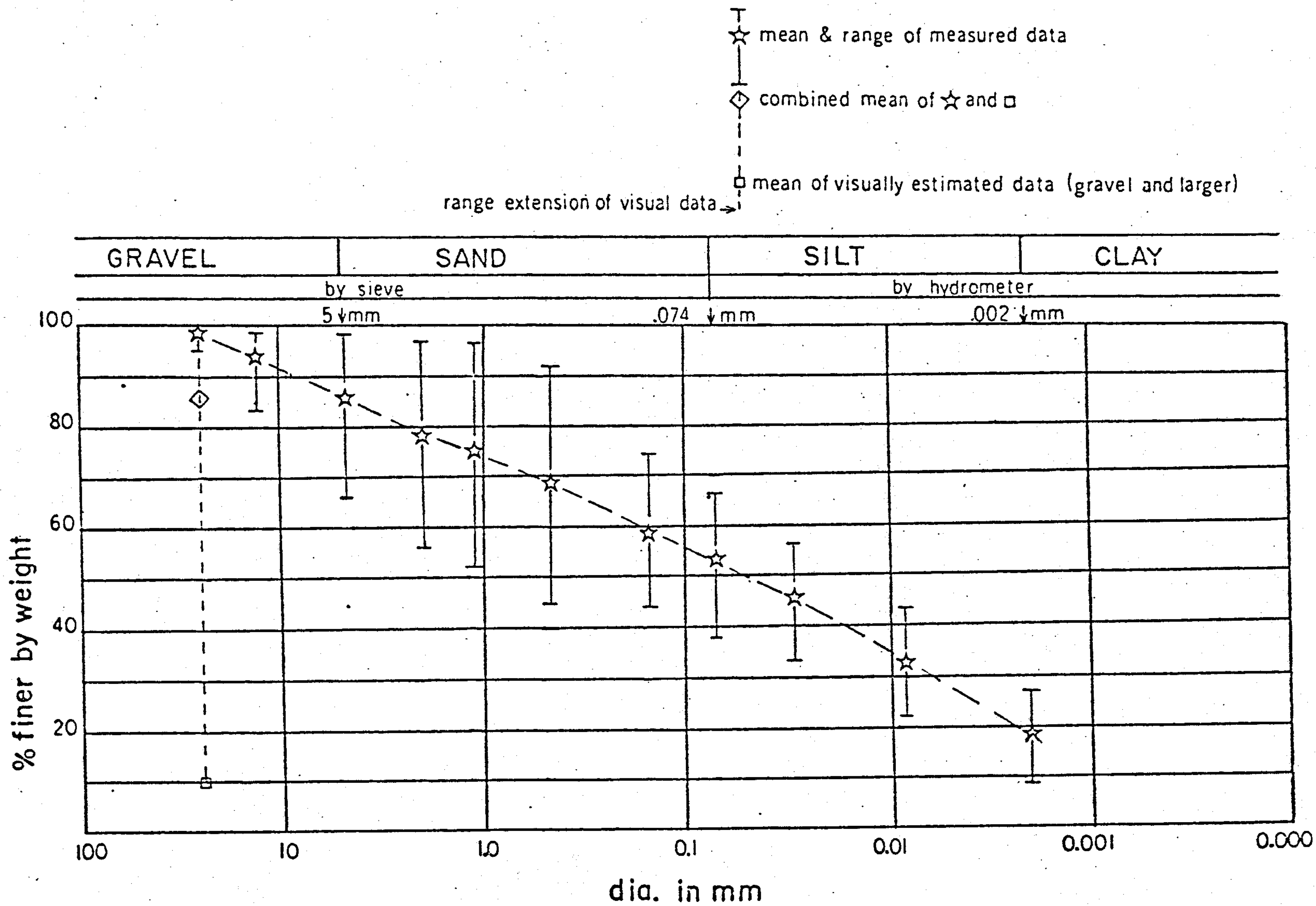

Figure III-3. Particle-size distribution for the 30 cm depth of the Hugo soil series (represented by 6 bulk samples and l visual estimate).

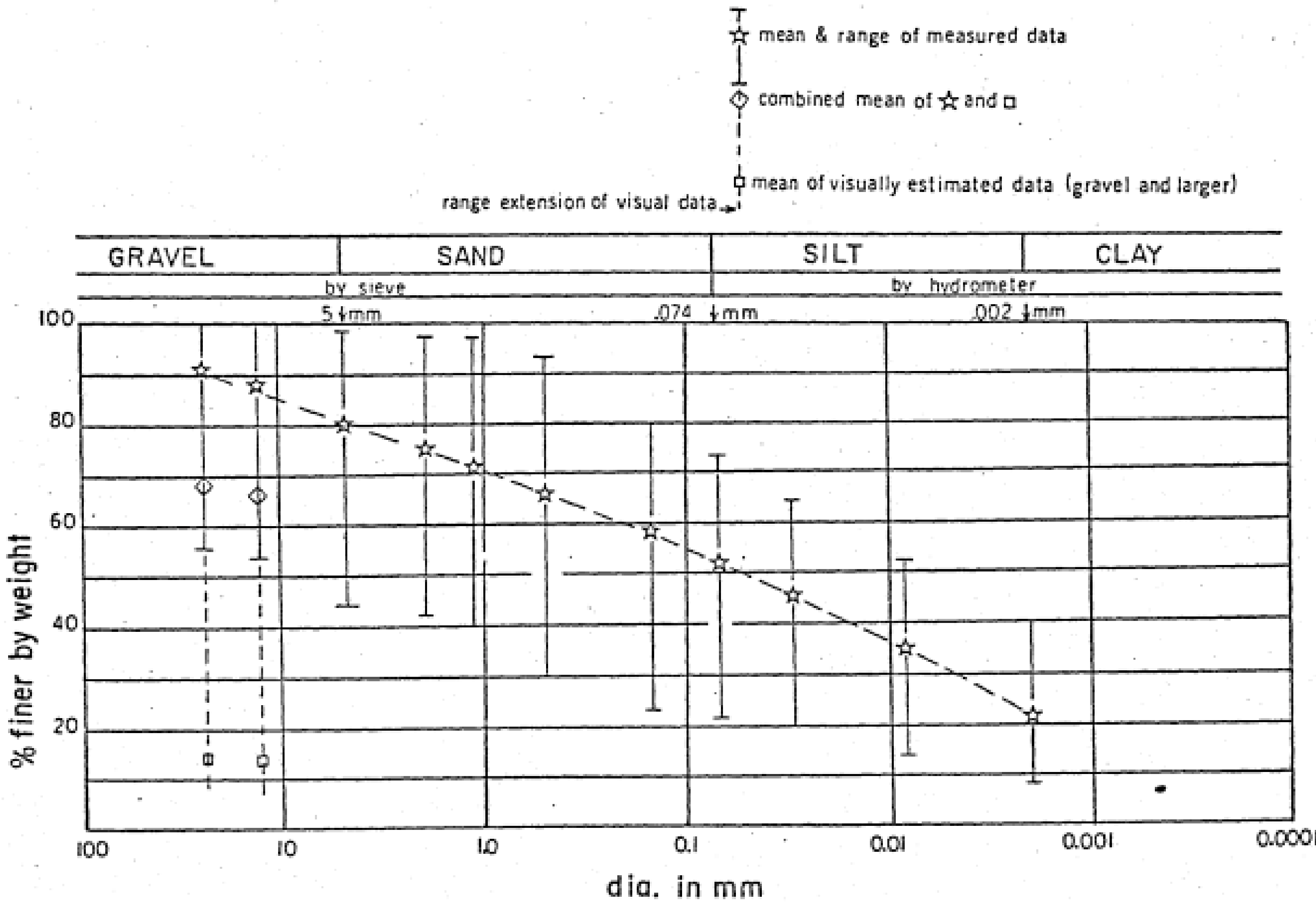

Figure III-4. Particle-size distribution for the 50 cm depth of the Hugo soil series (represented by 5 bulk samples and 2 visual estimates).

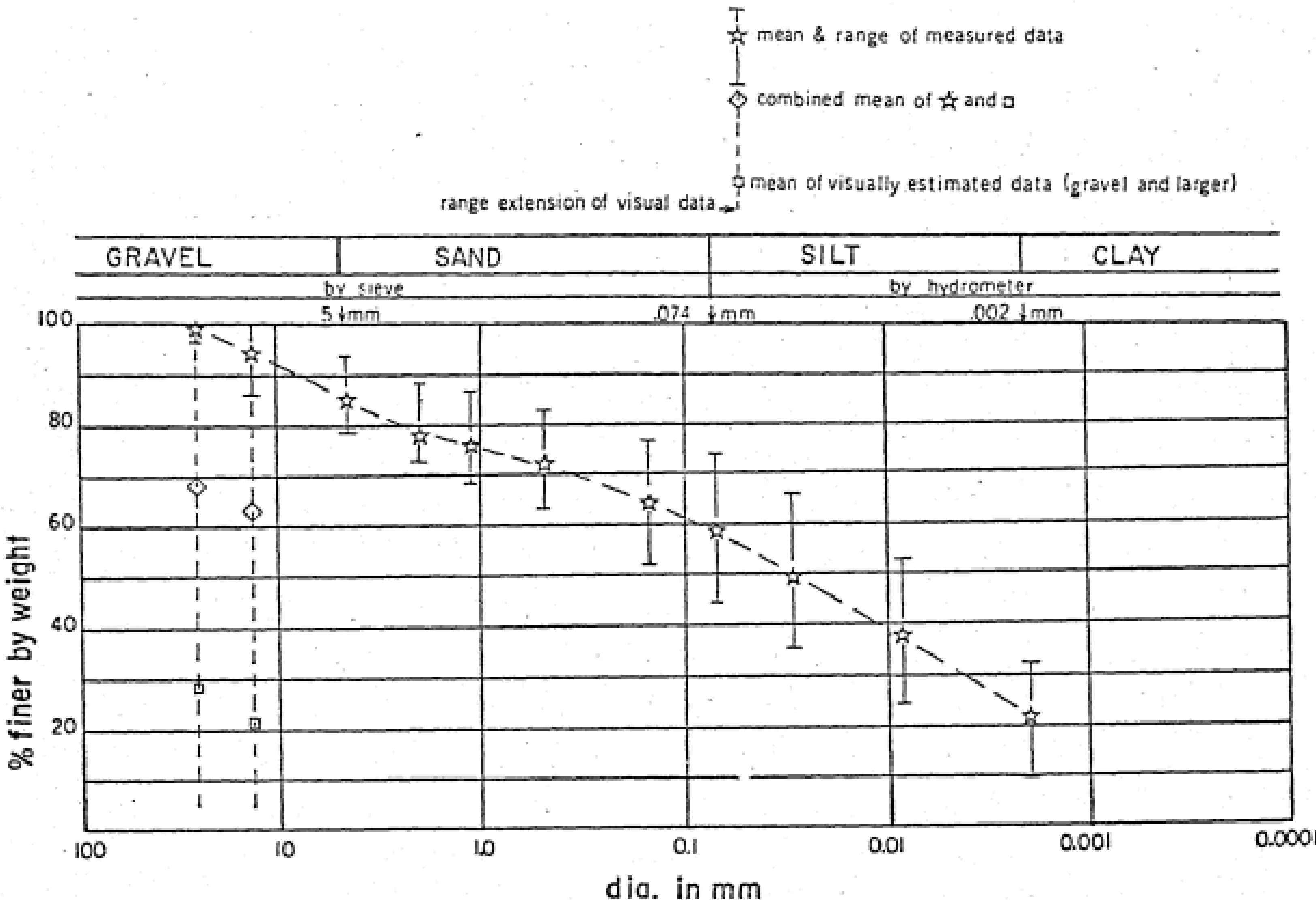

Figure III-5. Particle-size distribution for the 100 cm depth of the Hugo soil series (represented by 4 bulk samples and 3 visual estimates).

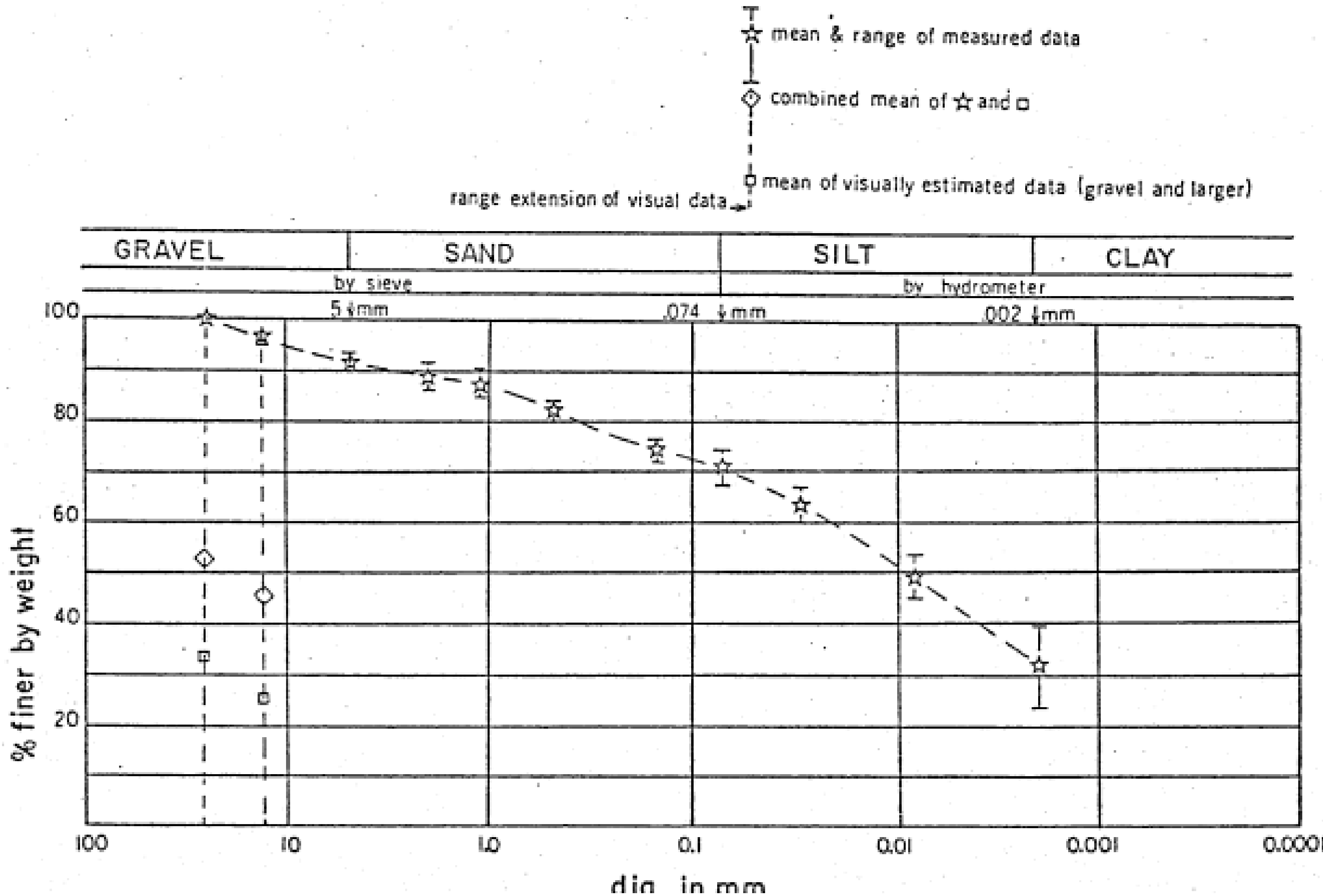

Figure III-6. Particle-size distribution for the 150 cm depth of the Hugo soil series (represented by 3 bulk samples and 4 visual estimates).

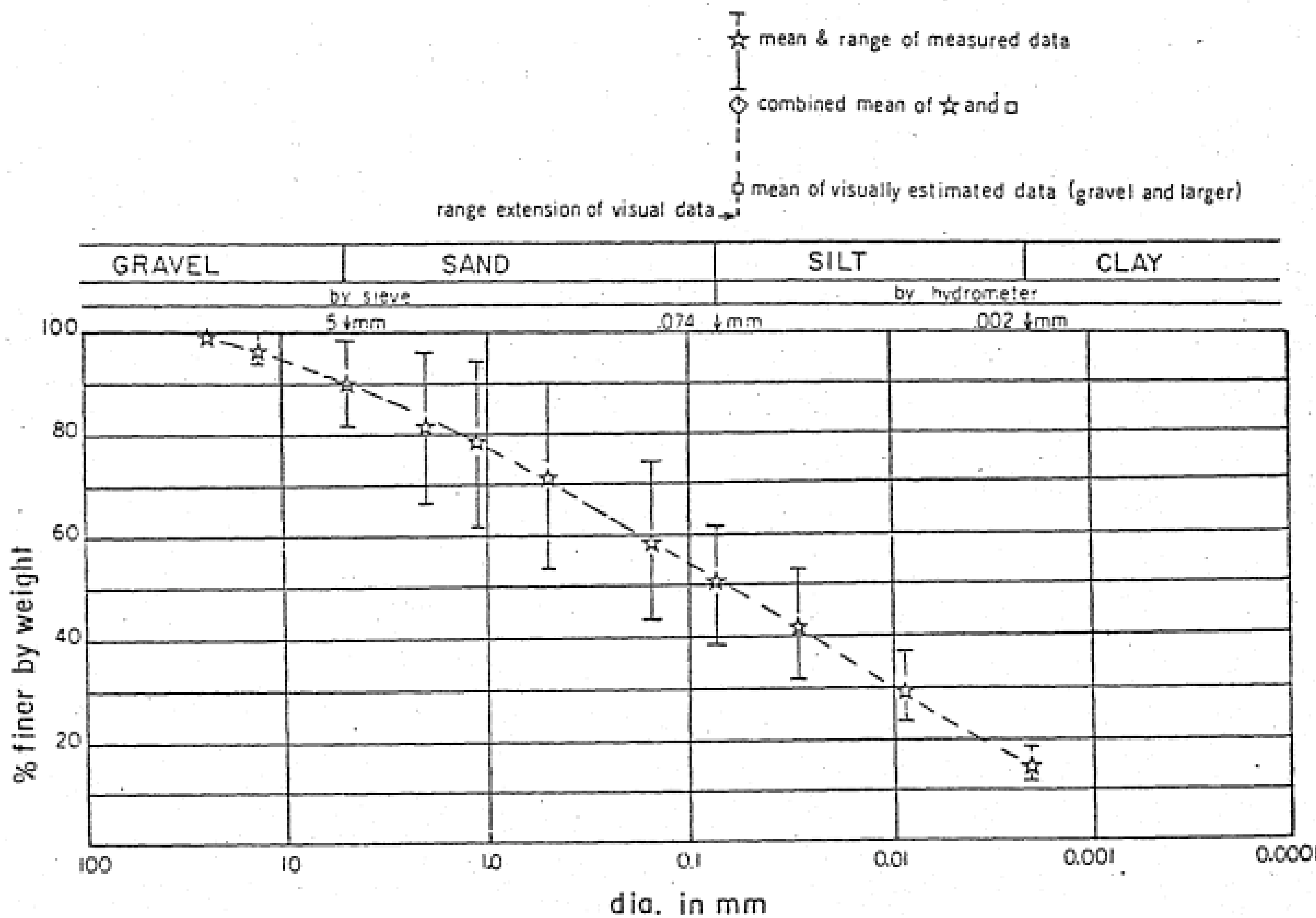

Figure III-7. Particle-size distribution for the 10 cm depth of the Mendocino soil series (represented by 2 bulk samples and 0 visual estimates).

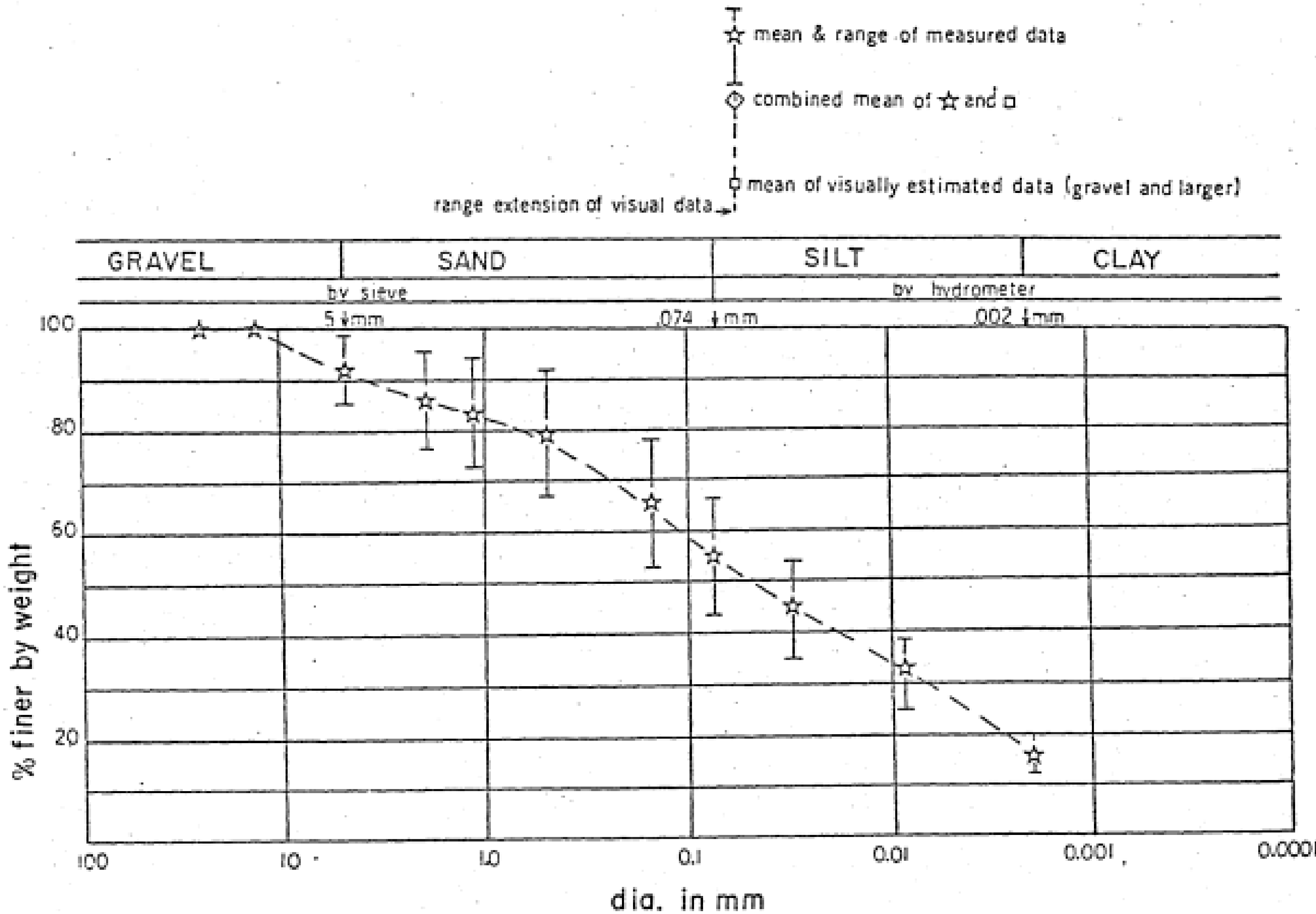

Figure III-8. Particle-size distribution for the 20 cm depth of the Mendocino soil series (represented by 2 bulk samples and 0 visual estimates).

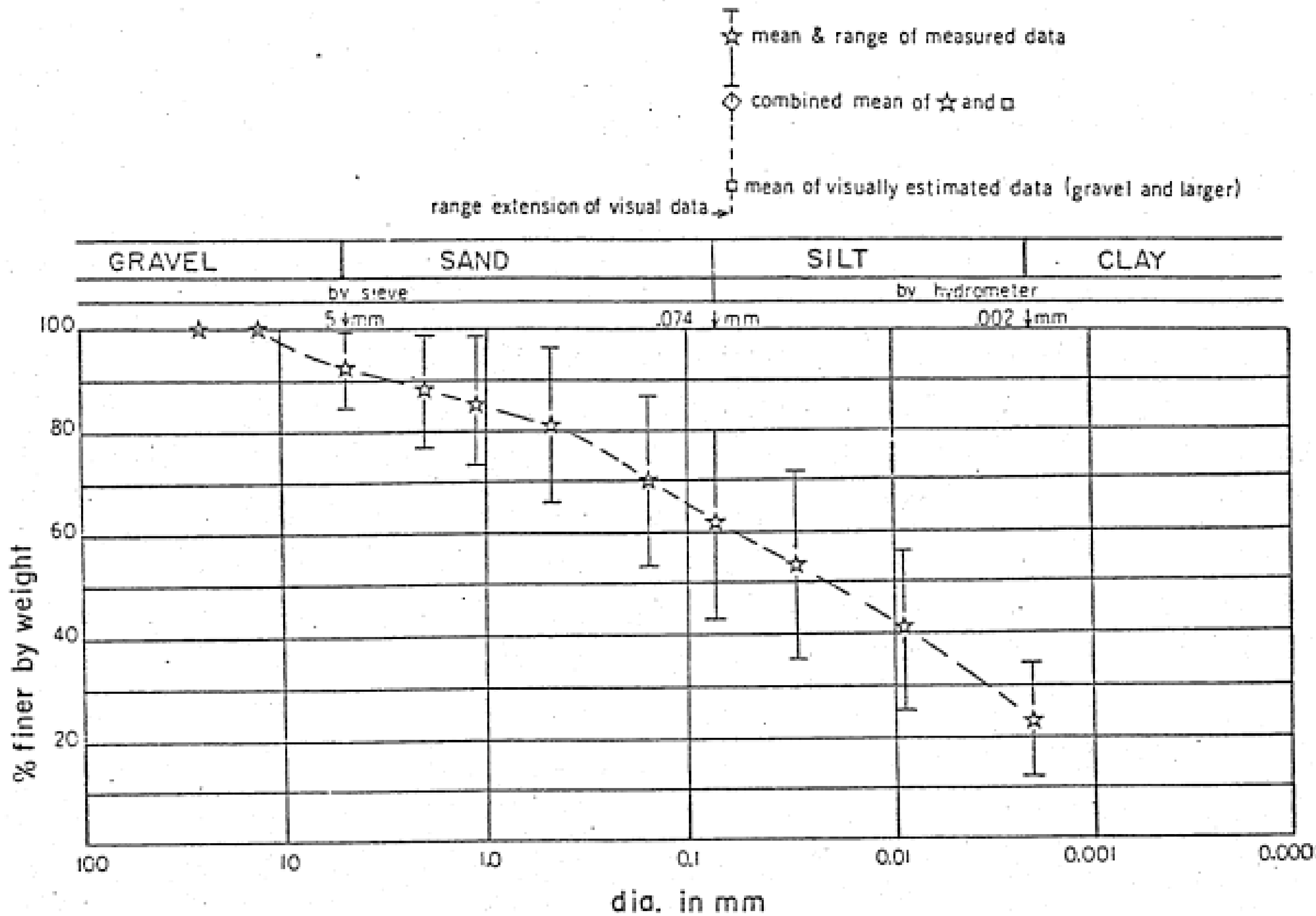

Figure III-9. Particle-size distribution for the 30 cm depth of the Mendocino soil series (represented by 2 bulk samples and 0 visual estimates).

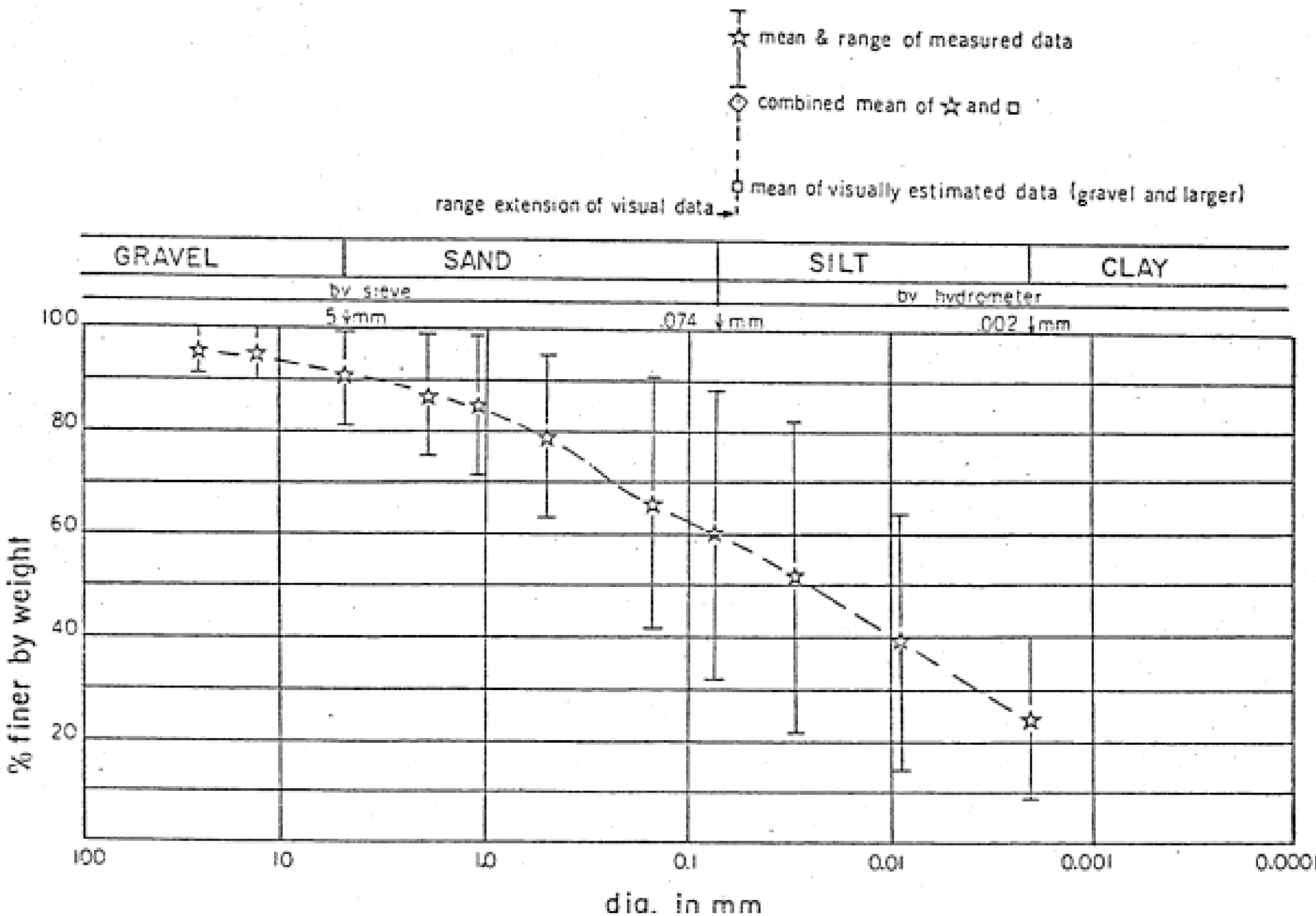

Figure III-10. Particle-size distribution for the 50 cm depth of the Mendocino soil series (represented by 2 bulk samples and 0 visual estimates).

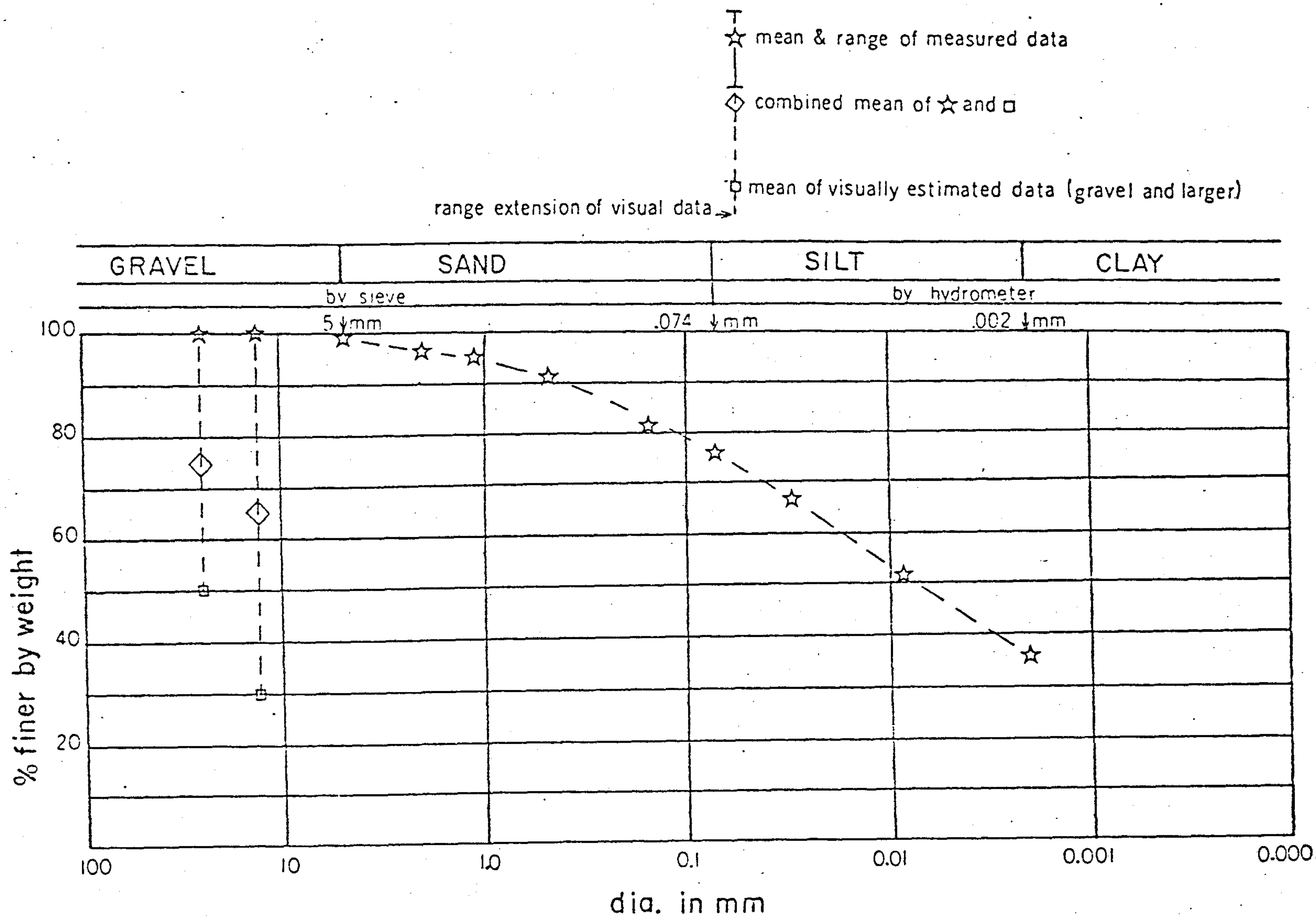

Figure III-11. Particle-size distribution for the 100 cm depth of the Mendocino soil series (represented by 1 bulk sample and 1 visual estimate).

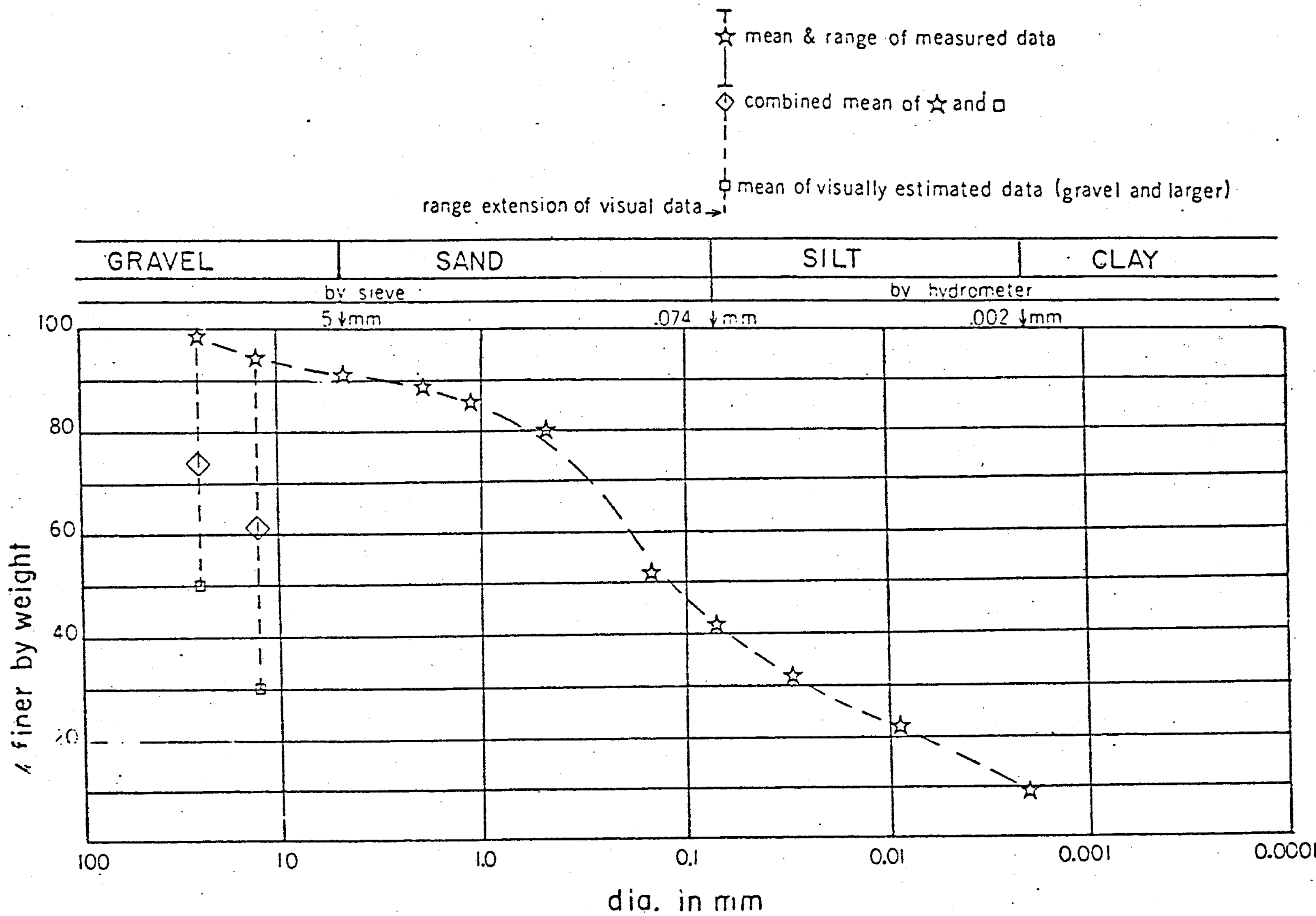

Figure III-12. Particle-size distribution for the 150 cm depth of the Mendocino soil series (represented by 1 bulk sample and 1 visual estimate).

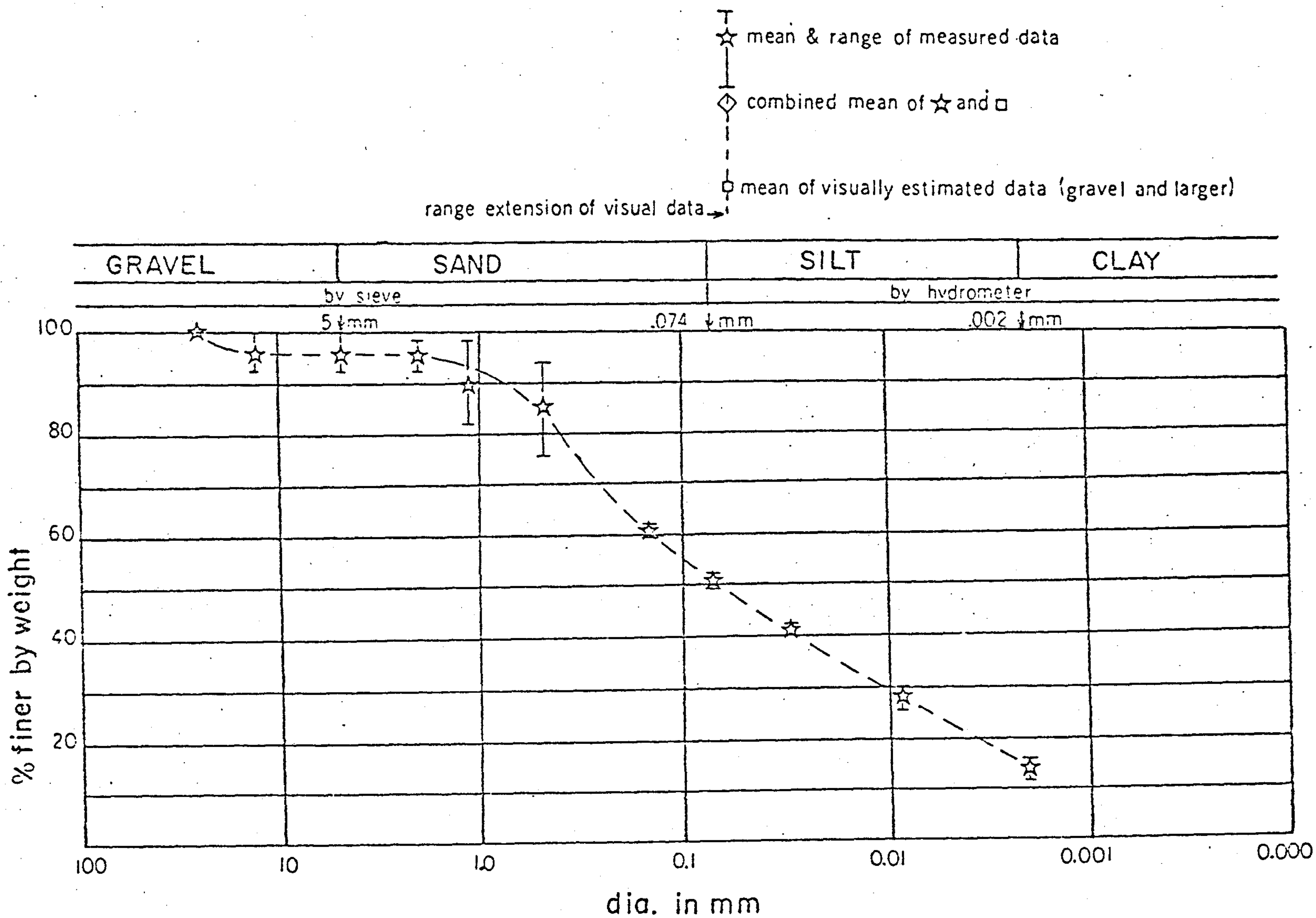

Figure III-13. Particle-size distribution for the 10 cm depth of the Caspar soil series (represented by 2 bulk samples and 0 visual estimates).

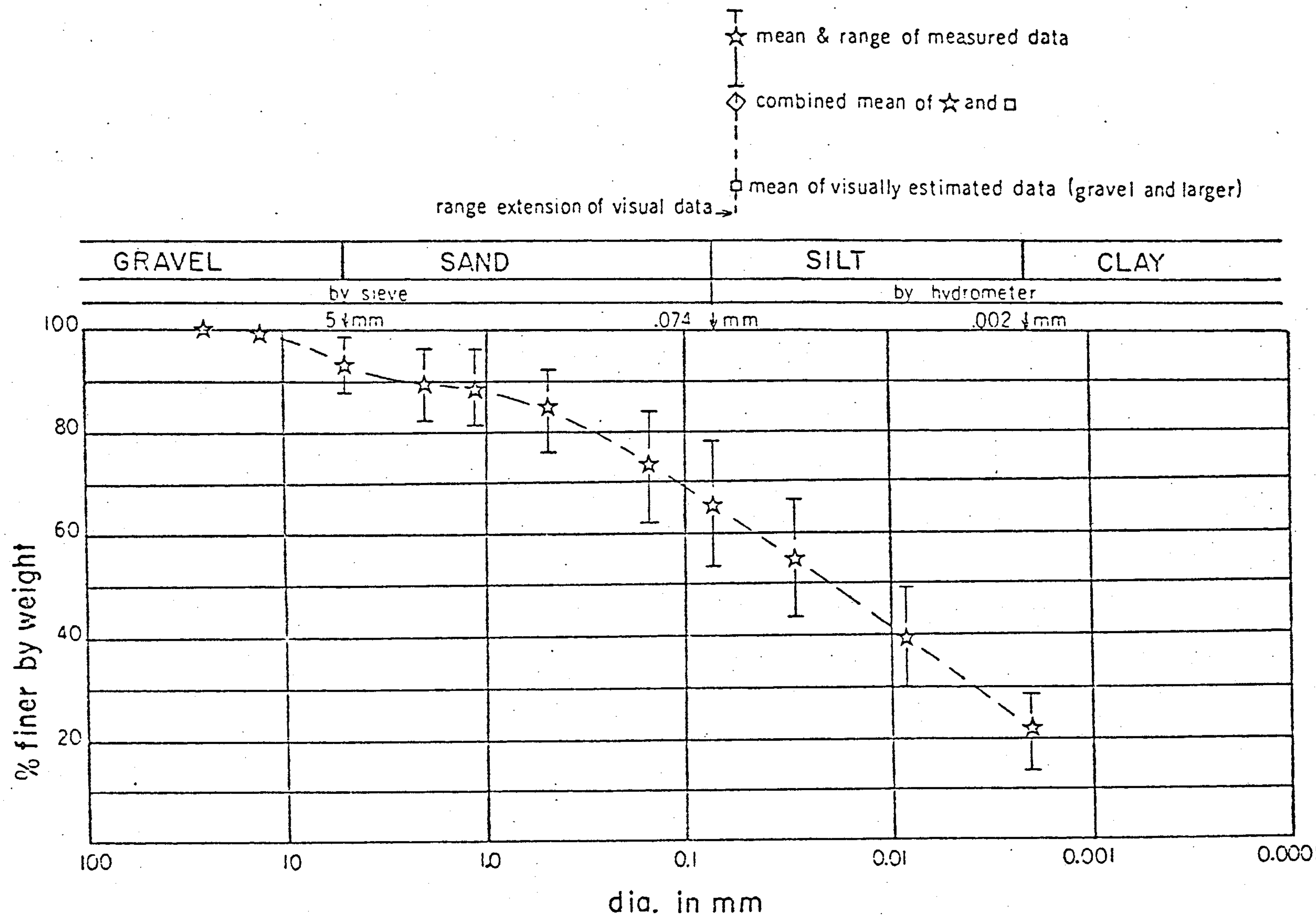

Figure III-14. Particle-size distribution for the 20 cm depth of the Caspar soil series (represented by 2 bulk samples and 0 visual estimates).

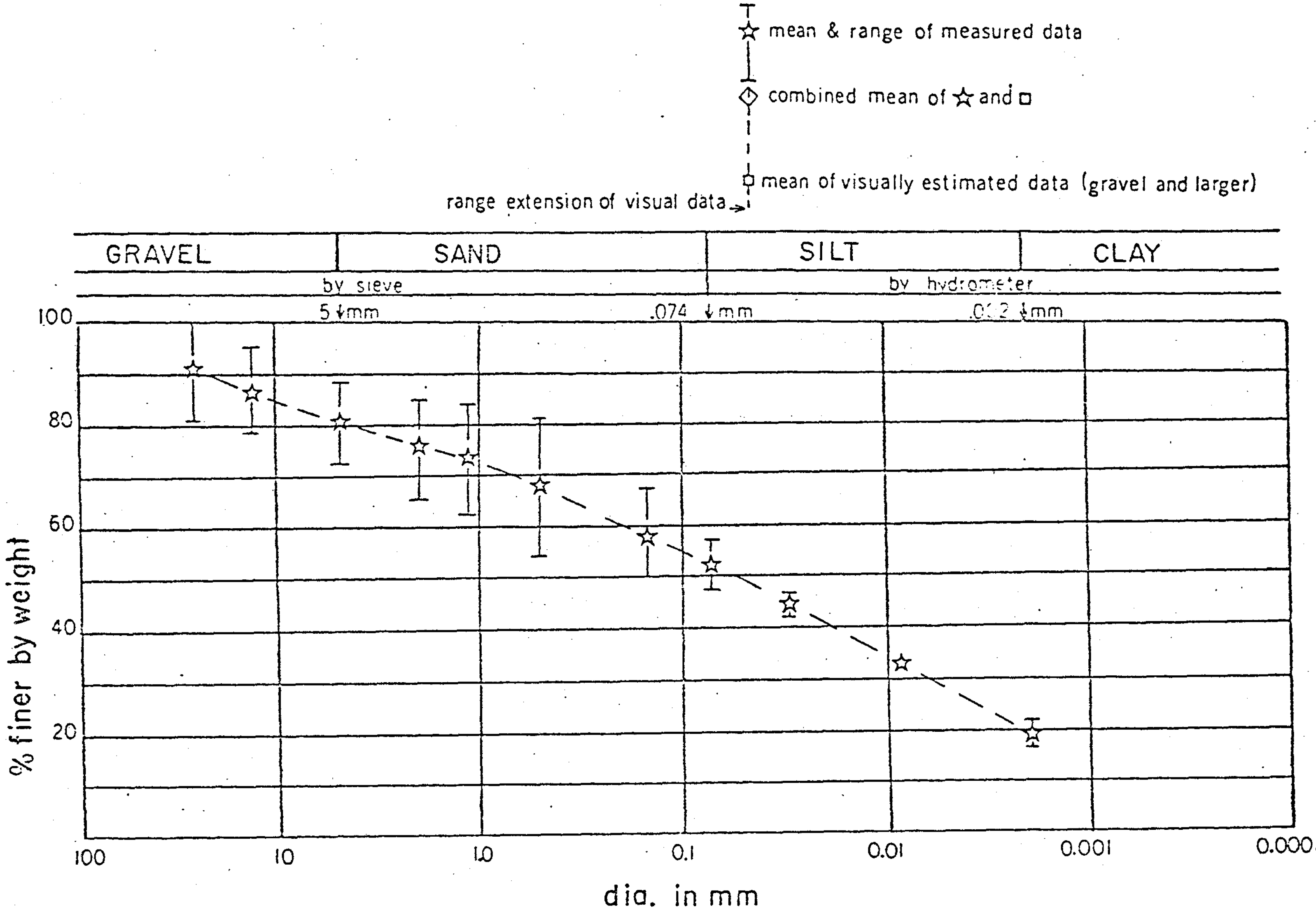

Figure III-15. Particle-size distribution for the 30 cm depth of the Caspar soil series (represented by 2 bulk samples and 0 visual estimates).

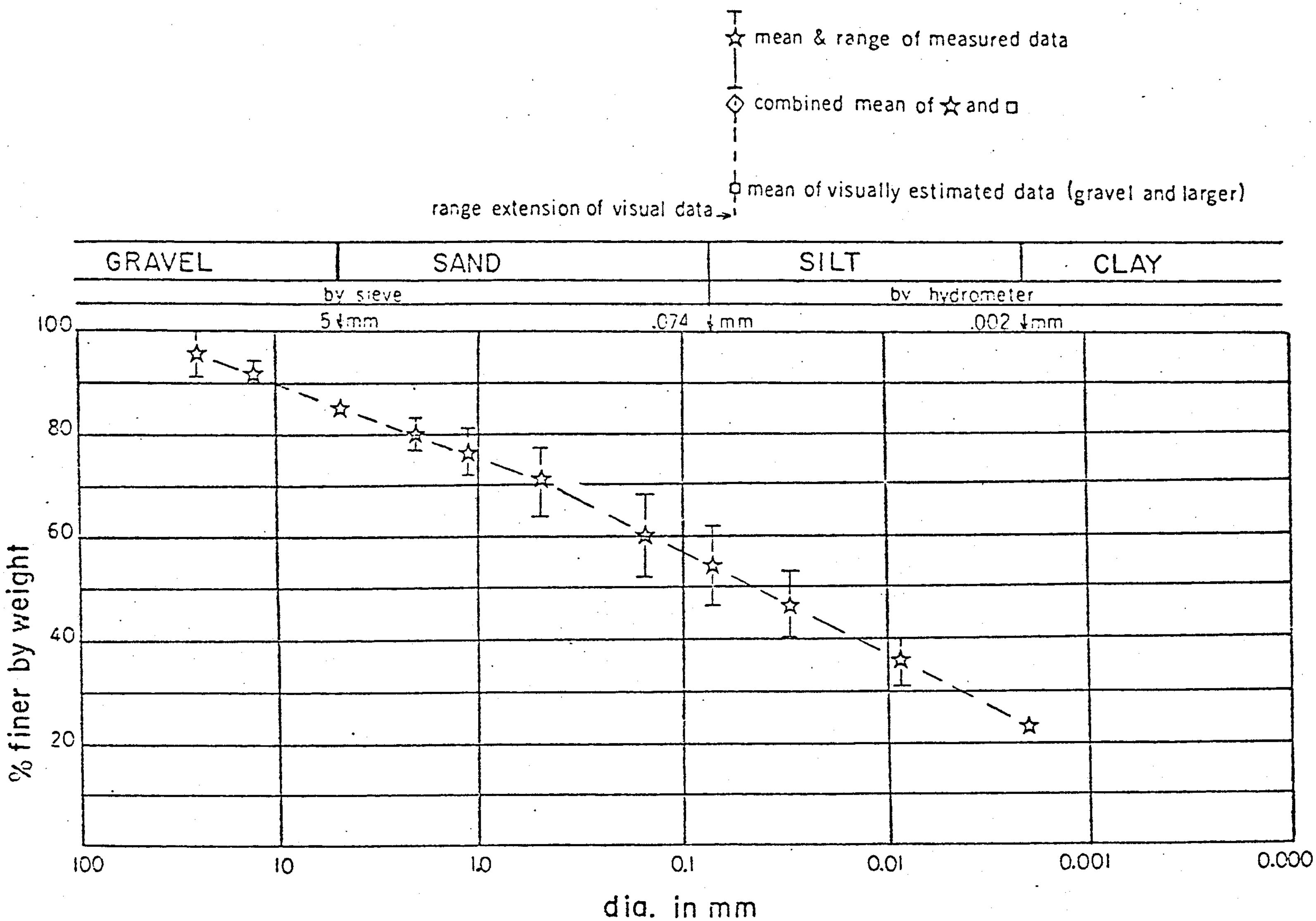

Figure III-16. Particle-size distribution for the 50 cm depth of the Caspar soil series (represented by 2 bulk samples and 0 visual estimates).

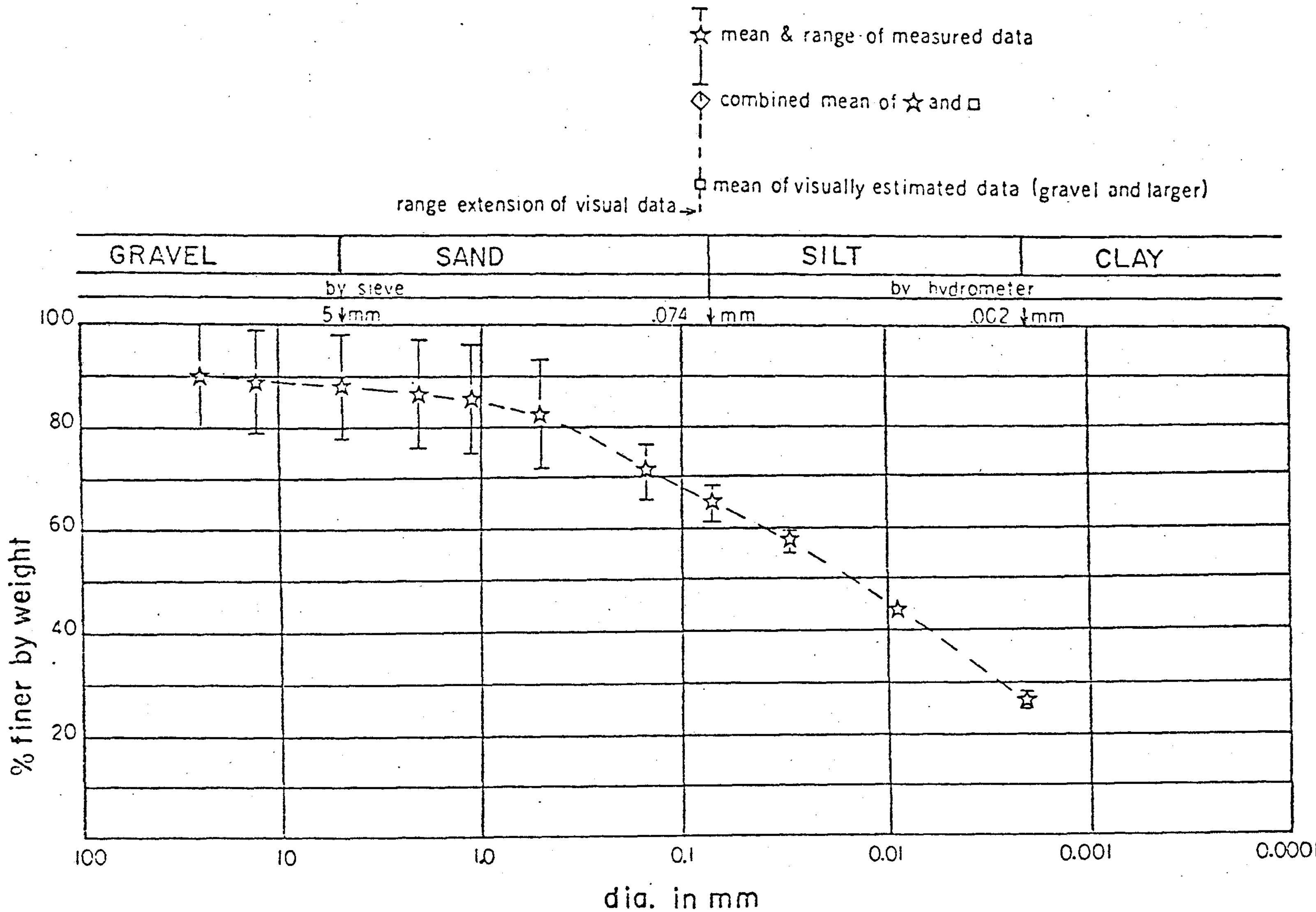

Figure III-17. Particle-size distribution for the 100 cm depth of the Caspar soil series (represented by 2 bulk samples and 0 visual estimates).

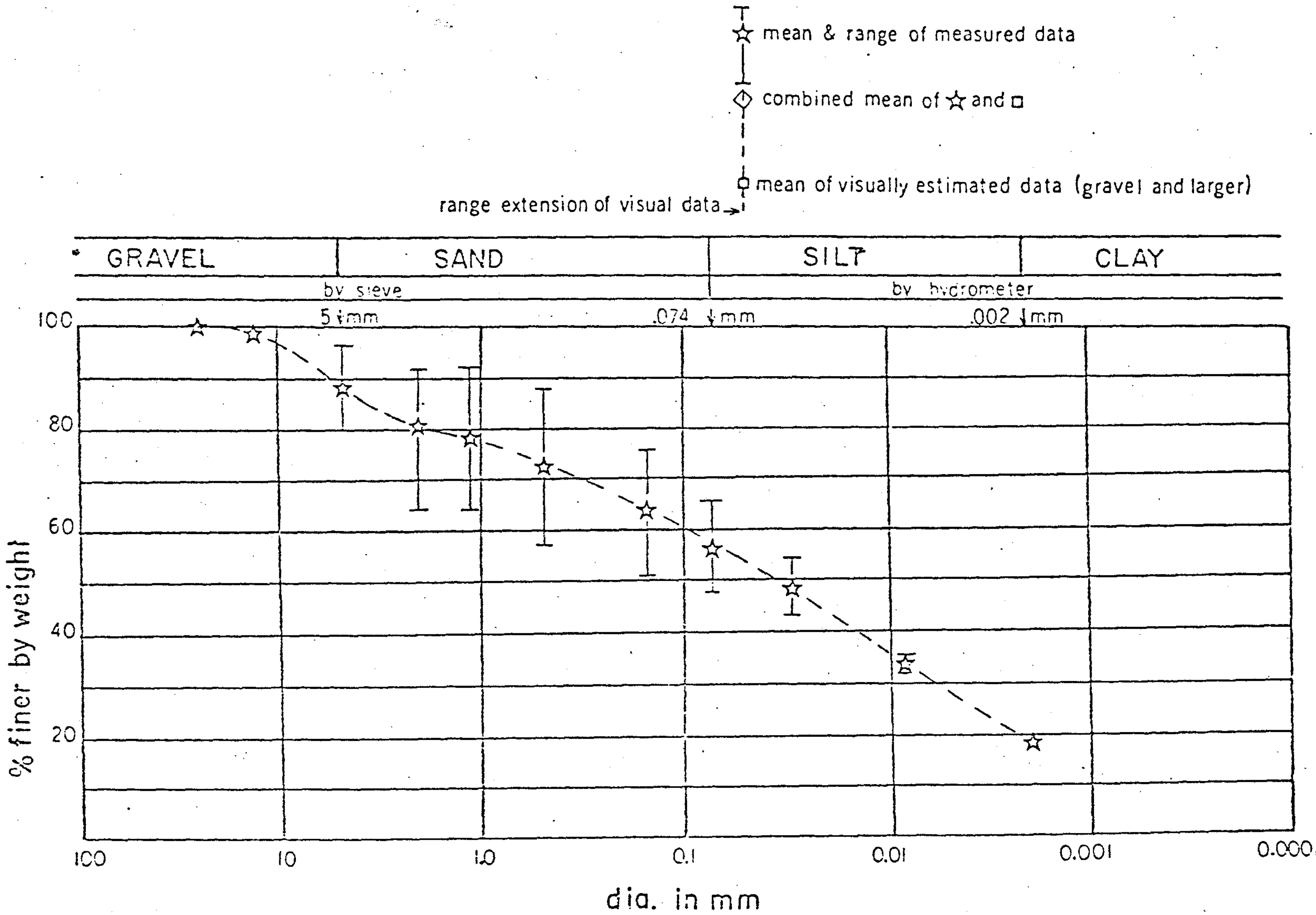

Figure III-18. Particle-size distribution for the 150 cm depth of the Caspar soil series (represented by 2 bulk samples and 0 visual estimates).

APPENDIX D

Hugo Soil Series (Pit No. 1)

Parent Material: Graywacke of the Franciscan formation
Landform: Colluvial slope, near crest
Slope: 50%, northerly aspect
Drainage: Well-drained
Elevation: 219 m MSL
Erosion: None evident
Vegetation: Sword fern understory, thinned second-growth redwood overstory

Horizon	Depth (cm)	Description
0_1	2-0	Litter, leaves, twigs .from redwood and sword fern.
A_1	0-20	Light yellowish brown (l0YR 6/4) dry, slightly dark brown (l0YR 4/3) moist, gravely (26%) loam; strong, fine and medium granular structure; soft, friable, slightly sticky, slightly plastic; many fine and very fine, and few coarse roots; many fine and very fine tubular and interstitial pores; very slightly acid (6.5pH); diffuse boundary.
B_l	20-40	Light yellowish brown (lOYR 6/4) dry, dark yellowish brown (l0YR 4/4) moist, gravely (21.5%) loam; fine and medium granular structure; soft, friable, slight ly sticky, slightly plastic; many fine and very fine, and few coarse roots; many fine and very fine tubular and interstitial pores; slightly acid (6.0 pH); diffuse boundary.
B_{21}	40-95	Light yellowish brown (l0YR 6/4) dry, dark brown (7.5YR 4/4) moist, gravely (266%)loam; strong fine and medium subangular blocky structure; slightly hard, friable, slightly sticky, slightly plastic; common fine and very fine tubular and interstitial pores; few medium clay films in pores and bridges; medium acid (5.5pH); clear wavy boundary.
B_{22t}	95-140	Light yellowish brown (lOYR 6/4) dry, strong, brown (7.5YR 5/6) moist, slightly gravely (14%) loam to clay loam; massive structure; slightly hard, friable, slightly sticky, slightly plastic; few fine, medium and coarse roots; many fine and very fine. tubular and interstitial pores; medium clay films in pores and bridges; medium acid (5.5pH); diffuse boundary.
C & R	140-150 +	Brown (l0YR 5/3) dry, shattered and weathered scoriaceous basalt, grading into unweathered scoriaceous basalt; no clay films.

APPENDIX D

Hugo Soil Series (Pit No. 2)

Parent Material: Graywacke of the Franciscan formation
Landform: Colluvial slope near crest
Slope: 50%, southerly aspect
Drainage: Well-drained
Elevation: 152 m MSL
Erosion: None evident
Vegetation: Sword fern understory, tanoak and chinquapin overstory.

Horizon	Depth (cm)	Description
0_1	20-15	Litter, leaves, twigs from tanoak, chinquapin, and sword fern.
0_2	15-0	Partially decomposed leaves, twigs, etc.
A_l	0-20	Pale brown (l0YR 6/3) dry, brown (l0YR 4/3) moist, slightly gravelly (13%) loam; strong fine and medium granular structure; soft, friable, slightly sticky, slightly plastic; many fine and very fine, and few coarse roots; many fine and very fine tubular and interstitial pores; medium acid (5.5 pH); diffuse boundary.
B_1	20-41	Yellowish brown (l0YR 5/4) dry and moist, very slightly gravelly (8%) loam; weak fine and medium granular structure; slightly hard, friable, slightly sticky, slightly plastic; many fine and very fine and few coarse roots; many fine and very fine tubular and interstitial pores; strongly acid (5.0 pH); diffuse boundary.
B_{21t}	41-79	Pale brown (l0YR 6/3) dry, brown (lOYR 4/3-4/4) moist, slightly gravelly (10%) clay loam; strong fine and medium subangular blocky structure; slightly hard, friable, slightly sticky, slightly plastic;. common fine and very fine, and few coarse roots; many fine and very fine tubular and interstitial pores; few medium clay films in pores and bridges; strongly acid (5.0 pH); clear wavy boundary.
B_{22t}	79-134	Pale brown (l0YR 6/2-6/3) dry, dark yellowish brown (l0YR 4/4) moist, slightly gravelly (5%) heavy clay loam; massive structure; slightly hard, friable, slightly sticky, slightly plastic; few fine, medium and coarse roots; many fine and very fine tubular and interstitial pores; few medium clay films in pores and bridges; strongly acid (5.0 pH); diffuse boundary.
C & R	134-150 +	Light yellowish brown (l0YR 6/4) dry scattered and weathered blocks of medium-grained graywacke, with some dark yellowish brown (l0YR 4/4) moist, slightly gravelly (7%) clay; massive hard, firm, slightly sticky, slightly plastic; medium clay films on rock fragments and along rock fractures strongly acid (5.0 pH); grades into shattered and weathered, very pale brown, hard, medium-grained graywacke.

APPENDIX D

Hugo Soil Series (Pit No. 3)

Parent Material: Graywacke of the Franciscan formation
Landform: Colluvial lower slope
Slope: 100%, southern aspect
Drainage: well-drained
Elevation: 122 m MSL
Erosion: extensive past slumping (hummocky topography); some ravelling
Vegetation: Sword fern understory, old second-growth redwood overstory

Horizon	Depth (cm)	Description
O_1	3-0	Litter, leaves, twigs from redwood, sword fern, tanoak, etc.
A_1	0-12	Yellowish brown (l0YR 5/4) dry, brown (l0YR 4/3) moist, gravelly (22%) loam; strong fine and medium granular structure; soft, friable, slightly sticky slightly plastic; many fine and very fine, and few coarse roots; many fine and very fine tubular and interstitial pores; medium acid (5.5 pH); diffuse boundary.
B_1	12-34	Yellowish brown (l0YR 5/4) moist, very gravelly (35%) loam; strong fine and medium granular structure; slightly hard, friable, slightly sticky, slightly plastic; many fine and very fine tubular and interstitial pores; strongly acid (5.0 pH); diffuse boundary.
C & R*	34-150	Slightly weathered, broken, graywacke (90% gravel and cobbles), with no clay films, having a large proportion of void spaces greater than 1 cm across the largest dimension (20% of soil volume).

* The utter lack of the B_{21} and B_{22} horizons, coupled with the negligible development of the C horizon points toward a long history of frequent mass movement.

APPENDIX D

Hugo Soil Series (Pit No. 4)

Parent Material: Graywacke of the Franciscan formation
Landform: Near bottom of colluvial slope
Slope: 20%, northerly aspect
Drainage: Well-drained
Elevation: 73 m MSL
Erosion: Past slumping, slight raveling
Vegetation: Recovering from a selection cut (1971); scattered redwood

Horizon	Depth (cm)	Description
O_1	2-0	Forest litter of leaves and twigs from redwood, sword fern, etc.
A_1	0-15	Light yellowish brown (10YR 6/4) dry, yellowish brown (10YR 5/4) moist, gravelly (32%) silt loam to loam; strong fine and medium granular structure; soft, friable, slightly~sticky, slightly plastic; many fine and very fine, and few coarse roots; many fine and very fine tubular and interstitial pores; medium acid (5.5 pH) diffuse boundary.
B_{1t}	15-41	Pale brown (lOYR 6/3) dry, brown (LOYR 4/3) moist, gravelly (14%) loam to clay loam; strong fine and medium granular structure; slightly hard, friable, slightly sticky, slightly plastic; many fine and very fine, and few coarse roots; many fine and very fine tubular and interstitial pores; strongly acid (5.0 pH); diffuse boundary.
B_{21t}	41-67	Pale brown (l0YR 6/3) dry, brown (l0YR 4/3-4/4) moist gravelly (16%) loam; strong fine and medium subangular blocky structure; slightly hard, friable, slightly sticky, slightly plastic; common fine and very fine, and few coarse roots; many fine and very fine tubular and interstitial pores; few medium clay films in pores and bridges; strongly acid (5.0 pH); clear wavy boundary.
B_{22t}	67-95	Pale brown (10YR 6/2-6/3) dry, dark yellowish brown (10YR 4/4) moist, gravelly (21%) loam (near clay loam); massive structure; slightly hard, slightly friable, slightly sticky, slightly plastic; few fine, medium, and coarse roots; many fine and very fine tubular and interstitial pores; few medium clay films in pores and bridges; strongly acid (5.0 pH); diffuse boundary.
C & R	95-109	Light yellowish brown (10YR 6/4) scattered and weathered medium-drained graywacke (60% boulders, 20% gravel), with some dark yellowish brown (10YR 4/4) moist silt loam; soil fraction is massive; hard, firm slightly sticky, slightly plastic; medium clay films on rock fragments and along rock fractures; strongly acid (5.0 pH); grades into shattered and weathered, massive, very pale brown, hard, medium-grained graywacke.

* Large blocks of indurated sandstone at the 109 cm depth precluded deeper excavation.

APPENDIX D

Huge Soil Series (Pit No. 5)

Parent Material: Grnywacke of the Franciscan formation
Landform: Colluvial slope near bottom
Slope: 60%, easterly aspect
Drainage: poorly drained below the A1 horizon
Elevation: 122 m MSL
Erosion: pit is located on an east-west trending fault of small size, which shows no control of the geomorphology
Vegetation: Sword fern understory, old second-growth redwood overstory

Horizon	Depth (cm)	Description
O_1	2-0	Litter, leaves, twigs from redwood, sword fern, tanoak, etc.
A_1	0-13	Pale brown (l0YR 6/3) dry, brown (10YR 4/3) moist, very gravelly (30%) loam; strong fine and medium granular structure; soft, friable, slightly sticky, slightly plastic; many fine and very fine tubular and interstitial pores; medium acid (5.5 pH); diffuse boundary.
C & R	13-150	Boulders and cobbles (50%) and gravel (25%) of faulted graywacke with interstitial black (l0YR 2/1) moist fault gouge; a perennial seep issues along the entire depth interval.

APPENDIX D

Hugo Soil Series (Pit No. 6)

Parent Material: Graywacke of the Franciscan formation
Landform: Colluvial slope near brow of ridge
Slope: 20% (top of back-rotated slump block; surrounding terrain is on 60% slope on the downhill side and 30% slope on the upphill side), northerly aspect
Drainage: Well-drained
Elevation: 244 m MSL
Erosion: extensive slumping prior to growth of present mature second growth forest
Vegetation: Sword fern understory, mature second-growth redwood overstory with some hardwoods

Horizon	Depth (cm)	Description
O_1	3-0	Litter, leaves; twigs from redwood and sword fern
A_1	0-20	Yellowish brown (l0YR 5/4) dry, dark brown (l0YR 3/3) moist, gravelly (18%); loam; soft, friable, slightly sticky, slightly plastic; many fine and very fine tubular and interstitial pores; neutral (7.0 pH; diffuse boundary.
B_1	10-25	Light yellowish brown (l0YR 6/4) dry, dark yellowish brown (l0YR 4/4) moist, slightly gravelly (8%) loam; poorly developed fine and medium granular structure; soft, friable, slightly sticky, slightly plastic; many fine and very fine and few coarse roots; many fine and very fine tubular and interstitial pores; slightly acid (6.0 pH); diffuse boundary.
B_{21t}	25-43	Light yellowish brown (l0YR 6/4) dry, dark brown (7.5 YR 4/4) moist, clay loam; strong fine and medium sub-angular blocky structure; slightly hard, friable, sticky, plastic; common fine and very fine tubular pores and bridges; medium acid (5.5 pH); clear wavy boundary.
B_{22t}	43-76*	Very pale brown (10YR 7/4) dry, yellowish brown (l0YR 5/6) moist, clay; massive structure; soft, sticky plastic; few fine, medium and coarse roots; few pores; exhibits mottling; medium acid (5.5 pH); diffuse boundary.
C & R	76-150	Occasional reddish yellow (7.5YR 7/6) dry, reddish yellow (7.5YR 6/8) moist clay films between gray (7.5YR 5/0) weathered, and light gray (7.5YR 7/0) clasts of broken graywacke; grading into unweathered bedrock

* Charcoal layer at the 50 cm level.

APPENDIX D

Hugo Soil Series (Pit No. 7)

Parent Material: Graywacke of the Franciscan formation
Landform: Colluvial slope, near crest
Slope: 75% westerly aspect
Drainage: Well-drained
Elevation: 268 m MSL
Erosion: slight soil creep evident
Vegetation: Sword fern understory, mature redwood overstory.

Horizon	Depth (cm)	Description
O_l	3-0	Litter, leaves, twigs from redwood and sword fern
A_l	0-13	Light yellowish brown (l0YR 6/4) dry, dark brown (l0YR 3/3) moist, slightly gravelly (l0%) loam to silt loam; soft, friable, slightly sticky, slightly plastic; many fine and very fine tubular and interstitial pores; neutral (7.0 pH); diffuse boundary.
B_1	13-37	Light yellowish brown (l0YR 6/4) dry, very dark grayish brown (lOYR 3/2) moist, gravelly (10.4%) loam; strong fine and medium granular structure; soft, friable, slightly sticky, slightly plastic; many fine and very fine and few coarse roots; many fine and very fine tubular and interstitial pores; very slightly acid (6.8 pH); diffuse boundary.
B_{21}	37-47	Brown (7.5YR 4/4) dry, dark brown (7.5YR 3/2) moist, very gravelly (40%) loam; strong fine subangular blocky structure; slightly hard, friable, slightly sticky, very slightly plastic; many fine and very fine tubular and interstitial pores; no clay films; very slightly acid (6.5 pH); clear wavy boundary.
B_{22t}	47-76	Very pale brown (l0YR 7/4) dry, yellowish brown (lOYR 5/6) moist, extremely gravely (70%) loam; fine subangular blocky structure; slightly hard, friable, slightly sticky, very slightly plastic; many fine and few coarse roots; many fine tubular and interstitial pores; few poorly developed clay films between peds, slightly acid (6.2 pH); diffuse boundary.
C & R	76-150	Light yellowish brown (l0YR 6/4) broken rocks (90%), with a little dark yellowish brown (l0YR 4/4) moist soil between clasts; few poorly developed clay films; grades into unweathered bedrock.

Note: this appears to be a very young Hugo soil whose lack of full development is a result of soil creep in the area.

APPENDIX D

Hugo Soil Series (Pit No. 8)

Parent Material: Graywacke of the Franciscan formation
Landform: Colluvial slope near bottom
Slope: 80%, southwesterly aspect
Drainage: Well-drained
Elevation: 122 m MSL
Erosion: Some past slumping evidenced by hummocky ground surface.
Vegetation: Sword fern understory, tanoak and old second-growth redwood overstory.

Horizon	Depth (cm)	Description
0_1	5-0	Litter, leaves, twigs from redwood, sword fern, tanoak, etc.
A_1	0-20	Brown (10YR 4/3) dry, very dark brown (10YR 2/2) moist, very gravelly, (32%) loam to clay loam; strong fine and medium granular structure; soft, friable, slightly sticky, slightly plastic; many fine and very fine, and few coarse roots; many fine and very fine tubular and interstitial pores; medium acid (5.5 pH); diffuse boundary.
B_1	20-34	Dark brown (10YR 3/3) dry, very dark brown (10YR 2/2) moist, very gravelly (35%) loam; strong fine and medium granular structure; slightly hard, friable, slightly sticky, slightly plastic; many fine and very fine, and few coarse roots; many fine and very fine tubular and interstitial pores; strongly acid (5.0 pH); diffuse boundary.
B_{21}	34-75	Dark brown (10YR 3/3) dry, very dark brown (10YR 2/2) moist, very gravelly (55%) silt loam to loam; strong fine and medium subangular blocky structure; slightly hard, friable, slightly sticky, slightly plastic; few fine, medium and coarse roots; many fine and very fine tubular and interstitial pores; few medium clay films in pores and bridges; strongly acid (5.0 pH); diffuse boundary.
C & R	75-150	Yellowish brown (10YR 5/6) moist very gravelly (40% cobbles, 20% gravel) silty loam; massive; hard, firm, slightly sticky, slightly plastic; medium clay films on rock fragments and along rock fractures; strongly acid (5.0 pH); grades into unbroken graywacke.

Note: The profile contains bits of charcoal throughout, testifying to strong colluvial overturning as a factor in the determination of the profile development.

APPENDIX D

Mendocino Soil Series (Pit No. 1)

Parent Material: Broken graywacke of the Franciscan formation
Landform: Brow of broad ridge
Slope: 30%, southerly aspect
Drainage: Well-drained
Elevation: 146 m MSL
Erosion: None apparent
Vegetation: Sword fern understory, old second-growth redwood overstory.

Horizon	Depth (cm)	Description
0_1	4-0	Litter, leaves and twigs from redwood and sword fern.
A_{ll}	0-10	Light brownish gray (l0YR 7/3) dry, very dark grayish brown (l0YR 6/27 moist loam; well developed fine and medium granular structure; slightly hard, friable, non-sticky, slightly plastic; many fine and very fine roots; many fine and very fine tubular and interstitial pores; very slightly acid (6.5 pH); clear wavy boundary.
A_{12}	10-16	Pale brown (l0YR 6/3) dry, dark brown (l0YR 4/3) moist, slightly gravelly (5%) loam; moderate fine and medium subangular blocky structure; hard, friable, slightly sticky, slightly plastic; many medium roots, many fine and very fine tubular and interstitial pores; neutral (7.0 pH); clear wavy boundary.
A_{13}	16-42	Very pale brown (l0YR 7/3) dry, dark yellowish brown (l0YR 4/4) moist clay to silty clay; moderate fine and medium subangular blocky structure; hard, friable, slightly sticky, slightly plastic; common medium and few coarse roots; many fine and very fine tubular and interstitial pores; slightly acid (6.0 pH); diffuse boundary.
B_{21t}	42-76	Dark yellowish brown (l0YR 4/6) moist silty clay, with brown (7.5YR 5/2) clay films; massive, firm, sticky, plastic; few medium and coarse roots; many fine and very fine tubular and interstitial pores; many very thin clay films in pores and filling former spaces between peds; slightly acid (6.0 pH); diffuse boundary.
B_{22t}	76-108	Dark reddish brown, dark yellowish brown, and very dark grayish brown (5YR 3/4, 10YR 4/4, 10YR 3/2) moist clay mottled together; moderate coarse angular blocky structure; hard, firm sticky, plastic; few coarse and fine roots; few fine tubular pores; medium acid (5.5 pH); diffuse boundary.
B_{23t}	108-120	Same colors as previous horizon (B_{22t}), clay loam; moderate coarse angular blocky structure; hard, firm, sticky, plastic; few fine and coarse roots; few fine tubular pores; continuous thick clay films in pores and filling former spaces between peds; slightly acid (6.0 pH); diffuse boundary.
C	120-150	Strong brown (7.5YR 5/6) dry and moist, slightly gravelly (8%) clay loam; massive; hard, firm, slightly sticky, plastic; very few fine roots; few fine tubular pores; continuous thick and moderately thick clay films along fracture planes; strongly acid (5.0 pH); grades into rotten and eventually into inaltered Franciscan graywacke at depth.

APPENDIX D

Mendocino Soil Series (Pit No. 2)*

Parent Material: Broken graywacke of the Franciscan formation
Landform: Colluvial slope near brow of ridge
Slope: 40%, northerly aspect
Drainage: Well-drained
Elevation: 122 m MSL
Erosion: Slight ravelling and colluvial movement of topsoil from upslope
Vegetation: Sword fern community understory, old second-growth redwood overstory

Horizon	Depth (cm)	Description
O_1	2-0	Litter, leaves, twigs from redwood, etc.
A_{ll}	0-12	Very pale brown (lOYR 7/4) dry, yellowish brown (l0YR 5/4) moist, gravelly (18%) loam; strong fine and medium granular structure; slightly hard, friable, non-sticky, slightly plastic; many fine and very fine roots; many fine and very fine tubular and interstitial pores; very strongly acid (4.5 pH); clear wavy boundary.
A_{12}	12-37	Yellowish brown (l0YR 5/4) moist, gravelly (14%) loam; moderate fine granular structure; slightly hard, friable, non-sticky, slightly plastic; some medium roots, many fine roots; many fine and very fine tubular and interstitial pores; medium acid (5.5 pH); clear wavy boundary.
A_{13}	37-51	Dark brown (l0YR 3/3) moist slightly gravelly (7%) loam to sandy loam; poorly developed subangular blocky structure (modified from colluvially deposited topsoil of granular structure); hard, firable, slightly sticky, slightly plastic; few medium roots; many fine and very fine tubular and interstitial pores; medium acid (5.5 pH); diffuse boundary.
B_{21t}	51-78	Dark yellowish brown (l0YR 4/6) moist, very gravelly (50% cobbles, 20% gravel) sandy clay loam, medium angular blocky structure; firm, sticky, plastic; common large roots, few medium roots; many fine and very fine tubular and interstitial pores; many very thin brown (7.5YR 5/2) clay films in pores and filling the former spaces between peds; very slightly acid (6.5 pH); clear wavy boundary.
B_{22t}	78-120	Mottled strong brown dark yellowish brown and light yellowish brown (7.5YR 5/8, l0YR 3/6, and lOYR 6/4) very gravelly (50% cobbles, 20% gravel) clay; moderate coarse angular blocky structure; hard, firm, sticky, plastic; few coarse and fine roots; few tubular pores; continuous thick clay films filling former spaces between ped faces and in pores; very slightly acid (6.8 pH); clear wavy boundary.
C & R	120-150	Mottled light brownish gray, dark brown, and yellowish brown (7.5YR 5/8, 10YR 3/3, and 10YR 5/6) moist, extremely gravelly (50% cobbles, 20% gravel) clay loam; massive strcuture; hard, firm, slightly sticky, plastic; very few fine roots; few tubular pores; continuous thick and moderately thick clay films along fracture planes; very slightly acid (6.5 pH) grades into Franciscan graywacke.

* This pit is not typical of the Mendocino series because the first 50 cm are essentially composed of colluvially deposited A_l horizon material from upslope. This has begun to be modified in the direction of the normal Mendocino profile. The first 50 cm of the profile also contain an unusually high gravel content (12%, as opposed to only 1.3% in Mendocino pit No. 2), which was presumably incorporated during the colluvial movement.

APPENDIX D

Caspar Soil Series (Pit No. 1)

Parent Material: Graywacke of the Franciscan formation
Landform: Brow of wave-cut terrace
Slope: 30%, northerly aspect
Drainage: Well-drained
Elevation: 146 m MSL
Erosion: Slight surface alteration from logging
Vegetation: Sword fern understory, with salal; overstory of heavily selection-cut second-growth redwood

Horizon	Depth (cm)	Description
0_1	2-0	Litter, leaves, twigs from redwood, sword fern, brush.
A_{ll}	0-10	Very pale brown (l0YR 8/3) dry, very dark grayish brown (l0YR 3/2) moist, slightly gravelly (13%) loam; soft friable, slightly sticky, slightly plastic; many fine and very fine, and few coarse roots; many fine and very fine tubular and interstitial pores; slightly acid (6.0 pH); clear wavy boundary.
A_{12}	10-16	Very pale brown (10YR 8/3) dry, brown (10YR 4/3) moist, slightly gravelly (5%) loam; moderate fine to medium subangular blocky with some granular structure; many fine and very fine and few coarse roots; many fine and very fine tubular and interstitial pores; slightly acid (6.0 pH); clear wavy boundary
B_{21t}	16-70	Very pale brown (l0YR 7/4) dry, brown (l0YR 4/3) moist, slightly gravelly (14%) clay loam; subangular blocky structure; firm, slightly friable, sticky, plastic; many fine and coarse roots; many fine and very fine tubular and interstitial pores; many clay films on ped faces; slightly acid (6.0 pH); clear wavy boundary.
B_{22t}	70-110	Dark yellowish brown (lOYR 4/4) dry, dark yellowish brown (l0YR 3/4) moist, gravelly (20%) clay loam; subangular blocky structure; firm, sticky, plastic; few fine and coarse roots; sparse fine and very fine tubular and interstitial pores; very acid (4.5 pH); clear wavy boundary.
B_{23t}	110-150	Mottled dark reddish brown, dark yellowish brown and very dark grayish brown (5YR 3/4, 10YR 4/4, l0YR 3/2) moist, gravelly (19%) clay loam; massive; hard, firm, sticky, slightly plastic; few fine and coarse roots; few fine tubular pores; thick clay films in proes; very strongly acid (4.5 pH); diffuse boundary.

APPENDIX D

Caspar Soil Series (Pit No. 2)

Parent Material: Graywacke of the Franciscan formation
Landform: Brow of wave-cut terrace
Slope: 20%, northerly aspect
Drainage: Well-drained
Elevation: 122 m MSL
Erosion: Some slight surface erosion due to surface run-off after logging
Vegetation: Sword fern and salal understory, overstory of thinned second-growth redwood, with some hardwoods

Horizon	Depth (cm)	Description
O_1	2-0	Litter, leaves, twigs from redwood, sword fern, brush
A_{ll}	0-15	Very pale brown (l0YR 8/4) dry, yellowish brown (l0YR 5/6) moist silt. loam to loam; very weak, fine granular structure; slightly hard, slightly friable, non sticky; non plastic; many fine and very fine roots; many fine and very fine tubular and interstitial pores; extremely acid (4.2 pH); diffuse boundary.
A_{21}	15-37	Brownish yellow (l0YR 6/6) dry, dark yellowish brown (l0YR 4/4) moist, gravelly (20%) clay loam to silt loam to loam; moderate subangular blocky structure; hard, friable, sticky, plastic; few medium roots; many fine and very fine tubular and interstitial pores; very strongly acid (4.5 pH); diffuse boundary
B_{21t}	37-78	Light yellowish brown (l0YR 6/4) dry dark brown (l0YR 3/3) moist, slightly gravelly (10%) clay loam; strong medium blocky structure; firm, lsightly sticky, slightly plastic; common large roots, and few medium roots; many fine and very fine tubular and interstitial pores; many very thin, brown (7.5YR 5/2) clay films in pores and on ped faces; strongly acid (5.0 pH); clear wavy boundary.
B_{22t}	78-110	Light yellowish brown (l0YR 6/4) dry, dark yellowish brown (l0YR 4/4) moist clay loam; coarse angular blocky structure; few tubular and interstitial pores; common clay films on ped faces; little mottling; very strongly acid (4.5 pH); clear, wavy boundary.
B_{23t}	110-150	Mottled strong brown dark yellowish brown, and light yellowish brown (7.5YR 5/8, 10YR 3/6, 10YR 6/4) moist, loam to clay loam; moderate coarse angular blocky structure; firm, sticky, plastic; few coarse and fine roots; few tubular pores; continuous thick clay films on ped faces and in pores; very strongly acid (4.5 pH); clear wavy boundary.
C	150+	Mottled light brownish gray, dark brown, and yellowish brown (l0YR 6/2, lOYR 3/8, 10YR 5/6) moist, slightly gravelly (4%) loam; massive structure; hard, firm, slightly sticky, plastic; very few fine roots; few tubular pores; continuous thick and moderately thick clay films along fracture planes; grades into reddish yellow, soft sedimentary rock.